UNIVERSITÄT
BERN

Graduate School for Cellular and Biomedical Sciences
University of Bern

Dynamics of Cortical Stability and Seizure Resilience In Vivo

PhD Thesis submitted by

Gregory Lepeu

for the degree of

PhD in Neuroscience

Supervisor
Ass. Prof. Dr. Maxime Baud
Center for Experimental Neurology
Faculty of Medicine of the University of Bern

Co-advisor
Ass. Prof. Dr. Stéphane Ciocchi
Department of Physiology
Faculty of Medicine of the University of Bern

External Co-referee
Prof. Dr. Premysl Jiruska
Department of Physiology
Second Faculty of Medicine of the Charles University, Prague

Accepted by the Faculty of Medicine, the Faculty of Science and the Vetsuisse Faculty of the University of Bern at the request of the Graduate School for Cellular and Biomedical Sciences

Bern, Dean of the Faculty of Medicine

Bern, Dean of the Faculty of Science

Bern, Dean of the Vetsuisse Faculty Bern

In memory of Caroline Lepeu

"The best model for a cat is another, or preferably the same cat"

Arturo Rosenblueth and Norbert Wiener (Rosenblueth and Wiener, 1945)

University of Bern - Faculty of Medicine - Center for Experimental Neurology

Abstract

Dynamics of Cortical Stability and Seizure Resilience In Vivo

by Gregory Lepeu

The sudden emergence of dangerous seizures is the defining feature of epilepsy, but how and when the brain changes dynamics remain enigmatic. In the formalism of dynamical systems theory, seizure onset can be described as a critical transition between two alternative states: interictal and ictal. My PhD research aims at studying these transitions, specifically by examining the concept of resilience, which, in the present context, refers to a system's ability to withstand perturbations without changing its state. It has been proposed that both the development of epilepsy and the emergence of seizures are a result of respectively a chronic and then transitory loss of resilience. Importantly, until the point of failure, changes in the system's resilience will have minimal impact on its observable state. By monitoring a system's reaction to minor perturbations, it has been theorized that changes in resilience could nevertheless be detected. In this study, we combined theoretical, experimental and clinical approaches to test this hypothesis, and to develop methodologies to delineate the landscape of physiological and pathological cortical excitability, including quantifications of seizure thresholds.

By using a mathematical model of seizures, and optogenetics stimulations in mice and intracranial electrical stimulations in patients with epilepsy, we were able to demonstrate how small perturbations can be used to gauge cortical stability and how larger perturbations can overcome cortical resilience in a measurable way, resulting in self-sustained seizures. Both phenomena were closely correlated and influenced by the underlying level of cortical excitability, which was tightly modulated in vivo through pharmacological intervention on the GABA-A receptor. Additionally, using a machine-learning approach on EEG snapshots, we confirmed that active and passive markers can be used to decode momentary states of cortical excitability and therefore the latent seizure resilience. Ultimately, this research helps to improve our understanding of the underlying mechanisms of seizure onsets and to develop new methods for predicting and preventing seizures.

Contents

List of Figures

List of Abbreviations

BZD	**B**enzodiazepine
CA1	**C**ornus **A**mmonis
Ch2R	**C**Channelrhodopsin-2
DG	**D**entate **G**yrus
DZ	**D**iazepam
EEG	**E**lectroencephalogram
GABA	**G**amma-Aminobutyric acid
IEA	**I**nterictal **E**pileptiform **A**ctivity
HYP	**H**ypersynchronous onset
LFP	**L**ocal **F**ield **P**ontential
LVF	**L**ow **V**oltage **F**ast Activity
LL	**L**ine-**L**ength
MEC	**M**edial **E**ntorhinal **C**ortex
NMF	**N**on negative **M**atrix **F**actorization
PC	**P**yramidal Cells
PTX	**P**icrotoxin
PTZ	**P**entylenetetrazol
PV	**P**parvalbumin
Sz	**S**eizure
TLE	**T**emporal **L**obe **E**pilpesy

Introduction

1.1 Epilepsy

1.1.1 Definitions and General Considerations

Epilepsy is a neurological disorder defined as a predisposition to generate unprovoked epileptic seizures. Seizures are periods of paroxysmal and transitory neuronal discharges which disturb normal brain function. They can be accompanied by various neurological symptoms depending on the localisation and extend of the seizure. Epilepsy can be caused by various etiologies (e.g. Trauma, stroke, brain tumor, infection or genetic predisposition) but the common mechanisms leading to seizures remain to be fully understand. In addition, non-epileptic brains can also produce seizures when neuronal homeostasis is acutely disturbed or when external sustained stimulations are applied.
Epileptogenesis is defined as the process by which the brain develops the tendency to seize after an initial injury or as a consequence of predisposing factors. These changes occur over time and may not manifest as seizures until months or even years after the initial trigger. They can also produce some cognitive deficits, even outside of seizures, due to alteration in the underlying circuits.
Epileptogenesis is typically considered as multi-level phenomenon with changes at the cellular level (inflammation, alteration in gene expression including voltage-gate channels and cell death in specific neuronal sub-populations), in the local microcircuit (synaptic reorganization and axonal sprouting) as well as brain-wide network reorganization (Goldberg and Coulter, 2013; Sheybani et al., 2018).

Even after all these changes, epileptic brains do not seize all the time and seizures are transient ("ictal") phenomenons lasting only tens of seconds to minutes and interspersed with long interictal period which can last up to weeks or month. Epilepsy can therefore be described as a condition of increase susceptibility to seizure. However, this susceptibility is not constant over time, and the probability of seizure varies over time, according to both exogenous and endogenous factors (Baud et al., 2020) .

1.1.2 Electrophysiological Correlates of Epilepsy

The gold standard characterization of epileptic activity is through electrophysiological recording of the brain. Electroencephalogram (EEG) is recorded through macroelectrode at the level of the scalp or intracranially (iEEG). Local Filed Potential (LFP) is the same type of signal but recorded from a smaller volume of cortex. These signals are generated by the superimposition of many ionic currents, reflecting the sum activity of a large number of neurons. Synaptic activity is classically considered as

the main source of EEG/LFP signals (Buzsáki, Anastassiou, and Koch, 2012). During an epileptic seizure, EEG and LFP show synchronous high-amplitude discharge (spikes), as well as abnormal dynamic oscillations and high frequency activity. In focal epilepsy, the seizures typically start in a restricted cortical area (called the seizure onset zone). The seizure can then expand to other parts of the brain, including to contralateral areas, following anatomical pathway. Clinical manifestations follow the spread of the seizure, and tonic-clonic convulsions correspond to the generalized stage of a seizure, with involvement of the motor cortex and the brainstem, and are reflected by bursts of spike-wave in the EEG.
In the epileptic brain, scalp EEG outside of the seizures can be normal (up to 50% for single short EEG) or present interictal epileptiform discharges (IED) (Pillai and Sperling, 2006). These can be spikes or sharp waves, high-voltage peaky waveform lasting respectively 20-70ms and 70-200ms, sometimes coming in bursts. As for seizure, IEDs present a non-random distribution and their probability of appearance is modulated by several factors, including brain states and circadian / multidien cycles (Karoly, Rao, et al., 2021).

Finally, high-frequency oscillations (HFOs) such as ripples (80-250Hz) or fast ripples (250-500Hz) have also been proposed to be interictal biomarkers of epilepsy, even if they can also occur physiologically (Zijlmans et al., 2009; Liu et al., 2022).

1.1.3 Temporal Lobe Epilepsy

Even if the seizure onset zone is usually in relation with the localisation of the initial insult, not all brain regions show the same sensibility toward seizure initiation. Temporal lobe epilepsy (TLE) represents around 60-80% of the cases of focal epilepsy in reference center (Ladino, Moien-afshari, and Téllez-Zenteno, 2014), and a vast majority of them can even be narrowed down to the mesial structures of the hippocampal formation. Classical clinical manifestations of focal mesio-temporal seizure include a feeling of déjà-vu, loss of awareness, fixed gaze and mouth or hand automatisms. Up to 30-40% of patients with mesial Temporal lobe epilepsy (MTLE) do not present any structural lesions, even after careful postmortem analysis (De Lanerolle et al., 2003). In the remaining patients, the most common finding is an hippocampal sclerosis.

The pathological findings of hippocampal sclerosis typically include shrinkage of the hippocampus, loss of neurons and gliosis; with the CA1 regions of the hippocampus being the most severely damaged. In addition, there are also changes in the structure and organization of the remaining neurons, as well as the formation of abnormal connections between them. In rodents, prolonged status epilepticus induced by pro-convulsive drugs such Kainic acid or Pilocarpine reproduce these findings and lead to the development of recurrent spontaneous seizures. These models have been extensively used to study temporal lobe epilepsy (Rusina, Bernard, and Williamson, 2021; Lévesque, Biagini, et al., 2021).

1.1.4 Anatomy of the hippocampal formation

The hippocampal formation (HF) is located bilaterally in the mesial part of the temporal lobes and is involved in different cognitive tasks including memory formation and spatial navigation (Strien, Cappaert, and M. P. Witter, 2009). The classic definition encompasses the dentate gyrus (DG), the Cornu Ammonis area (CA) one, two

and three and the subiculum (M. Witter, 2012). The main input to the hippocampal formation is the entorhinal cortex (EC). It is a six layered cortex situated, in the rodent, at the back of the telencephalon. The upper layers (I to III) receive input from other limbic corticies (perirhinal and postrhinal) as well as non-limbic structure, such as the prefrontal cortex. They are also receiving strong commissural connections from the contralateral entorhinal(M. Witter, 2012).

The two main projections from the entorhinal cortex to the hippocampal formation are the perforant path, going to the Dentate Gyrus, and the temporoammonic path, going directly to CA1 and the subiculum.[1]
Both lateral (LEC) and medial entorhinal cortices (MEC) contribute to these projections, with the LEC targeting the distal part of CA1 and the MEC targeting the more proximal part(Igarashi et al., 2014). Finally, there is also a topological organization of connections between the dorso–ventral axis of the EC and dorso-ventral axis of the HF: In both LEC and the MEC, the more dorsal parts project to the dorsal hippocampus, and the more ventral parts project to the temporal/ventral hippocampus(M. Witter, 2012).

The neurons giving rise to these projections are spatially segregated, with layer II glutamatergic neurons (called stellate cells) projecting to the Dentate Gyrus (DG) and layer III glutamatergic neurons (called pyramidal cells) projecting directly to the CA1 and the subiculum (see Fig.1.1). These neurons are also molecularly distinct: layer II stellate cells are positive to reelin staining but not calbidin, whereas layer III pyramidal cells are reelin negative and calbidin positive. In addition, small clusters of pyramidal cells (reelin -, calbidin +) have been also described in the layer II ("island cells") and their projections pattern matches pyramidal cells from layer III (CA1 and subiculum)(Kitamura et al., 2014).

After leaving the entorhinal cortex, the fibers projecting to the hippocampal formation enter the underlying white matter in the angular bundle. They then cross the subiculum and either target the molecular layer of the subiculum and the CA-fields (temporoammonic path) or perforate the hippocampal fissure to enter the dentate gyrus. In addition to the ipsilateral connections, entorhinal cortex also sends crossed hippocampal projections to the contralateral hemisphere. In the mice, crossed projections from layer III pyramidal cell to CA1 represent a density of 20% of the ipsilateral one's (Groen, Miettinen, and Kadish, 2003).

The CA1 region of the hippocampus can be divided into four layers: the dense central one contains the excitatory glutamatergic pyramidal cells and is therefore called the stratum pyramidale. The more dorsal one, just below the alveus, is the stratum oriens which contains the pyramidal cells axons and basal dendrites and inhibitory interneurons cell bodies. Just below the stratum Pyramidale are the stratum radiatum and then the stratum lacunosum-moleculare containing the pyramidal apical dendrites and others subtypes of interneurons. Direct projections from EC layer III make synapses in the stratum lacunosum-moleculare (shown in dark blue in Fig.1.1), whereas inputs going to the DG will follow the classical trisynaptic route

[1] In the literature, the nomenclature can vary and the term "perforant path" can refer to either both tracts (subdivided in 'indirect' and 'direct perforant path') or only to the one going to the DG. For clarity, in this work we will restrict this term to this latter sense and used temporoammonic path for projection to CA1.

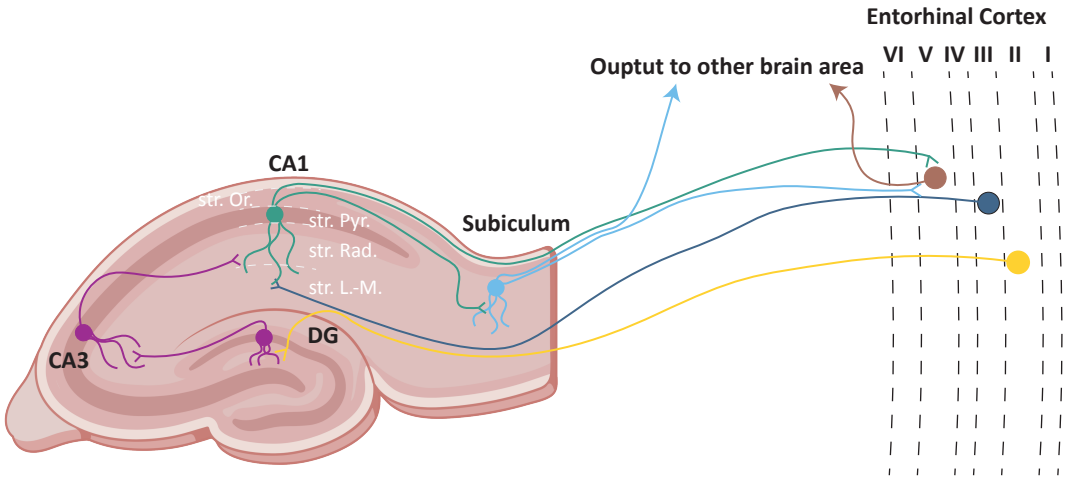

FIGURE 1.1: Main excitatory connections inside the hippocampal formation.

(DG -> CA3 -> CA1) through the Schaffer collaterals, arriving in the stratum radiatum(M. Witter, 2012) (purple in Fig.1.1).
These projections are largely glutamatergic and provides mainly excitatory inputs. However, some of these projections contact directly local interneurons, including PV-positive basket and chandelier cells, providing feed-forward inhibition(Kiss et al., 1996) (Fig.1.2a). Finally, some long-range interneurons projecting from the MEC to the stratum lacunosum-moleculare of CA1/CA3 and the stratum moleculare of DG have also been described (Melzer et al., 2012). These interneurons contact preferentially other interneurons, leading to a disinhibitory net effect of HF pyramidal cells.

The main outputs from the hippocampal formation are CA1 and subiculum projections that return to layer V of EC, with a less dense projection to layers II and III. Layer V neurons in turn are the main origin of EC projections to widespread cortical and sub-cortical regions in the forebrain. In additions to this standard unilateral pathway, smaller back-propagation projections have been described, such as the one between CA3 and the DG. Local collateral connections between pyramidal cells have also been reported within each region (Strien, Cappaert, and M. P. Witter, 2009). Finally, commissural projections to the contralateral hippocampus arise at every step of the path, with the main one being from CA3 pyramidal cells to the opposite CA1 stratum radiatum.

The highly circular organization of these excitatory connections leads to the possibility of recurrent excitatory loops. A recurrent excitatory loop occurs when there is a feedback loop between neurons in which the output of one neuron excites the input of another neuron, which in turn excites, directly or indirectly, the input of the first neuron. These loops are believed to be important for neuronal computation in the HF, but might generate 'runaway excitation' and explain the specific vulnerability of this structure to seizures(McCormick and Contreras, 2001).

1.1.5 Dysregulation of cortical inputs in TLE

A classic view of this circuit disruption in TLE is the "dentate gate theory": in physiological condition, the dentate gyrus acts as a "gate" that controls the flow of inputs reaching to the hippocampal formation and protects it from overexcitation (Heinemann et al., 1992; Lothman, Stringer, and Bertram, 1992). In persons with TLE, the gate function of the DG would breakdown, allowing too much input to flow into the hippocampus, leading to the possibility of uncontrolled excitatory loops which would develop into seizures (see figure 1.2b). This idea was first supported by in-vitro observations that DG granule cells have really high firing threshold, due to both intrinsic properties and strong feedforward / feedback inhibition, and act as a filter on EC inputs. Later, observations in rodent TLE model showed both a loss of DG inhibitory interneurons and an increase collateral excitatory synapses between granule cells ("mossy fiber sprouting"), resulting in hyperexcitable granule cells (W. Zhang, Huguenard, and Buckmaster, 2012; Sloviter, 1987).
However, these observations are purely correlative and rescuing some of them didn't result in any changes in seizure counts (Buckmaster and Lew, 2011).

An alternative option would be that, in TLE, the dentate gate be bypassed by an hyperactivation of the temporoamonic pathway. In a slice study, Wenzy and colleagues showed that entorhinal discharges propagate to CA1 through the temporoammonic path only in epileptic animals, due to a loss of feed-forward inhibition (Wozny et al., 2005). This findings were confirmed by a second group, showing an unchanged gating function of the DG but at >10fold increase in temporoammonic transmission in TLE mice (Ang, Carlson, and Coulter, 2006). This specific overactivation could then give rise to uncontrolled excitation looping between the entorhinal cortex and CA1 (see figure 1.2c).

Both these views are not mutually exclusive and a combination of the two could underlie epileptogenesis in TLE. Regardless of exactly which circuit is affected, the two main characteristics of acquired epileptogenesis at the circuit level are believed to be (1) a formation of new recurrent excitatory circuits and (2) a selective loss of GABAergic interneuron functions (Noebels et al., 2012).

1.1.6 Alteration of the GABA system in Epilepsy

γ-Aminobutyric acid (GABA) is the main inhibitory neurotransmitter is the mammalian brain. In physiological conditions, it exerts a powerful control on cell and network excitability. In particular, feedforward and feedback inhibition are necessary to maintain a dynamic balance of the excitation / inhibition (E/I) ratio in the cortex: an increase in activity of glutamatergic excitatory cells is matched with a mirror increase in GABAergic interneurons activity (Dehghani et al., 2016). This fast synaptic inhibition is mediated by the GABA-A receptor. The GABA-A receptor is a ligand-gated ion channel, selectively to chloride (Cl-). In presence of GABA, it opens and produces an inward chloride current, leading to hyperpolarization of the neuron under physiological condition(Chuang and Reddy, 2018).

Alteration of the GABAergic system has been long believed to be one of the main causes of epilepsy. Mutation in the GABA-A receptor is directly involved in some genetic cases of epilepsy(Baulac et al., 2001) and variant of the gene has also been linked to increase susceptibility to non-monogenic epilepsy(Skotte et al., 2022).

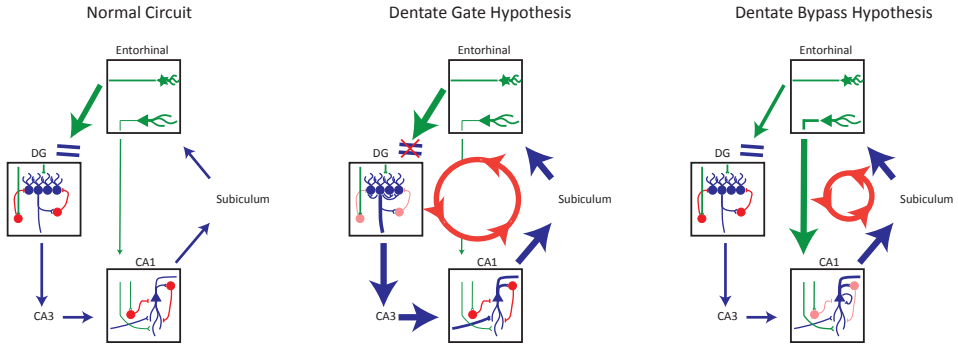

FIGURE 1.2: Dysregulation of cortical inputs in TLE

Schematic of two main theories of circuit dysregualtion in temporal lobe epilepsy. Entorhinal inputs are in green, excitatory connections in blue and GABAergic interneurons in red. The double horizontal line before the dentate gyrus represents its gating ability lost in the "dentate gate hypothesis". Red circles represent loops of runaway excitation.

As described previously, mesial temporal epilepsy in human is associated with cell death visible in histopathological studies. This cell loss touches both excitatory and inhibitory cells. The question of whether there is an overall decrease inhibition in the epileptic hippocampus is still debated (Wittner et al., 2005; Mathern et al., 1995; Dubanet et al., 2021). Compensatory mechanism and synaptic reorganization could explain the unchanged inhibition reported both at the level of both CA1 pyramidal cells and DG granule cells (Morin, Beaulieu, and Lacaille, 1998; L. Wittner et al., 2001; Wittner et al., 2005; K. Wu and Leung, 2001). However, specific subtypes of interneurons, such as the somatostatin or neuropeptide Y positive ones, show selective loss both in human tissue and experimental epilepsy (Lanerolle et al., 1989; Robbins et al., 1991; Sloviter, 1987; Mathern et al., 1995; Cossart et al., 2001). Somatostatin interneurons in CA1 (oriens-lacunosum-moleculare interneurons) and DG (Hilar-perforant-path-associated interneurons (HIPP cells)) are crucial for feedback inhibition and therefore their loss is congruent with a reduce ability to gate inputs from the entorhinal cortex (Figure1.2B-C). Using specific optogenetic activation of these cells, Hofmann and colleagues (Hofmann et al., 2016) confirmed a reduced ability to gate EC input in a TLE model.

Lastly, a few studies causally link interneurons involvement in epilepsy. Drexel and colleagues (Drexel et al., 2017) showed that selective ablation of PV positive interneurons in the hippocampal formation was enough to induce the occurrence of spontaneous seizures for several weeks as well as lowering the threshold for chemically induced seizures. On the other hand, the transplantation of GABAergic interneurons progenitors has been shown to be sufficient for a 84% reduction in seizure rate in epileptic mice.

Taken together, these results point toward an hippocampus still capable of maintaining E/I balance but which loses some of its key safeguards toward runaway excitation. It results in a structure vulnerable to any destabilizing inputs or changes in homeostasis. In that sense, observations at the microcircuit level correspond well with the idea that epilepsy represents a condition of increased fragility toward a

transition to seizure (Baud et al., 2020).

1.2 Ictogenesis

1.2.1 Pre and proictal state

The term ictogenesis describes the processes of transition from a non-seizure to a seizure state (also called ictal state). It encompasses the cases of both provoked seizure in a non-epileptic brain or spontaneous (unprovoked) seizure in epilepsy. In patient or animal with epilepsy, the non-ictal state is often referred as the interictal state, the state in between two seizures.

The pre-ictal state refers to a putative detectable state preceding the onset of spontaneous seizures. It would correspond to specific underlying brain dynamics that will result in a seizure. Several studies reported detectable changes in EEG or blood flow dynamics in a range going from seconds to hours before a seizure. After some promising results, methodological concerns, low replicability and lack of result in the few prospective study have questions the specificity of such measurements (Mormann et al., 2007). These studies are often purely phenomenological, applying complex linear or non-linear signal analysis methods in absence of physiological hypothesis. A better understanding of the biological correlates of these changes has been suggested to improve detection of pre-ictal states (Mormann et al., 2007).

Pre-ictal states are usually thought about in a deterministic view of seizure, corresponding to retrospectively defined periods containing a distinct phenomenon leading to a seizure (Baud et al., 2020). In contrast, pro-ictal state refers to a period of increase probability of seizure. Due to some intrinsic stochasticity, this increased risk could be realized in an actual seizure or not. This idea is supported by the long time observation that seizure occurrences are not completely random. They tend to occurs in clusters (Griffiths and Fox, 1938; Kudlacek et al., 2021; Williams et al., 2009), preferentially in a given brain state (Ng and Pavlova, 2013), and in given phases of the circadian time (Griffiths and Fox, 1938; Langdon-Down and Brain, 1929; Leguia et al., 2021; Quigg et al., 2000) or longer multidien cycles (Leguia et al., 2021; Karoly, Rao, et al., 2021). Additionally, several factors are well known to increase seizure risk such as medication non-compliance, alcohol, sleep deprivation or stress (Baud et al., 2020).
In the last decades, the development of chronic EEG recording device allowed the acquisition of long term EEG in epileptic patient. They confirmed the cycling nature of seizure risks and linked it to underlying cycle of cortical excitability, detectable as increase of interictal epileptiform discharges (Leguia et al., 2021; Maturana et al., 2020; Karoly, Rao, et al., 2021). The discovery of these biomarkers corroborates the probabilistic view of the pro-ictal states: seizures do not occur every time the brain is in a pro-ictal state, and the raise of cortical excitability precedes seizure, excluding the idea of an increase susceptibility caused by the seizure itself. The biological mechanisms underlying these fluctuations at different timescales remain to be understood. Here again, the GABA-A receptor could have a central role as it is directly modulated by steroid hormones which are known to cycle with both circadian and multidien periods (Maguire et al., 2005; Karoly, Rao, et al., 2021).

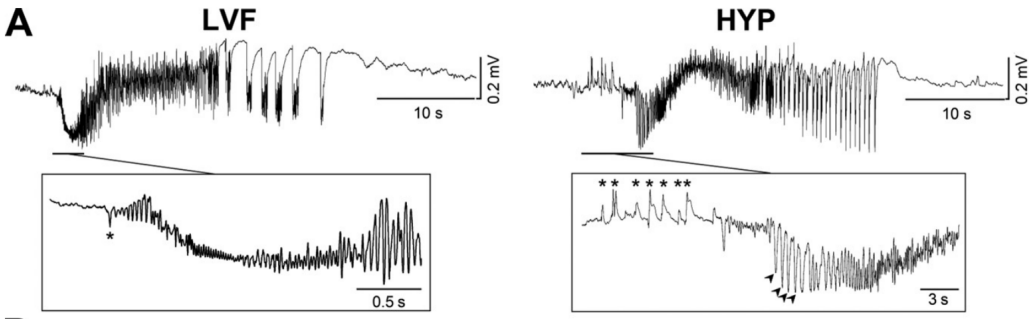

FIGURE 1.3: Example of seizure onsets with low voltage fast activity (left) and Hypersynchronous discharges (right). Adapted from Avoli et al., 2016

1.2.2 Clinical recording of seizure onset

Seizure can start with different electrographic patterns. Up to eight have been described in humans (Lagarde et al., 2019), but in the temporal lobe the distinction can usually be reduced to two main categories: seizures starting with slow hypersynchronous discharges or seizures starting with low voltage fast activity (LVFA) (Avoli et al., 2016). These EEG patterns correspond also to different patterns of neuronal activity. Hypersynchronous discharge are believed to reflect population spike of glutamatergic cells (Chvojka et al., 2021) whereas LVFA has been associated with an increase in activity of inhibitory interneurons (Truccolo, Ahmed, et al., 2014; Elahian et al., 2018). More recent studies revealed that neuronal firing pattern at seizure onset are highly heterogeneous with a majority of cells which do not seem to be involved at all (Lambrecq et al., 2017; Truccolo, J. A. Donoghue, et al., 2011; Weiss et al., 2016).

1.2.3 Mechanisms of Ictogenesis

Pyramidal cells are the main contributors of epileptic discharges and are also strongly involved during seizure. Their rhythmic stimulation is sufficient to induce seizure in non-epileptic animal (Osawa et al., 2013) in vivo. Increase glutamate release during seizure onset has been demonstrated in human (During and Spencer, 1993) and glutamate AMPA/NMDA receptors activity are necessary to seizure initiation in vitro (Huberfeld et al., 2011).

The contribution of inhibitory interneurons is more contested. GABAergic inhibition is crucial to prevent any brain from seizing. Blockade of the GABA-A receptors by pharmacological antagonist (pentylenetetrazol, picrotoxin, bicuculline) is a potent and easy way to induce seizures both in vivo and in vitro (Velíšková, Shakarjian, and Velíšek, 2017). The recent development of cell-type specific optogenetic and chemogenetic tools allow progress in understanding the role of interneurons in seizure generation and showed that GABAergic inhibition plays a key role in regulating seizure likelihood (Y. Wang, Liang, et al., 2018), threshold (Khoshkhoo, Vogt, and Sohal, 2017), duration (Krook-Magnuson, Armstrong, Oijala, et al., 2013) and severity (Y. Wang, Xu, et al., 2017; Krook-Magnuson, Armstrong, Bui, et al., 2015).

1.2.4 Optogenetic induction of seizures

Although repetitive electrical stimulations are known to induce seizures for decades, the development of optogenetics in animal research has afforded the long-needed cell-type and circuit specific probing of brain stability. Optogenetics refers to the combination of light sensitive ion-channels and optic stimulations to achieve fast excitation or inhibition of specific neurons (Tye and Deisseroth, 2012). If not specify otherwise, all of the cited studies below used either the original or a variant of the Channelrhodopsin-2 protein, leading to depolarization and excitation of the targeted neurons.

Optogenetics train stimulations in both neocortex, limbic cortices and the hippocampal formation have been shown to induce self-sustained seizures in non-epileptic rodents and in Drosophilia flies (Saras et al., 2017). Whereas the pioneer study of Osawa and colleagues used stimulations unspecific to neurons type, several other studies have since demonstrated that the specific activation of excitatory neurons is sufficient to induce seizures in rodents (see figure1.4).
The ability of interneurons stimulation to start a seizure is more controversial. Optogenetic interneurons activation can start seizures in presence of pro-convulsive drugs but does not seem to be sufficient in its absence (Assaf and Schiller, 2016; M. Chang et al., 2018; Lévesque, Chen, et al., 2019). In chronic epileptic model, activation of PV interneurons might rarely induce seizures above chance level but data are inconsistent (Lévesque, Chen, et al., 2019; Lévesque, S. Wang, et al., 2022). Rebound excitation after then end of stimulation and indirect increase synchronization of pyramidal cells could explain these findings, and it should be noted that chemogenetic activation of interneurons - which doesn't produce an artificial synchronization - systematically showed anti-seizure effect (Călin et al., 2018; Y. Wang, Liang, et al., 2018). Vasoactive intestinal peptide (VIP) expressing interneurons could be an exception as they inhibit mostly other interneurons resulting in a net disinhibitory effect. A previous study showed a potential pro-ictal role (Khoshkhoo, Vogt, and Sohal, 2017), but to my knowledge their activation has never been shown to be sufficient to induce seizure.

Seizure induction by pyramidal cells stimulation has been demonstrated in several brain regions (see figure 1.4), but the ictogenicity (i.d. the propensity to induce seizure) of the different structures is difficult to assess due to important differences in stimulation protocol. To my knowledge, only one study has tested the same protocol across different structures and observed a 10x increase in seizure probability in the hippocampus compared to neocortex(Osawa et al., 2013). The two other studies reporting optogenetic seizure induction in the neocortex required kindling protocols and didn't show seizure induction on the first stimulation train (Khoshkhoo, Vogt, and Sohal, 2017; Cela et al., 2019). These findings suggest an intrinsic higher ictogenicity in the hippocampal formation compared to neocortex. Interestingly, limbic cortices (entorhinal and piriform) seem to share high excitable proprieties with the hippocampal formation.
Finally, recent developments in the activity-dependent labeling technique could allow the study of seizure initiation with even more finesse. Lai and colleagues recently showed that optogenetic stimulation of a mixed population of seizure active, but not interictal active, neurons are actually more prone to induce generalized seizures compared to stimulation of just excitatory cells (Lai et al., 2022).

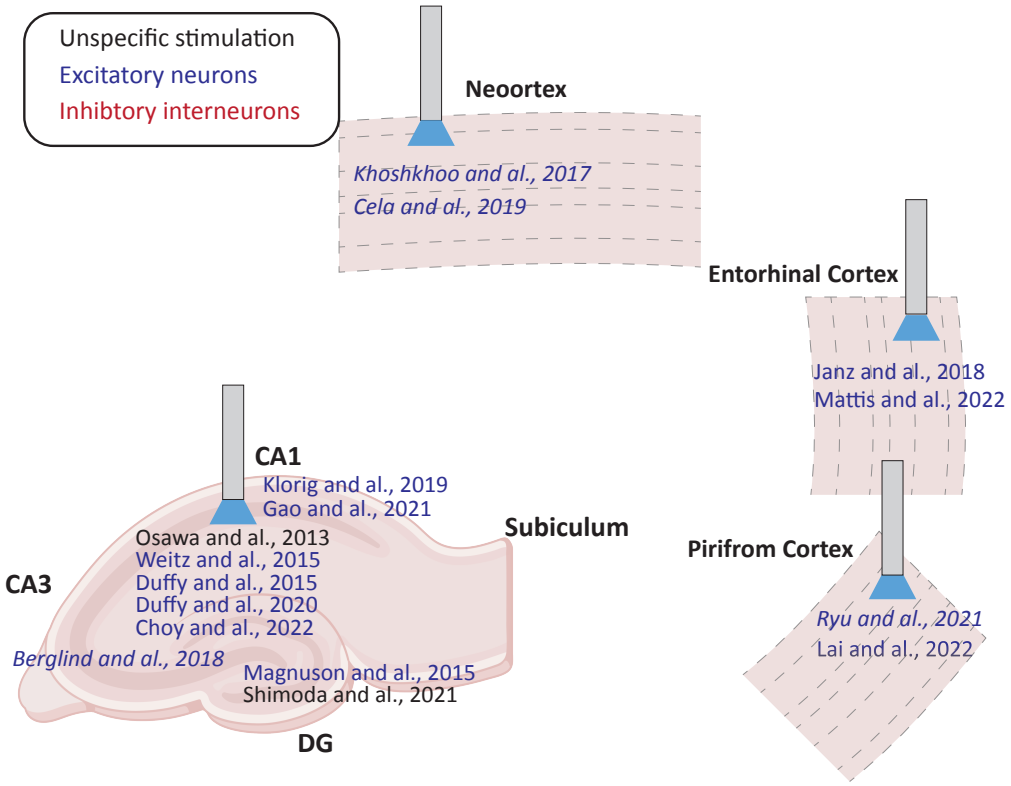

FIGURE 1.4: Optogenetic induction of seizures

Review of in vivo optogenetic seizure induction. PubMed research using the search: (optogenetics) AND (seizure). From the 230 results, 15 studies were then manually selected based on abstract and paper inspection. Inclusion criteria were: 1) in vivo studies 2) with data in non-epileptic animals and 3) in absence of pro-convulsive drugs. Seizure criteria were the same as in our study: sustained (>10s) electrographic ictal activity after the end of stimulation. Color-code indicated cell type stimulation, italic font indicate study where kindling protocols were necessary prior to the first induce seizure. With these criteria, no study showing seizure induction by interneurons stimulation has been found.

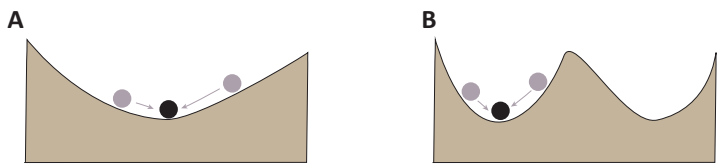

FIGURE 1.5: stability landscapes

Two different examples of stability landscapes, with respectively one (A) and two attractors (B).

1.3 Dynamical system

Cells, organisms, populations, ecosystems or even entire planets can be described as dynamical systems. They change through time and a limited set of differential equations is able to capture their behavior. While some of them follow slow and linear transformations, many present seemingly unpredictable abrupt shifts. Coral reefs collapse, volcanos erupt and brains seize. In dynamical system theory, these abrupt transformations are described as 'critical transitions' between alternative states and happen in highly complex and interconnected systems. In this section, I will briefly introduce a few concepts from dynamical system theory and then expand on their applications to epileptic seizures.

1.3.1 Alternative stable state

A state refers to one possible configuration of a system. Although a system can potentially adopt a myriad of different states, its internal dynamics usually push them toward a limited number of stable states (Scheffer, 2009). This can be visualized by the means of stability landscapes, where all the different possible states are represented on the x-axis and the slope of the landscape corresponds to the local rate of change (Fig.1.5). The system will then be visualized as a ball which will naturally settle for the lowest points of the landscape. Note that at the bottom of these valleys, the slope is 0, therefore the rate of change is null: it's at a stable equilibrium point. [2]

A given system, in a given set of conditions can possess one (Fig. 1.5A) or more (Fig.1.5B) stable equilibrium points. In the latter case, the system is described as multi-stable as it possesses more than one alternative stable state. As all the other states are attracted to them, stable equilibriums are commonly referred to as attractors and their basins of attraction - the valleys of the landscape - are defined as the set of states from which the system will spontaneously move toward the corresponding

[2] In a stability landscape, the hilltops also possess a rate of change of 0. For this reason, they are also referred to as equilibriums but have very different properties from the stable ones, as any perturbations will move the system away from them. Therefore they are referred to as unstable equilibriums and can act as 'separatrix', the delimitation between the basins of attraction of two stable attractors Fig.1.5B).

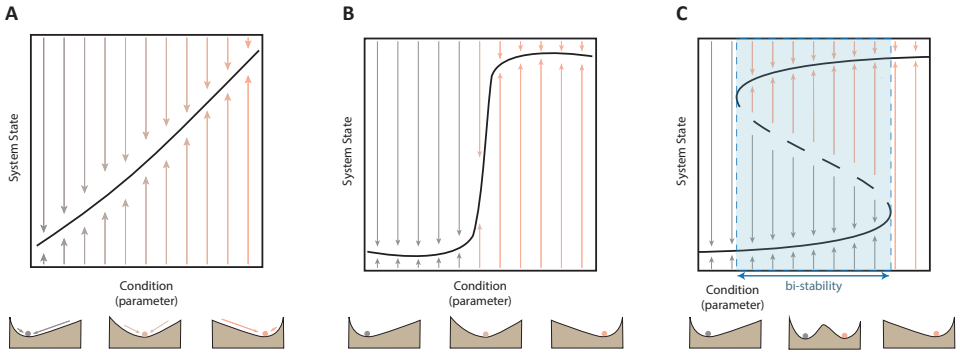

FIGURE 1.6: Fold and bifurcation diagram

Bifurcation diagrams representing the location of the stable equilibrium ('fixed point') against the parameter. The arrows correspond to the direction in which the system moves when it's not at equilibrium, and correspond to the slope of the landscape. The stability landscapes depicted below correspond to vertical slices of the bifurcation diagrams at different values of the control parameter. Modified from (Scheffer, 2009).

attractor. [3]

In reality, most dynamical systems are never completely stable but are constantly subject to internal and external perturbations. These perturbations can be visualized as small stochastic movements applied on the ball and correspond to transient changes in the system's variables.
Furthermore, the stability landscapes themself can also be modified through time. Conditions that modify the landscape are called control (or state) parameters; they evolve at a much slower timescale and are generally assumed to be constant during the time the system is observed (Scheffer, 2009). As they change the landscape, control parameters also modify the equilibrium states' locations. In some cases, the equilibrium state can change smoothly in response to variations of the control parameter (Fig.1.6 A). In other cases, it can be rather insensible to changes in a certain range of value, but changing drastically when a threshold is crossed (Fig.1.6 B). Finally, the curve can be folded, creating a range of parameter values where the system possesses more than one stable state (blue box in Fig.1.6 C). Note that in this latter case, the system's state is not only dependent on the parameter, but also on its starting position. For a given parameter value in the bi-stability range, the system could be attracted either to the upper or the lower part of the curve depending on its past trajectory. The middle part of the fold is separating the two basins of attraction and is therefore called the separatrix (dashed line in Fig.1.6 C). It acts as a threshold: any state under it will fall into the first attractor, and any state above it will fall toward the second one.

If this threshold is passed, the system shift from one attractor to the other is a process called a critical transition and it will result in an abrupt change in the system state (Fig. 1.7). Note that such a result can be obtained in two different ways: 1) by

[3]The attractors described here correspond to point attractors, which are the simplest cases. Other types such as limit cycle, torus or strange attractors also exist but will not be discussed here for the sake of simplicity.

applying on the system a perturbation large enough to pass the separatrix and fall into the second basin of attraction (in black) without changing the control parameter or 2) by modifying the parameter until the first attractor disappears, forcing the transition into the second attractor, even in the absence of perturbations. This special case, where the transition is accompanied by a qualitative change in the stability landscape, is called a catastrophic bifurcation because an equally small change in the control parameter leads to a radical change in the system's behavior.[4]
In real-world situations, both are generally combined: as the system gets closer to the bifurcation point, the distance to the separatrix gets smaller until even an infinitesimal perturbation can induce a critical transition (Scheffer, 2009).

In this context, the system's resilience can be defined as the maximum perturbations that can be taken without transitioning to an alternative state (Scheffer, 2009; Holling, 1973). On the bifurcation diagram, it corresponds to the distance to the separatrix and in the landscape schematic to the depth of the basin of attraction. [5]

The emergence of such a system with multiple attractors typically occurs in the coexistence of both negative and positive feedback mechanisms (Scheffer, 2009). Negative feedback will assure the stability of the state up to a certain point (i.e. the threshold), but when it is passed, a positive runaway process will push it into a completely different state. Brain circuits, such as the hippocampal one described in the section 1.1.4, possess both mechanisms and therefore are good candidates for critical transition. In neuroscience, critical transitions have been proposed to govern spiking in neurons (Izhikevich, 2007), sleep-wake cycle and onset of depressive state (Van De Leemput et al., 2014; M. Zhang, Riddle, and Frohlich, 2022) but their most natural application are onset and termination of epileptic seizures which present prototypical rapid shift between two alternative state, easily observable in the EEG.

1.3.2 Dynamical model of seizures

A simple dynamical model of seizure transition can be implanted as a slow-fast process, where the interaction of two variables running at two different time-scales is sufficient to give rise to a fold bifurcation as described above (see figure 1.6). In such a model, the fast variable represents the mean neuronal firing and the slow one represents the gradual change in cortical excitability. As it is much slower than the first variable, the excitability can act as to the control parameter of the system and is set in such a manner that it is increasing when the system is in the non-ictal state (first attractor) but decreasing during ictal state (seizure, second attractor), giving rise to periodic alternations between the two states which resemble in vitro epilepsy model (red arrows in Fig.1.8) (W. C. Chang et al., 2018). Despite its simplicity, such a

[4] This particular case of bifurcation is referred to as a fold or more commonly a saddle-node bifurcation. The node refers to the stable equilibrium (bottom of the valley) and the saddle to the unstable equilibrium (hilltop). On this particular point (bifurcation point), both coalesce, leading to their mutual destruction. Other types of bifurcation exist but they will not be discussed here.

[5] At least two different definitions of resilience coexist in the dynamical system framework. We used the one after Scheffer and Holling's work (Scheffer, 2009; Holling, 1973). It is also the one previously applied to the context of epilepsy by Chang and colleagues. An alternative definition, which is not specific to critical transition, would be "the speed with which the system recovers upon perturbations". As discussed below, these two phenomena - resilience to transition and rate of change - are well correlated in most models but remain different (Scheffer, 2009). In this work, we will restrict the term resilience to this first usage, the resilience to critical transition, and use the term stability to refer to the rate of change.

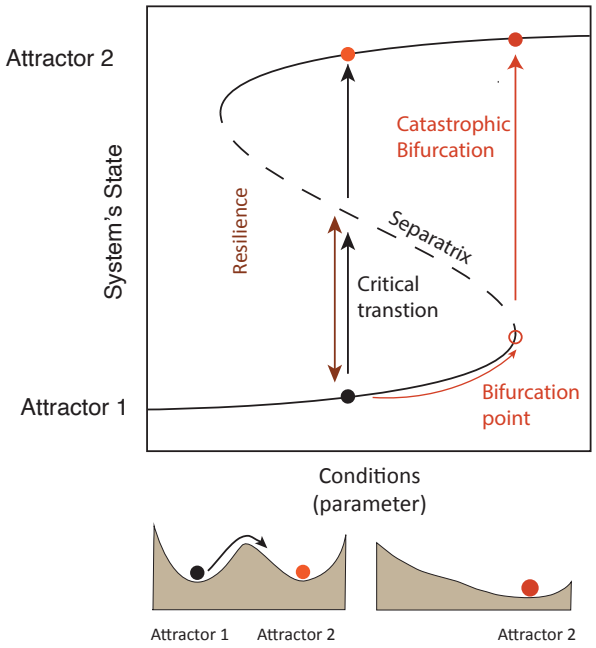

FIGURE 1.7: Two different path to critical transition

Bifurcation diagram and corresponding stability landscape representing respectively 1) a large perturbation which overcomes the system resilience and results in a critical transition toward an alternative attractor (black arrows) 2) a shift in the control parameter until the bifurcation point, resulting in a catastrophic bifurcation.

model can already capture interesting aspects of seizure dynamics such as the state dependent effect of external stimulation (W. C. Chang et al., 2018).

Importantly and in contrast to most previous seizure models, it does not require parameter modification to give rise to a seizure. Due to the intrinsic bi-stability of the system, even at a fixed excitability, strong perturbations can pass the threshold and change the state of the system (black arrows in Fig1.8) (W. C. Chang et al., 2018).

Modeling seizure as an alternative state in a multi-stable system has also been replicated in more sophisticated models. Bio-realistic models try to replicate the complexity of biological systems and typically focus on the interactions of individual neurons, while phenomenological models aim at capturing the global dynamics and behavior of a system and abstract away from the detailed mechanisms.
Using a bio-realistic cortical model, Fröhlich and colleagues (Fröhlich, Sejnowski, and Bazhenov, 2010) described seizures as a network transition into coexisting alternative states, which could be induced by transient perturbations even in absence of parameter modification. The proposed mechanism was a positive feedback between neural activity and extracellular potassium accumulation, which, when a certain threshold value is passed, overcomes the natural feedback inhibition.

In order to faithfully describe the complex dynamics before, during and after seizures, more advanced phenomenological models have also been proposed. One of the most widely used is the Epileptor. It is a well established seizure model capable of simulating a vast range of epileptic activity such as interictal spikes,

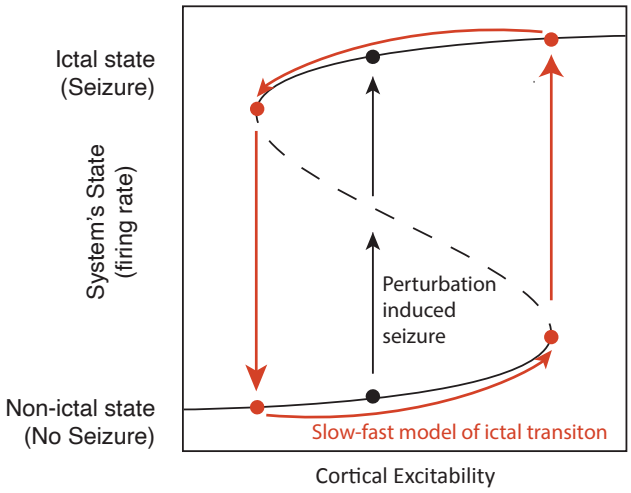

FIGURE 1.8: Slow-fast process

Schematic of the slow-fast process model, giving rise to a fold bifurcation and alternating between two stable states: no seizure and seizure. Adapted from (W. C. Chang et al., 2018)

spreading depression, refractory status epilepticus and both induced and spontaneous seizures.
This model could have a direct clinical application as recent studies suggest that it can be combined with structural imaging to produce individualized patient-specific virtual brain models (Proix, Bartolomei, et al., 2017). This would allow testing of clinical hypotheses in silico and a multi-center clinical trial is currently ongoing (EPINOV).

Intuitively, Epileptor can be seen as an extension in five dimensions of the slow-fast process (Jirsa et al., 2014), and contains multiple bifurcation respectively governing the epileptogenicity (system capacity to produce spontaneous seizures), the onset of epileptic spike as well as the onset and termination of seizure per se (Jirsa et al., 2014; El Houssaini et al., 2015; Proix, Jirsa, et al., 2018). Importantly, the bifurcation governing seizure transition is of the same type as the one described above (a fold / saddle-node bifurcation), and the core of the model is based on the conceptualization of seizures as critical transitions between two alternative stable states.

As described above, modeling work proposed that epilepsy can be conceptualized as a chronic loss of resilience in the context of a bi-stable system. Seizures then emerge by the alignment of a transient loss of resilience with some internal stochastic events. From a clinical perspective, these transient losses of resilience would correspond to the pro-ictal states described in the section 1.2.1 (Baud et al., 2020; Karoly, Rao, et al., 2021). In addition, the fundamental bi-stable nature of the cortex matches the clinical observation that seizures can occur in any brain, whether as a result of a sudden disruption in homeostasis or due to prolonged external stimulation (S.

Kalitzin et al., 2005; Lisanby, 2007; Zangaladze et al., 2008).

1.3.3 Anticipating ictal transition

The hope of describing seizure onsets as critical transitions resides in being eventually able to anticipate and ultimately control them. However, observing the bifurcation diagram (Fig1.7), we can observe that changes in the system's resilience (x-axis) are hard to capture as they correspond to very slight changes in the system state (y-axis) until the bifurcation point. Nevertheless, both mathematical (Kuehn, 2011), computational (Dakos et al., 2012) and empirical evidence (Scheffer, Carpenter, et al., 2012) from various fields show that a subset of these transitions are accompanied by the presence of 'warning' or 'precursor' signs, preceding the critical transition. When the system approaches the bifurcation, it displays a slower recovery rate from small perturbations, measurable in a given time series describing the system state. They can be observed in response to imposed perturbations, or indirectly through passive recordings. In the latter case, an increased impact of stochastic events can be seen as an increase of the signal variance and skewness as well as their longer recovery time as an increased autocorrelation and a decrease in the signal frequency composition.
In the case of epilepsy, several studies in silico suggested that such precursor signs could be detected in the EEG signal. They also suggested the superiority of active probing versus passive metrics (Suffczynski et al., 2008; Carvalho et al., 2021).

1.3.4 In vitro evidence for precursors signs

Some of the most convincing evidence for seizure precursors signs come from in vitro seizure models. In these models, seizures happen frequently and in a very deterministic way, as modeled by the slow-fast process (Fig1.8), allowing to effectively capture changes in the signal across many events.
Using hippocampal slices in the high potassium model, Chang and colleagues (W. C. Chang et al., 2018) showed a progressive increase of both active (response to stimulation) and passive (increase variance, autocorrelation, spatial correlation and slowing in the signal frequency composition) markers. Some of these markers (variance and frequency composition) present mostly an increase in the last seconds before the seizure, when the system is putatively in the vicinity of the bifurcation. In contrast, responses to stimulation presented a steady increase in between two seizures, suggesting that active probing might capture changes in resilience at distance from the bifurcation.
Using two different in vitro models (low magnesium (Mg2+) and the K+ channel blocker 4-aminopyridine (4AP)), Graham and colleagues (Graham et al., 2022) also showed an increased response to perturbations in the seconds before seizure. However, they described only small changes at the time of the pharmacological manipulation (Mg 2+ wash-out), and then an abrupt "all-or-nothing" increase in the seconds before the seizure. This could indicate a rapid shift in the underlying resilience in opposition to the gradual drift described by the slow-fast model.

1.3.5 In Vivo evidence

EEG recordings from patients have also been studied to detect these predicted precursor signs for spontaneous seizures. The first approach was to examine the EEG

signal preceding the seizures, but as for the other pre-ictal makers discussed before, most of the patients didn't display any specific increases (Milanowski and Suffczynski, 2016; W. C. Chang et al., 2018; Wilkat, Rings, and Lehnertz, 2019).
These differences with in vitro and in silico findings could be explained by several factors: 1) the shift toward the bifurcation could happen at a timescale not captured by these analyses (either in the range of milliseconds or several hours); 2) in vivo brain's dynamics could be dominated by other effects, hiding these subtle changes which are known to be really sensitive to noise (Kuehn, 2011); 3) the loss of resilience may be confined to a specific brain area and not detectable on EEG recordings from the scalp or sparse intracranial electrode; 4) retrospective methods may not be effective in capturing changes due to the unpredictable nature of seizures. Some seizures may be triggered by strong internal perturbations that occur outside of times of low resilience, while other temporary reductions in resilience may not lead to seizures.

Tacking advantages of multi-site chronic recordings, Maturana and colleagues (Maturana et al., 2020) were able to circumvent some of these limitations by investigating precursor signs on a longer timescale (month to years) and capturing their probabilistic relationship with seizure occurrences. They showed that, in the majority of the patients, variance and autocorrelation vary in a cyclical manner on a long time-scale (several hours to several days), and that seizures tend to happen on the rising phase of these cycles. Based on these markers, they were able to produce reasonably accurate probabilistic seizure forecasting. Interestingly, the cycles correlated well with previously described cycles in the interictal epileptiform activity (IEA) ((Leguia et al., 2021)), suggesting the IEA itself can be a marker of the distance toward the bifurcation.
In rodents, Chang and colleagues report an increase in IEA events in between seizure clusters as well as changes in the IEA features (line-length, duration, spatial correlation).

As suggested by in silico and in vitro studies, active perturbation in vivo could improve detection of latent shift in cortical stability. Two studies provided a 'proof of principle' (S. Kalitzin et al., 2005; S. N. Kalitzin, Velis, and Lopes da Silva, 2010; Freestone et al., 2011) but to my knowledge no study investigated it systematically, either in patients or in rodent models of epilepsy.

1.3.6 Prediction and intervention

In situations of major transitions such as seizures, the causative event is often assumed to be in close proximity, which can lead to the formulation of false causal relationships (W. C. Chang et al., 2018; Scheffer, 2009). The notions of dynamical systems developed in this section imply that seizures occurrences may rather stem from a slow alteration in the resilience to seizures.
Implementation of real-time estimation of cortical excitability based on markers of critical transition, both active and passive, has the potential of improving current seizure prediction models and facilitating the development of dynamically targeted interventions. Cortical stimulations have been shown to either prevent or start seizures depending on the underlying dynamics (W. C. Chang et al., 2018). Measuring adequately these dynamics seems therefore a prerequisite for the developments of closed-loop therapeutic devices (Vonck and Boon, 2015).
In addition, in most dynamical systems, increasing the resilience is easier and much

more potent than the suppression of stochastic perturbations (Scheffer, 2009). A better understanding of the biological determinants that govern seizure resilience and their fluctuations could help develop new pharmacological intervention. However, current research on the dynamics of cortical stability and resilience has primarily focused on EEG signal analysis only, with a lack of connections to underlying biological mechanisms.

Aims and hypothesis

2.1 Aims and hypothesis

Dynamical system theory provides scientific explanations and predictive power on natural phenomena by abstracting dynamic features from their complex system-level behavior (Ross, 2014). A correct modelisation requires a precise understanding of these dynamics. In the case of epileptic seizure, a profound understanding of their dynamical nature is still lacking. Further, the available data are intrinsically limited, as most of the current work relies either on passive in vivo recordings in patients (Jirsa et al., 2014; Saggio et al., 2020; W. C. Chang et al., 2018) or on in-vitro models kept in artificial milieu (Jirsa et al., 2014; Graham et al., 2022; W. C. Chang et al., 2018). Moreover, this line of work made assumptions on latent features, such as cortical excitability and/or seizure resilience, which are presumably key, but has been assumed through proxies and rarely directly measured experimentally. Thus, a thorough demonstration of presumed dynamical mechanisms making use of active probing of the involved circuits in a behaving animal is lacking at the present stage.

The overall goal of this thesis is to develop a comprehensive understanding of cortical stability and seizure resilience with a triple approach, including computational modeling (in collaboration with Dr. Proix), in vivo experiments in mice and clinical investigations in patients with epilepsy (in collaboration with Mrs. Van Maren).

Our working hypothesis is that the limbic circuit operates as a bi-stable dynamics system, which can be triggered into a seizure state at any given time. Furthermore, as suggested by recent modeling work, that seizure resilience is directly dependent on the underlying cortical excitability and can be precisely measured in vivo or inferred from evoked cortical activity.

To test this hypothesis, our first aim was to develop a triple model (computational, experimental and clinical) of 'on demand' induced seizures that can be used to quantify and model seizure resilience. To achieve this, we used a modified version of the Epileptor model, circuit and cell type specific optogenetic stimulations in non-epileptic mice and intracranial electrical stimulation in patients with epilepsy.

The second aim of this thesis is to characterize how seizure resilience changes as a function of cortical excitability across all three paradigms. In the dynamical model, this will correspond to changes in the control parameter, and in vivo, we will adjust cortical excitability using different doses of both agonist and antagonist of the

GABA-A receptor.

The third aim of this thesis is to test whether changes in seizure resilience can be inferred from measurable changes in cortical activity. We will directly correlate responses to small perturbations with measurable changes in seizure resilience and use a machine-learning approach to validate and compare both active and passive proposed markers of seizure resilience.

2.2 Contributions

The following section of this thesis will present the results of a collective effort to tackle these questions in a translational manner. The mice experiments (Fig. 3.2C, 3.3C, 3.4A-E, 3.5, 3.6C-L as well as all supplementary figures (7-16) are the core of my PhD work. They were designed by Professor Maxime Baud and myself with invaluable inputs from Professor Antoine Adamanditis on optogenetic manipulations. Krsitina Slabeva, another PhD candidate in the lab, initially contributed to set up the optogenetics 'seizure on demand' model. Once in place, I alone performed all the data collection and analysis.
For the human investigation (Fig. 3.2D, 3.3D and 3.4H-I), Ellen Van Maren, Maxime Baud and myself designed the stimulation protocol based on my preliminary data in mice. Ellen, Maxime and Dr. Juan Anso set up the hardware and software for concomitant intracranial stimulation and recording. Ellen performed all the human data acquisition, preprocessing, and most of the data analysis, which I complemented for consistency with the animal work. Finally, a large clinical team was involved including Mr. Markus Fuchs, Professor Claudio Pollo, Professor Kaspar Schindler and Professor Werner Z'Graggen.
The dynamical modeling part (Fig. 3.2A-B, 3.3A-B and 3.6B) was done by Dr. Timothée Proix, based on weekly discussion between him, Maxime and myself. I generated the final figures and wrote the manuscript under Maxime's supervision, with occasional inputs from Timothée and Ellen. The work presented here will be the basis of a forthcoming publication where I will be the first author. A preprint was already published in February 2021 but contained only a marginal part of these data (<10%, https://doi.org/10.1101/2021.02.18.431873).

Methods

3.1 Animals

All mice experiments were conducted in accordance with protocols approved by the veterinary office of the Canton of Bern, Switzerland (license no. BE 19/18 and BE 51/2022).
A total of 32 C57BL/6JRj male mice aged between 2 and 4 months old were used. Before surgery, mice were housed in groups in ventilated cages, with food and water ad libitum under controlled conditions (12:12h light-dark cycle, constant temperature 22°C and humidity 30-50%).

3.1.1 Virus targeting

Mice were anesthetized with Isoflurane (5% in ambient air for induction and 1.5-2% for maintenance, Abbvie, Switzerland). They were then placed in a digital stereotaxic frame (David Kopf Instrument, USA) and body temperature was kept at 37°C using a rectal probe and closed-loop heating system (Harvard Apparatus, USA). Eyes were protected with ointment (Bepanthen, Bayer, Germany) and analgesia was given as subcutaneous injection of Meloxicam 2mg/kg (Boehringer Ingelheim, Switzerland). Scalp fur was removed using a depilatory cream (Weleda, Switzerland) and the scalp was disinfected with Betadine (Mundipharma, Switzerland). After skin opening, the periosteum was scratched, and bur holes were drilled at the targeted coordinates. To express Channelrhodopsin (Ch2R) specifically in pyramidal cells projecting from the medial entorhinal cortex (MEC) to the CA1 region of the hippocampus ($PC_{MEC->CA1}$), we used an intersectional strategy with two recombinant adeno-associated viruses (AAV) injected in two different target brain regions, such that only neurons transfected with both viruses would express ChR2 (Supp. Fig. 8 A-C) : 1) 450nl of a retrograde virus containing the opsin on inverted cassette (AAVretro-EIFa-DIO-Ch2R(H134R)-eYFP from UNC Vector Core, USA) were injected into CA1 right (coordinates: antero-posterior (AP) -2.0mm from Bregma, medio-lateral +1.3mm from Bregma and dorso-ventral -1.6mm from the skull level). 2) 450nl of an anterograde virus containing the Cre recombinase under CamKII promoter to target pyramidal cells (AAV1-CamKII-Cre-SV40, Addgene, USA) were injected into the right MEC (+3.2mm laterally from Lambda along the lambdoid suture and DV -2.5mm from skull level). Viruses were loaded on a 500nl Hamilton syringe (Model 7000.5, Hamilton Company, USA) and injected using a micro-infusion pump (Pump 11 Elite Nanomite, Harvard Apparatus, USA) at the rate of 50nl/min, with 10 min pause before syringe retraction. The skin incision was then sutured and animals were put back in their home-cage. They were monitored and received analgesia (Meloxicam 2mg/kg) for 3 days.

Three other virus constructs were used for different kinds of control (see Supp. Fig. 9, 10, 11A): 1) To control that Channelrhodopsin was necessary to induce seizure, two mice received the same two viruses at the same coordinates, but without the Channelrhodopsin (AAV1-CamKII-Cre-SV40 and AAVretro-EIFa-DIO-eYFP (8). 2) To control that seizure could also be induced by direct stimulation of CA1 pyramidal cells, four mice received an anterograde virus in CA1 (450nl of AAV2-EIFa-DIO-Ch2R(H134R)-eYFP)(9). 3) To control if seizure could also be induced by stimulation of inhibitory cells, four PV-ires-Cre mice received a cre-dependent anterograde virus in CA1 (AAVdj-EIFa-DIO-Cheta-eYFP)(10). The cheta ospin was chosen to allow stimulation at higher frequencies (80 and 100Hz) in fast spiking neurons. Details of every animal used can be found in the supplementary tables 2 (18) and 3 (19) .

3.1.2 Mice electrodes implantation

Three weeks after viral injection, mice were implanted with intracranial electrodes for multisite intracranial EEG recordings. . To obtain faster recovery after long surgeries, a reversible mix (10 l/g) was used for anesthesia, with the following composition: 10% Midazolam 5mg/ml (Sintetica, Switzerland), 2% Medetomidine 1mg/ml (Graeub AG, Switzerland), 10% Fentanyl 0.05mg/ml (Sintetica, Switzerland) and 78% NaCl 0.9%. Otherwise, surgery was carried out as described above through the same incision. Bilateral frontal skull EEG screws (1.9mm, Paul Korth GmbH, Switzerland) were soldered to a stainless-steel cable (W3 wire, USA) and inserted at coordinates -1.0AP, ±2.0ML. Reference and ground EEG screws were inserted above the cerebellum and the olfactory bulb, respectively. Intraparenchymal depth electrodes, made of tungsten wires (76.2m, model 796000, A-M System, USA), were pinned in an 18-EIB board (Neuralynx, USA) and inserted one by one and glued in place at the following coordinates: MEC on the lambdoid suture, ±3.2ML, - 2.5DV; CA1 -2.0AP, ±1.3ML, -1.6DV; DG -2.0AP, ±1.3ML, -2.3DV; CA3 -2.0AP, ±2.2ML, -2.2DV and Subiculum -3.2APm, ±1.6ML and -1.8DV (All DV coordinates are calculate from skull level). The right entorhinal electrode was glued to a homemade optical fiber implant (200m, 0.39 NA Core Multimode Optical Fiber, FT200EMT inserted and glued into CFLC128 ceramic ferrules, Thorlabs, USA) (Sup. Fig. 3E). In three mice, linear 16 channels silicon probe (A1x16-3mm-100-177, NeuroNexus, USA) were implanted in the right hippocampus, instead of the CA1/DG R homemade electrodes.

Mice were woken up with a mix for reversing anesthesia (10 l/g), composed of 5% Atipamezole 5mg/ml (Graeub AG, Switzerland), 2% Naloxone 4mg/ml (OrPha Swiss GmbH, Switzerland), 50% Flumazenil 0.1mg/ml (Anexate, Roche, Switzerland) and 43% NaCl. After the surgery, mice were monitored in their home-cage for a week and received analgesia (Meloxicam 2mg/kg) for three days. During a brief isoflurane anesthesia, the mice were connected to the EEG recording system, and habituated for another week to freely move with the cables fixed to a moving hook.

3.1.3 EEG Data Acquisition

The implanted EIB board was connected to either a HS-16-CNR-MDR50 Neuralynx or a RHD 16-channel Intan (Intan Technologies, USA) headstage, and the optic fiber

to a home-made optical patch cord (optic fiber FT200EMT glue in a FC/PC connector, 30230G3, Thorlabs, USA). EEG, EMG and LFP signals were amplified and digitized at 2KHz using either the Digital Lynx SX data acquisition system (Neuralynx, USA) or the Intan RHD USB interface board (Intan, USA).

3.1.4 Optogenetic stimulation

For opto-stimulation, a patch-cord was connected to a 473nm blue laser (Cobolt 06-MLD, HÜBNER Photonics GmbH, Germany) controlled by a Matlab (Mathworks, USA) script through a pulse train generator (PulsePal 2, Sanworks, USA). The digital trigger signal was recorded along with the electrophysiology data. The analogue modulation mode of the lasers was used to stimulate with different light intensities by employing varying input voltages. Maximum intensity was calculated to be around 30mW at the tip of the optic fiber. The reliability of the laser outputs and modulation was ensured previously by recording laser power for each of the stimulation protocols with a photodiode (PM100A, Thorlabs) connected to the Digital Lynx with a Universal Signal Mouse board (Neuralynx Inc., USA).

3.1.5 Scoring seizure severity

Video of the seizures were recorded using zenithal webcams (HD Pro C920, Logitech, Switzerland) and the OBS Studio software (https://obsproject.com/). Video recordings of the induced seizures were scored offline and blinded to pharmacological condition, using a modified Racine scale as follow: 0: no visible change, 1: behavioral arrest, 2: clonus without rearing, 3: clonus with rearing, 4: clonus and falling on side, 5: wild jumping, 6: death.

3.1.6 GABAergic agonists and antagonists

Diazepam (Valium 10mg/2ml i.m./i.v., Roche, Switzerland) and Pentylenetetrazole (PTZ, P6500, Sigma-Aldrich, USA) were diluted in NaCl 0.9% in order to inject a constant volume (2l/g i.p.) across conditions. Diazepam dose was set at 5mg/kg if not specified otherwise. Sub-threshold PTZ dose was set at 20mg/kg. If this dose led to an unprovoked seizure, data from this protocol were discarded and the next dose for this animal was reduced by 75%.
In some animals, Picrotoxin (PTX, P1675, Sigma-Aldrich, USA), another GABA antagonist, was also used at a sub-threshold dose of 0.75mg/kg and diluted in DMSO.

3.1.7 Recording sessions

Each of the recording blocks included three 90-min afternoon sessions (second half of the light phase) with three different pharmacological conditions (Diazepam (BZD), Sub-threshold Pentylenetetrazole (PTZ) and NaCl) (Supp. Fig.7), in a random order at intervals of 48-72h to allow for drug elimination and avoid excessive kindling (i.e. the tendency for seizures to become more severe over time). To avoid changes in cortical excitability related to vigilance stages, mice were kept awake by gentle poking.

Each session contained first a 10min baseline recording, and then 3 different stimulation protocols preceded each time by an i.p. injection of the same drug (BZD, PTZ or NaCl) 3min before (See Sup. Fig. 3A). The protocols were, in a fixed order:
1) 270 paired pulses (PP) at varying inter-pulse intervals (6-2000ms) over 45 min,

with three different intensities (1/3 max intensity, 2/3 max intensity or max intensity) for the first ('conditioning') pulse and a fixed intensity (2/3 max) for the second ('probing') pulse.
2) 60 single pulses (SP) at 12 different intensities, linearly distributed in the range of the laser analogue modulation (0.45V to 1V), over 45min. 10 additional low intensities (analogue modulation 0.45V-0.55V) were used to determine the minimal intensity necessary to obtain a detectable response (rheobase) in the EEG.
3) Train stimulations (20 Hz) of increasing duration (0.25 to 30sec, presented at one-minute intervals) for seizure induction until a seizure occurred (Sup. Fig. 3A).Seizures were visually detected by a trained experimenter as sustained (>10s) ictal activity continuing after the end of the stimulation. All animals (non-epileptic, n=17) showed seizures from the first session.

All pulse simulations consisted of 3ms light pulses. During their respective protocol, SP and PP were present in a random order every 8-12 seconds. Second and third i.p. injections in-between protocol were necessary due to the fast PTZ elimination 1,2.These additional injections were respectively, for PTZ and Dz, of 50% and 10% of the initial doses due to differences in elimination rate (Yonekawa, Kupferberg, and Woodbury, 1980; Yoong et al., 1986).

Seizure induction protocol at different stimulation frequencies (4, 7, 10, 20, 40Hz) were also tested on 5 animals. Each recording block consisted of three sessions at a given frequency, corresponding to the three different pharmacological conditions randomized. Some animals (n=8) underwent a similar experiment to test an eventual dose-response effect of Diazepam. The experimental protocol was the same (PP, SP and seizure induction) but the block consisted of a control condition (NaCl) and four different doses of Diazepam (1, 3, 5 and 7mg/kg) in a randomized order. Finally, 5 mice also undergo the same protocol with a subthreshold dose of another GABA-A antagonist, the picrotoxin 0.75mg/kg.

3.1.8 PTZ chemically-induced seizures

For this experiment, recording sessions were planned as follow: 10min baseline recording, followed by a first protocol of stimulation with only single pulse (20 pulses at maximum intensities, every 8-12 seconds) to probe cortical excitability before PTZ injection (baseline), and then a second similar 1h SP protocol following after an i.p. injection of a supra-threshold PTZ dose (30-40mg/kg). Seizures were detected off-line by a trained experimenter as sustained (>5s) ictal activity. Control animals (receiving supra-threshold PTZ but not single pulse) underwent the same protocol but without receiving any light.

3.1.9 Mice histology

Animals were euthanized after the end of the recording blocks. They were anesthetized with 250mg/kg Pentobarbital (Esconarkon 1:20, Streuli Pharma AG, Switzerland) and transcardially perfused first with cold NaCl 0.9% and then with 4% formaldehyde for 5min each. Extracted brains were post-fixed in 4% formaldehyde (Grogg Chemie, Switzerland) for 24h, then transferred in sucrose for 48h before being flash-freezed with -80° methylbutane. Brains were then sliced along the sagittal axes (40µm slices) on a cryostat (Hyrax C 25, Zeiss, Germany), and collected in PBS. For immunostaining against the GFP and NeuN proteins, slices were first incubated

1h in a blocking solution composed of PBST and 4% bovine serum albumin. Free-floating slices were then incubated 48h at 4° with a mix of anti-GFP (1:5000, Ref. A10262, Invitrogen, USA) and anti-NeuN (1:1000, Ref. 2931160, Millipore, USA). They were then rinsed 3x10min with PBS containing 0.1% Triton and incubated 1h at room temperature with two secondary antibodies of different colors, AlexaFluor 488 (1:500 Abacam, ab96947) for the anti-GFP primary antibody and AlexaFluor 555 (1:500, Ref. A21422, Invitrogen, USA) for the anti-NeuN primary antibody. Finally, slices were washed again 3 x 10 minutes and mounted on glass slides. Images were obtained using an epifluorescence microscope (Olympus BX 51, Olympus Corporation, JP) at different magnifications (4-10x).

3.2 Human subjects

Human data were collected from 7 patients with intractable epilepsy undergoing invasive presurgical evaluation with stereo-EEG at Inselspital, Bern. Electrodes were implanted as necessary for seizure localization purposes and without relationship to the present research study. These intracranial EEG electrodes enable direct cortex stimulations with pulses of electrical current to probe cortical excitability in the form of cortico-cortical evoked potentials (CCEPs), hereafter termed cortical responses for simplicity. The patients provided informed consent for participation and this study was approved by the ethics committee of the Canton Bern (ID 2018-01387).

3.2.1 Data acquisition

Each intracerebral electrode (DIXI medical, Microdeep®, France) consists of 8-18 platinum channels with a diameter of 0.8 mm and a length of 2 mm with varying spacing. The MRI and postsurgical CT were co-registered using the Lead-DBS software (www.lead-dbs.org) to determine the exact location of each electrode contact. A neurologist (MOB) labeled the channels based on their anatomical locations. The intracranial EEG recording was amplified using a 128 channel Neuralynx ATLAS system (Neuralynx Inc., USA), with a sampling frequency of 2KHz, a voltage range of ± 2000µV along with a digital trigger signal to identify stimulation onsets.

3.2.2 Cortical electrical stimulations

A neurostimulator (ISIS Stimulator, Inomed Medizintechnik GmbH, Germany) was used to deliver a single or a train of bipolar (neighboring contacts) stimulations at varying intensity and with a square-biphasic pulse of total width 1ms. The same stimulation protocol was repeated before and after the intravenous administration of clonazepam 0.5-1 mg, a GABA-A receptor agonist of the benzodiazepine class (BZD), given for medical reasons (end of clinical work-up). The single pulse protocol (SP) consisted of varying intensities ranging from 0.2 – 10mA, each pulse repeated three times and randomly delivered with an inter-stimulation-interval (ISI) of at least 4 s. The paired-pulse protocol (PP) consisted of a first conditioning pulse varying in intensity (1, 2 or 4mA) followed by a second probing pulse with fixed intensity of 2mA at varying inter- pulse-interval (IPI) ranging from 10 to 2000ms. The inter-stimulation-interval (ISI, between blocks of paired-pulses) randomly varied between 9- 24 seconds (See Sup. Fig. 7).

Seizure inductions in the human subject were done only as part of the clinical investigation (focus localization). It consisted of 60Hz bipolar stimulations at 1-3mA

for a few seconds (1-5s). In one patient, the procedure was repeated after the intravenous administration of clonazepam 0.75 mg, allowing a direct comparison with baseline condition.

3.3 Signal Processing and data analysis

3.3.1 Pre-processing

The human EEG signals were preprocessed in Matlab (The MathWorks, Inc., Natick, Massachusetts, United States) in the following steps: 1. calculating bipolar derivations by subtracting monopolar recordings from two neighboring channels on the same electrode lead, discarding most of the stimulation artifacts. 2. removing remaining stimulation artifact by interpolation of a 12ms window ([-2, 10]ms from trigger onset). A kriging technique is applied where a linear fit with random noise (gaussian distribution of standard deviation of 50ms preceding data) connects the beginning and the end of the interpolation window. 3. bandpass 0.5 – 200Hz and 50Hz (and harmonics) notch filtering followed by resampling to a frequency of 500Hz.

The mice EEG signals were preprocessed in Python (Python Software Foundation, https://www.python.org/) with a 0.5-800Hz band-pass and a 50Hz (and harmonics) notch filter.

3.3.2 Single channel-level cortical response analysis

All the remaining signal analysis was carried out using custom Python scripts and following identical steps for mouse and human data.
The evoked response to a stimulation pulse was measured as the line-length (LL) per millisecond (ms) of the LFP signal as follows:

$$LL = \frac{\sum_{i=1}^{N} |(x_i - x_{i-1})|}{N} * sf/1000 \tag{3.1}$$

Where N is the number of datapoints over which the LL is calculated, sf is the sampling frequency and x the EEG signal measured as voltage difference at each datapoint. For single and paired pulse responses, the LL was calculated over the first 250ms (Sup. Fig. S3 B). For humans, this window includes both negative peaks of a typical CCEP described in human (Keller et al., 2018). For the 20Hz train stimulations on mice, the LL was calculated during the 53ms window in between two pulses. LL in train stimulations could not be calculated for human data due to the electrical artifacts.
For each session and each intensity, the pulses with the higher LL were visually checked to ensure that there was no artifact and removed otherwise. This process was done blind to the session condition.

3.3.3 Network-level cortical response analysis

To measure differences in single pulse evoked-responses across multiple electrodes and stimulation intensities and summarize it in a single value, we used non-negative matrix factorization (NMF). For each subject (mice or human patients), responses to

each single stimulation across session and condition were measured in each electrode using the LL as described above and stacked into an input matrix V of dimension $N_{electrodes}$ x $N_{stimulations}$. The NMF algorithm (sklearn implementation) then decomposes (factorizes) in a non-supervised manner the input matrix V into two smaller matrices W (size $N_{electrodes}$ x Rank) and H ($N_{stimulations}$ x Rank) using the multiplicative updates algorithm (Devarajan, 2008). In our context, W represented the weights assigned by the algorithm to each electrode and H the activation coefficient of these weights for each stimulation. The rank corresponds to the number of sub-networks in which the input matrix can be decomposed. The value of H then estimates the activation, for a given stimulation, of each sub-network.
In mice optogenetic experiment, only one stimulation site was used (MEC) and all EEG electrodes, implanted in limbic areas, showed robust evoked responses. Therefore, a rank of 1 was always selected (Sup. Fig.7 D). In humans, for each patient two different stimulation sites were used and only part of the recording electrodes showed evoked responses.
Consequently, we performed a stability NMF analysis (S. Wu et al., 2016) for each patient and chose the optimal rank number between 2 and 8. For each stimulation site, sub-networks that show increased response to increasing stimulation intensity were then selected as the responsive sub-networks and kept for analysis, effectively discarding background noise from non-responsive electrodes (Sup. Fig.7 E).

Finally, for each sub-network and each pharmacological condition, we compute an input-output response curve by computing the average H coefficient in response to each stimulation intensity. The area under this curve (I/O AUC) was used to measure the overall network responses across intensities and electrodes.

3.3.4 Passive indicators of critical transition

In addition to active probing, several passive metrics have also been used in the past to evaluate the proximity to a bifurcation. To measure them, we used EEG signal at distance (4s) from the single and paired pulse stimulations (See Sup. Fig. 3B). Six classical markers of critical slowing in the time- and frequency-domain were computed: variance, skewness, line-length, autocorrelation, spatial correlation and 1/f spectral exponent (Scheffer, Bascompte, et al., 2009).

Variance, skewness and width-half of the autocorrelation function were respectively calculated for each channel on 4s EEG epochs, bandpassed between 0.5-100Hz, respectively with the Numpy, Scipy and statsmodels functions following these equations:

$$Variance = \frac{\sum_{i=1}^{N}(x_i - \bar{x})(x_i - \bar{x})}{N} \tag{3.2}$$

$$Skewness = \frac{\sqrt{N(N-1)}}{(N-2)} \frac{\sum_{i=1}^{N}(x_i - \bar{x})^3}{N\sigma^3} \tag{3.3}$$

$$Autocorr = \frac{\sum_{i=k+1}^{N}(x_i - \bar{x})(x_{i-k} - \bar{x})}{\sum_{i=1}^{N}(x_i - \bar{x})(x_i - \bar{x})} \tag{3.4}$$

Where N is the number of datapoints, x the measured EEG voltage at each datapoint, $\bar{x}$ the mean EEG voltage, and σ the standard deviation, i.e. the square root of the variance.
For the autocorrelation, the measure taken was the width of at the half maximum of the autocorrelation function. For the spatial correlation, the Pearson correlations

were calculated in-between each electrode pair and then averaged to obtain a mean spatial correlation.
Finally, to assess potential shifts in non-oscillatory spectral content, the 1/f power law exponent from 10 to 250Hz were extracted from the signal after removing oscillatory peak using the FOOOF toolbox (T. Donoghue et al., 2020).

3.3.5 Statistics

Statistical testing was performed using bootstrap estimation statistics methods on group averages and graphical representations(Ho et al., 2019). Differences between conditions are calculated and reported as the mean difference (i.e. the effect-size) and its 95% confidence interval (95%CI) in brackets, obtained by performing bootstrap resampling 5000 times. For comparison across conditions, data were always either paired or normalized by block to control condition (NaCl in mice, baseline in human) (See Sup. figures 7).

3.3.6 Classifer

To investigate the consistency of our effects at the single trial level, we trained logistic regression classifiers to determine the pharmacological condition based on the EEG signal. We build 3 different classifiers: 1) one taking as input the EEG traces after a single pulse for all the channels, in a 250ms window 2) one using the six passive indicators of critical transition described above, calculated on a 4s EEG epochs in-between two pulses for each channel (see Sup. figures 7 B)and 3) one using all the passive indicators and also the magnitude of the response to the single pulse.

The classifiers were built using the sklearn multiclass implementation of the logistic regression with l2 regularization to avoid overfitting. The classifier was then trained to attribute to a given vector X_i a probability p_k to belong to a given class k as follow :

$$p_k(X_i) = \frac{e^{X_i W_k + W_{o,k}}}{\sum_{l=0}^{K-1} e^{X_i W_l + W_{o,l}}} \tag{3.5}$$

Where K is the total number of classes and W the coefficient matrix. As a classification problem, the objective for the optimization is then:

$$minW \quad C_i = 1^n \sum_{k=0}^{K-1} [y_i = k] \log(p_k(X_i)) + l2 \tag{3.6}$$

With y_i being the label of the observation X_i, n the total number of observations and l2 the penalty term.

Each classifier was trained animal by animal to discriminate between three classes (NaCl, PTZ subthreshold and Diazepam) using a 5-folds cross-validation strategy. Performance were calculated with the F1-score as follow:

$$F1 = \frac{TP}{TP + 0.5(FP + FN)} \tag{3.7}$$

Where TP, FP and FN are respectively the number of true positives, false positives and false negatives. To determine the chance level, classification scores were compared with the ones obtained from surrogate dataset in which the class labels were

permuted 100x. P-values were then obtained using this formula:

$$p - value = \frac{C+1}{n_{perm}+1} \tag{3.8}$$

Where C is the number of permutations whose score is higher than the true score, and n_{perm} the total number of permutations.

3.4 Epileptor Model

The Epileptor is a well-established five-dimensional neural mass model of seizure activity (Jirsa et al., 2014; El Houssaini et al., 2015; Proix, Jirsa, et al., 2018; W. C. Chang et al., 2018). Conceptually, this model is divided into three interconnected subsystems: a fast subsystem (variables x1 and y1) models fast ictal discharges, a slower subsystem (variables x2 and y2) models slower spike-wave events, and a very slow permittivity variable z which governs the switching between ictal and interictal states (Jirsa et al., 2014). We used a slightly modified version of the original Epileptor, by adding a coupling from the spike-and-wave subsystem onto the fast subsystem, implemented as follows:

$$x_1 = y_1 - f_1(x_1, x_2) - z + I_1 + 0.2(x_2 + .7) \tag{3.9}$$

$$y_1 = y_0 - 5x_1^2 - y_1 \tag{3.10}$$

$$x_2 = -y_2 + x_2 - x_2^3 + I_2 + 0.002g(x_1) - 0.3(z - 3.5) \tag{3.11}$$

$$y_2 = \frac{1}{\tau_2}(-y_2 + f_2(x_2)) \tag{3.12}$$

$$z = \frac{1}{\tau_0}(x_1 - z) \tag{3.13}$$

with:

$$g(x_1) = \int_{t_0}^{t} e^{-\gamma(t-\tau)} x_1(\tau) d\tau \tag{3.14}$$

$$f_1(x_1, x_2) = \{ x_1^3 - 3x_1^2 \text{ if } x_1 < 0 (x_2 - 0.6(z-4)^2)x_1 \text{ if } x_1 \geq 0$$

$$f_2(x_1, x_2) = \{ 0 \text{ if } x_2 < -0.256(x_2 + 0.25)x_1 \text{ if } x_2 \geq -0.25$$

Stimulation occurs on I_2

with τ_0 = 20000, τ_2 = 10, I_1 = 3.1, I_2 = 0.45 + $Istim_2$, and γ= 0.01. Note that compared to the original Epileptor parameters, tau_0 was chosen with a larger value, to obtain longer seizure and interictal period duration.
In our in vivo experiments, seizures did not occur spontaneously, but were the result of electrical or optogenetic stimulations which resulted in synchronous population discharges. Unless otherwise stated, we thus chose the excitability (or epileptogenicity) parameter x_0 such that no seizure occurs spontaneously, i.e. x_0=-2.12 for the NaCl condition, x_0=-2.09 for the PTZ condition, and x_0=-2.15 for the BZD condition. We modeled electrical stimulations as an additional input $Istim_2$ to I_2 to the spike-and-wave (x_2,y_2) subsystem. The stimulation amplitude $Istim_2$ was set to 5, unless stated otherwise. To allow repetitive stimulation to induce seizures, we added a

coupling term ($0.2(x_2 + 0.7)$ in the first equation) in the fast subsystem (x_1,y_1). Initial conditions were chosen for each excitability condition such that the system was lying on the fixed point at the beginning of the simulation.

The time correspondence between simulations and experiments was chosen such that one time step in the simulation corresponds to 10 ms of real time. Temporal stimulation parameters were then chosen as in the experimental setting (frequency: 20Hz, stimulation duration: 3 ms). The system was simulated using a fourth-order Runge–Kutta methods.

Results

To characterize how small and large perturbations can respectively probe cortical stability and overcome seizure resilience, we adopted a combination of theoretical, experimental and clinical approaches. Predictions of the well-established Epileptor model (Fig.3.2A-B) were systematically tested using optogenetic stimulations in non-epileptic mice (Fig 3.2C) and electrical stimulation in patients with epilepsy (Fig 3.2D).

3.5 Dynamics of ictal transitions in the Epileptor model

The Epileptor is a well-established five-dimensional neural mass model of seizure activity (Fig. 3.2A)(Jirsa et al., 2014). Intuitively, Epileptor is divided into three interconnected subsystems which capture dynamics at different timescales and represent the building blocks of the interictal-ictal sequence in epilepsy: 1) a fast subsystem (variables x_1, y_1) generating high-frequency activity (i.e. 100Hz) corresponding to the ones seen at the onset and during seizures (HFA, e.g. 30-150Hz, sometimes called 'tonic' discharges), 2) a slower subsystem (variables x_2, y_2) which models slower spike-wave discharges (SW) and corresponds to the pathognomonic sharp deflections (70-200ms) followed by an aftergoing slow-wave, visible both during seizures (sometimes called 'clonic' discharges) and during interictal periods (the 'epileptic spikes'), 3) and a very slow variable z which governs the switching between ictal and interictal states at longer timescale (Jirsa et al., 2014). Importantly, this variable z is directly dependent from the control parameter x_0 which sets the system level of excitability, defining the existence and stability of the ictal and non-ictal states (Fig. 3.1). In contrast to previous usage of the model, we explored brain stability mostly for cortical state where no seizure occurs spontaneously and studied how it reacts to small and large perturbations.
The ensemble of the explored dynamics can be captured in a bifurcation diagram (Fig. 3.1C) that summarizes changing cortical stability (so-called stability landscapes in Fig. 3.1A) as the cortical excitability is varied. Central to our study, we induced short and long excursions away from a point of stability, reflected in transient cortical response or self-sustained seizures to small and large perturbations, respectively.

3.6 Probing cortical stability

Small perturbations, delivered as single-pulses at discrete time-points, can be used to probe cortical stability: perturbations will lead to a stable excursion away from the attractor and return, whereas a large-enough perturbation will lead to an unstable excursion into a seizure (effectively crossing the seizure threshold). In Epileptor, perturbations are implemented as single-pulse stimulations of the subsystem in charge of the spike-wave events, mimicking the population discharges visible in vivo for

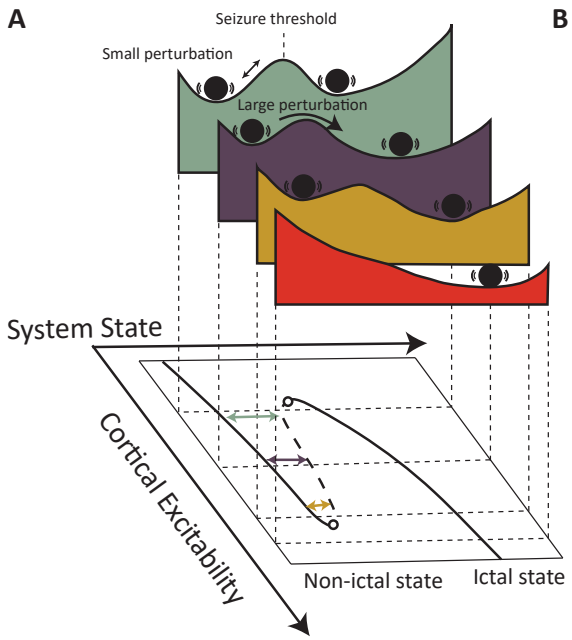

B

	Dynamical system concept	Epileptology
1	Basin of attraction 1	Non-ictal state
2	Separatrix	Seizure threshold
3	Basin of attraction 2	Ictal state
4	Resilience	Distance to seizure threshold
5	Control parameter	Cortical excitability
6	Critical transition	Ictal transition
7	Catastrophic bifurcation	Spontaneous Seizure

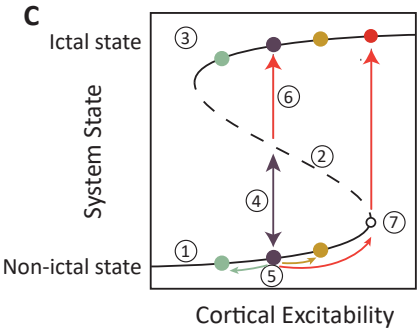

FIGURE 3.1: Dynamics of ictal transitions

A. From a dynamical system perspective, the brain can be conceptualized as a bistable system forming a stability landscape with two coexisting basins of attraction (also called fixed points or attractors, full thick line) - the "non-ictal" and "ictal" states - on either side of a separation - the seizure threshold (also called separatrix, dashed thick line). At any given time point, the system (black ball) can orbit within one of the basins of attraction or travel over the threshold, consisting in an ictal transition. In physiological conditions(brown landscape), the brain is excitable, but the "non-ictal" attractor is deep, preventing spontaneous ictal transitions, and presenting high seizure resilience. In the presence of small perturbations, the system's trajectory is slightly deviated from its attractor (bottom of the basin), before returning to it. Strong enough perturbations can nevertheless lead to ictal transitions. Bi-directional changes in cortical excitability redefine the stability landscape and lower (yellow) or heightens (green) seizure resilience. If the excitability reaches the bifurcation point (empty black dot), the "non-ictal" attractor disappears and the system is forced to transition to the ictal state (red landscape). Here, cortical excitability is a control parameter which defines the existence and stability of the ictal and non-ictal states in this bifurcation diagram. B. Table of the different concepts of dynamical system theory with their application in the context of epileptology. C. Bifurcation diagram represents the location of the stable equilibriums (full thick lines) against the parameter. It is a 2-dimensional version of the diagram in A. Numbers correspond to the concepts in the table in B.

single pulse stimulations (Fig. 3.2 A-B2).
In vivo, they correspond respectively to 3ms optogenetic single-pulse stimulations in mice (Fig. 3.2 C2) and intra cortical electrical 1ms single-pulse stimulations in humans (Fig. 3.2 D2). Although their exact shape could vary, the evoked response in silico, in mice and in human shared invariant features such as a sharp deflection, followed by an after-going slow wave over a total of 500ms that resemble interictal discharges in epilepsy (Fig. 3.2 B2-D2). The magnitude of the response to perturbation was quantified as the line-length, an integrative measure of voltage changes over time (see methods). Intuitively, line-length directly reflects the length of the path traveled on an excursion around the attractor upon perturbation (small double-arrows in Fig. 3.1A and Fig. 3.2 A2). In the three paradigms, single-pulses of increasing intensity resulted in a non-linear increase in evoked cortical responses, with a floor effect, a rapid rise in magnitude and a plateau (Fig. 3.2 B3-D3). Dynamically, this sigmoid input-output response curve results from an increase in gradients (the landscale slope in Fig. 3.1A) at a distance from the non-ictal attractor (Fig. 3.2 A3).

When the system is far from the bifurcation (brown landscape in Fig. 3.1), small perturbations are insufficient to challenge cortical stability. However, large enough perturbations can overcome seizure resilience and push even healthy cortex into the ictal state. In the model, non-epileptic mice and humans with epilepsy, trains of simulations over seconds induced self-sustained seizures, revealing the fundamentally bistable nature of the cortex (Fig. 3.2 C4-D4). The amount of imposed perturbation necessary for an ictal transition directly reflects the distance between the attractor and the seizure threshold (Fig. 3.2 A4). Practically, we quantified this distance by imposing series of pulse-trains of increasing duration and measured: 1) The 'time-to-seizure': practically, the time of stimulation necessary to induce a seizure for some given stimulation parameters (amplitude, frequency) (Fig. 3.2 B7-C7), which could be derived in all three paradigms. 2) The 'Distance-to-seizure (threshold)': the total path necessary to reach the seizure threshold, measured from the EEG signal as the cumulative line-length until the seizure onset. For electrical stimulation in humans, the presence of stimulation artifacts during the train stimulation forbids this more sophisticated measurement. In mice and in silico, a pulse by pulse analysis of the responses to train stimulation showed that the response is not constant but follows a bell curve, rising and then declining before the seizure starts. Dynamically, this bell-shaped curve results from changes in gradients encountered in the trajectory to the seizure threshold (Fig. 3.2 B7-C7).

Epileptor also makes negative predictions, for example on the lack of resonance properties of the system, and the resulting impossibility to trigger seizures with inhibitory inputs. To verify these additional predictions in vivo, we tested several ways of inducing seizures in the healthy CA1 region of the hippocampus in mice (Suppl. Fig. 9,9,10,11A). Limbic seizure could be triggered by both stimulation of entorhinal excitatory inputs (layer III pyramidal cells, Supp. Fig. 1) or downstream stimulation of the CA1 pyramidal cells (local excitation, Supp. Fig. 9) but not local parvalbumin interneurons (local inhibition, Supp. Fig. 11) . Additionally, we did not find any specific resonance frequency, but merely a faster integration for higher frequency stimulations (Suppl. Fig. 11B). Further suggesting a lack of resonance, seizures could also be triggered by irregular train of stimulations (Suppl. Fig. 11C) . These features are characteristics of an integrator type of bifurcation (saddle-node or saddle-node on invariant circle bifurcations (Izhikevich, 2007)), which correspond to

the ones mathematically implemented in Epileptor for seizure and epilepsy onsets (Jirsa et al., 2014).

3.7 Modulation of cortical response to perturbation

Changes in cortical excitability (i.e. the control parameter) predictively lead to changes in cortical stability, resulting in modification of cortical responses to perturbation and seizure resilience (Fig. 3.3 A1). In Epileptor, decreases or increases in cortical excitability (variable x_0 set at different values) redefines the stability landscape (Fig. 3.1 A) and modifies the gradient field towards the non-ictal state (Fig. 3.3 A1-A2). Consequently, when small perturbations are applied (single-pulse, same as in Fig. 3.2 B2), the cortical response will decrease (Fig. 3.3 B1 green) or increase (yellow). These changes, quantified as the line-length of the cortical response in each condition, are particularly visible for intermediate stimulation intensities (Fig. 3.3 B2). For experimental verification of these effects in mice, we used pharmacological agonists (Benzodiazepines, diazepam i.p. in mice) or antagonist (subthreshold PTZ, i.p. 10-20mg/kg) of the GABA-A receptor, established drugs which respectively decrease and increase cortical excitability (Yonekawa, Kupferberg, and Woodbury, 1980; Yoong et al., 1986). As predicted, optogenetically evoked cortical responses in mice were significantly decreased in presence of the Benzodiazepine (BZD) and increased in presence of PTZ (quantification in CA1 R at max intensity: mean difference across mice after bootstrapping: -22.5%, 95%CI [-18, -26], for BZD and +10% [5,17] for PTZ, Fig3 C1). The effect was most prominent for intermediate intensities and resulted in both a vertical and a horizontal shift of the sigmoid input-output curve (Fig. 3.3 C2). Capturing the modulation of cortical response across stimulation intensities, the area under the curve (AUC) showed significant modification as a function of cortical excitability (mean difference after bootstrapping: -17% [-14,-20] for BZD and +15% [8,23] for PTZ). In the case of benzodiazepines, this reduction was dose-dependent (tested for doses between 1 and 7 mg/kg, See Supp. Fig. 12 A-D).

For verification of these effects in humans, we compared cortical responses before and after administration of i.v. clonazepam given for clinical reasons. Decreased responses to small perturbations were also observed in the human cortex (Fig. 3.3 D1), mostly for intermediate intensities (3-7 mA, Fig. 3.3 D2). Each patient had a different electrodes montage dictated by clinical need and received only a low number of single pulses; therefore statistical analysis has only been performed at the group level with network responses (see below).

3.8 Modulation of cortical resilience

Further, these detectable changes in cortical responses to small perturbation at different degrees of cortical excitability were systematically associated with corresponding changes in seizure resilience. In silico and in mice, seizure induction was achieved at three different degrees of cortical excitability (Fig. 3.3 B3-C3) and the differences in seizure resilience were calculated both as 'distance to seizure threshold' and 'time to seizure' (Fig. 3.3 B5-C5). Modulation of cortical excitability also induced changes in the dynamic cortical response during the train stimulations. The bell curves described previously were respectively shrunk or elongated, in presence of increased or decreased cortical excitability (Fig. 3.3 B6-C6). Across 18 mice and 107 sessions, 'Time-to-seizure' and 'Distance to seizure' were significantly increased with BZD

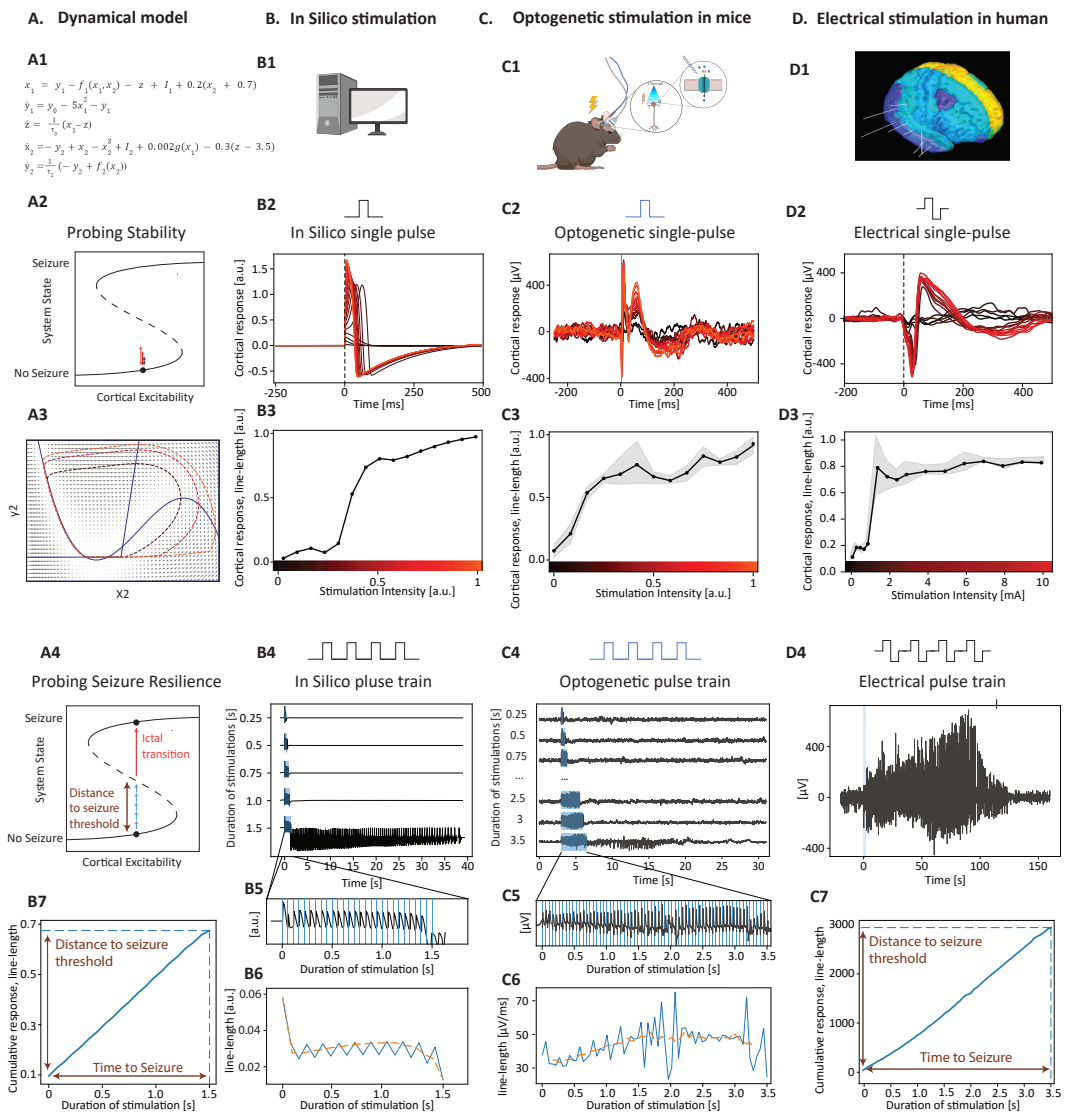

FIGURE 3.2: Probing cortical stability and seizure resilience

Modeling (A), simulation (B), experimentation in mice (C) and study in humans (D) of the dynamics of cortical responses and ictal transitions. A1: Cortical stability is modeled by the differential equations of the Epileptor model. B1: Simulation of the effect of stimulation by an in-silico implementation of the equations. C1: Cortical stimulations in healthy mice with 3ms optogenetic pulses to control the firing of projecting pyramidal neurons from the Entorhinal (layer III) to the hippocampal cortex (supp. Fig. 8). D1: Cortical stimulations in human patients with epilepsy undergoing an invasive diagnostic work-up with stereotaxic EEG. Implanted electrodes were used to deliver 1ms electrical pulses to the hippocampal and entorhinal cortex. A2: Prediction that stimulations of increasing intensity will lead to trajectories of increasing path-length. B2-D2: Measuring cortical responses to a range of single-pulse stimulations of varying intensity (dark to bright red) in silico (B2), in mice (evoked potentials in CA1 hippocampus, C2) and in humans (evoked potentials in the entorhinal cortex, D2). In each case the input-output curve takes the shape of a sigmoid. A3: Trajectories of single pulse evoked response in the phase space of the Epileptor's spike-and-wave subsystem. Nullclines are shown in blue, and arrows show the instantaneous gradients. Three color-coded trajectories are shown and correspond to evoked responses to a single-pulse stimulation at different intensities. B3-C3: Relationship between increasing single-pulse stimulation intensity and cortical response magnitude, quantified as the line-length of the evoked response over a 250ms window. A4: Prediction that trains of stimulation progressively move the system states until it crosses the seizure threshold and induce an ictal transition to self-sustained seizures.

B4-D4: Experimental verification using train stimulation of increasing duration until an ictal transition occurred in silico (B4, 20Hz), with optogenetic stimulation in mice (C4, 20Hz) and with electrical stimulation in humans (D4, 60Hz for the clinical investigations). B5-C5: Zoom-in on the stimulation train leading to a seizure. B6-C6: During the stimulation train, the magnitude of the cortical response follows a bell shaped curve. B7-C7: Seizure resilience can be quantified either as the time of stimulation necessary to induce a seizure ('Time-to-seizure') or the total amount of perturbation necessary to reach the threshold ('Distance-to-seizure', corresponding to the total line-length of the EEG during the stimulation train).

(respectively, +71% [53,97] and +97% [72,140], Supp. Fig. 13, absolute values in Fig. 3.4 F) and decreased with PTZ (-19% [-5,-30] and -17% [-8,-28], Fig. 3 C5-C8, Fig. 4F). Dynamically, these observations in the EEG correspond to bidirectional changes in the gradients of the stability landscape.Additionally, shifts in the bell curve were quantified as the time of stimulation to reach the peak of the bell curve ('Time-to-peak', Fig. 3.3 B6-C6) and were significant across mice after bootstrapping (Fig. 3 C7, mean difference: +104% [71,152] in presence of BZD, -18% [-7,-28] in presence of PTZ). These effects were dose-dependent and already present at low doses (Supp. Fig. 12 and 13).
Finally, similar increases in cortical excitability were also observed upon picrotoxin injections, another GABA-A receptor agonist (Supp. Fig. 14).

In human patients, seizure inductions were done strictly for clinical reasons. In one patient, seizure induction was performed both before and after the administration of BZD, allowing direct comparison in seizure resilience. In line with the mouse results, the time to seizure time to seizure increased from 2s at baseline to 4s with BZD (+100%, Fig. 3.3 D3).

3.9 Network excitability

We next took advantage of our optogenetics experimental set-up in mice to quantify cortical stability more exhaustively over a range of drug dosage. We also asked whether changes in cortical responses could be observed at the network level using multi-site EEG recordings (Entorhninal, CA1, CA3, DG and subiculum bilaterally) . Optogenetic single pulse stimulation of the right entorhinal layer III pyramidal cells produced an evoked response in all electrodes, propagating from the right entorhinal to the hippocampal cortex, and ending in the contralateral limbic circuit (Fig 3.4 A). When compared to the control condition (NaCl), all electrodes showed a significant pharmacological modulation in cortical response to max stimulation intensity (Fig. 3.4B). To capture changes in cortical response across all channels and intensities into a single value, we used a dimensionality reduction algorithm (Non-negative Matrix Factorization (NMF)) attributing weights to each electrode and calculating an activation coefficient of these weights for each stimulation (see methods and Supp. Fig. 7D-F). As before for single channel value (Fig. 3.3 C2), the area under the input-output response curve of this coefficient was calculated for each session, resulting in a global measure of the network response.
Extending our prior single-channel observations, network responses to small perturbations were decreased in a dose-dependent manner by Benzodiazepine, and increased by sub-threshold PTZ, (Fig. 3.4C), (Dz 7mg/kg: -31% [-25,-39], Dz 5mg/kg: -18% [-14,-22], Dz 3mg/kg: -13% [-4,-21], Dz 1mg/kg: -9% [-4,-21], sub-threshold

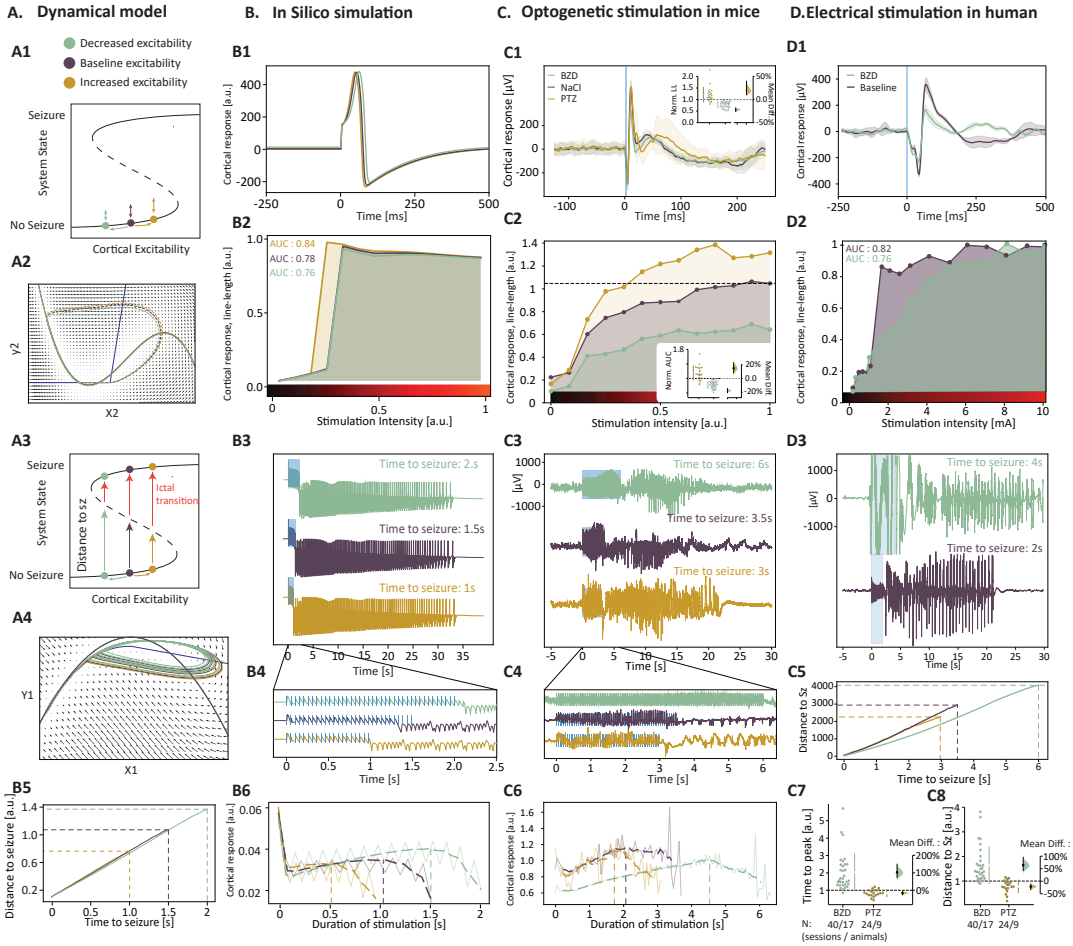

FIGURE 3.3: Modulation of cortical excitability

Characterization of the changes in cortical responses and seizure resilience under high (yellow) and low (green) cortical excitability regime, using changes in the control parameter in the Epileptor model (A-B), an agonist benzodiazepine (BZD, diazepam) and an antagonist Pentylenetetrazole (PTZ) of the GABA-A receptor in mice (C) and a benzodiazepine (BZD, clonazepam) in humans (D). A1: Prediction that different cortical excitability (i.e. starting positions) will lead to different cortical responses for the same input. B1-D1: Modulation of cortical excitability results in detectable changes in cortical responses to single-pulse stimulation in silico (evoked potentials at half-maximum intensity B1), in mice (evoked potentials at maximal intensity in CA1, C1), and in humans (3mA, evoked potentials in entorhinal cortex, D1). Insert shows measured magnitude of responses, quantified as the line-length of the signal on a 250ms window. A2: Trajectories of single pulse evoked response as in Fig 2 A3, but for three different cortical excitability (color-coded). B2-D2: Measured cortical responses (line-length) to a range of single-pulse stimulations of varying intensity under high and low cortical excitability in silico (B2), in mice (C2) and in humans (D2). Insert shows modification of the area under the curve (AUC) as a function of changes in cortical excitability. A3: Predicted changes in seizure resilience as a function of changes in cortical excitability. B3-D3: Representative example of seizure induction with different 'time-to-seizure' under higher and lower cortical excitability in silico (A3 and B3), in mice (C3) or in humans (D3). A4: Trajectories of induced seizures in the phase space of the Epileptor's high-frequency activity subsystem. Nullclines are shown in blue, and arrows show the instantaneous gradients. The three trajectories correspond to the different levels of cortical excitability (color-coded). B4-C4: Zoom-in on the stimulation trains. B5-C5: Modulation of cortical excitability results in a higher or lower distance to seizure threshold for the in silico (B5) and in mice (C5). B6-C6: the maxima and length of Bell-shaped curves (calculated as in Fig. 2 B7-C7) were displaced as a function of cortical excitability. C7: In mice, quantification of this shift as the normalized distance until the peak (vertical dashed line in C6). C8: In mice, quantification of the normalized distance-to-seizure threshold. N for mice experiment, n: 18 animals, 107 sessions across animals and conditions. For humans, example data from one electrode in one subject.

PTZ: +11% [+5,+18]). Further, the modulation of responses was greater for electrodes with higher response latency (Fig. 3.4B), suggesting a cumulative modulation by GABAergic drugs in polysynaptic connections. Similarly, electrodes weights, attributed by NMF in an unsupervised manner, also positively correlated with latency (Supp. Fig. 15).

3.10 Correlation of network excitability with seizure resilience and severity

As described before, seizure resilience, measured as 'time-to-seizure', is modulated bi-directionaly and in a dose-dependent manner by GABAergic drugs (Fig. 3.4D, normalized value and statistics in Supp Fig. 13A). Bidirectional and dose-dependent changes in seizure resilience were negatively correlated with the network response to small perturbation in the same session (Fig. 3.4E, Pearson correlation: R^2=0.20, p <10-6), suggesting that cortical probing can inform about momentary levels of seizure resilience.
Optogenetically-induced limbic seizure can produce different severity of symptoms, from clinically undetectable to behavioral arrests and full-blown clonic-tonic seizures. Seizure severity (modified Racine scale, see methods) was correlated with the level of cortical excitability, set by the GABAergic drugs (Fig. 3.4F, normalized value and statistics in Supp Fig 13B). For a given session, the difference in seizure severity with control condition was positively correlated to the difference in network response to perturbation (Fig. 3.4G, Pearson correlation, R^2=0.30, p <10-8). Taken together these results indicate that GABAergic agonists and antagonists modulate seizure initiation and propagation in the limbic circuit.

3.11 GABAergic modulation of subnetworks in the human brain

In humans, input-output curve calculations using NMF as above allowed for the characterization of GABAergic modulation of response to small perturbations across many electrode contacts (up to 80 by patient). For each stimulation site, a responsive subnetwork of contacts was derived (see Fig. 3.4H) and its activation by a range of single-pulse stimulations in the presence or absence of BZD was calculated. Across 19 stimulation sites and 7 patients, sub-network responses showed a significant decrease in the presence of clonazepam 0.5-1mg (mean difference after paired bootstrapping: -16% [-11,-21], see Fig. 3.4I). Note that most stimulations and response networks were in the limbic structures. However, a few were extra-limbic, where the same modulatory effects held true.

3.12 Passive markers of cortical excitability

In addition to active probing, several passive markers have been proposed to reflect cortical excitability in vitro and in vivo (W. C. Chang et al., 2018; Maturana et al., 2020; Meisel and Kuehn, 2012), with some evidence that they could help measure the distance to the bifurcation in epilepsy. These markers are believed to reflect slower recovery from natural stochastic perturbation ("critical slowing") and do not require any imposed stimulation to be measured (Fig. 3.5A) . As we were able to vary cortical excitability and seizure resilience in a controlled manner, we asked which of the

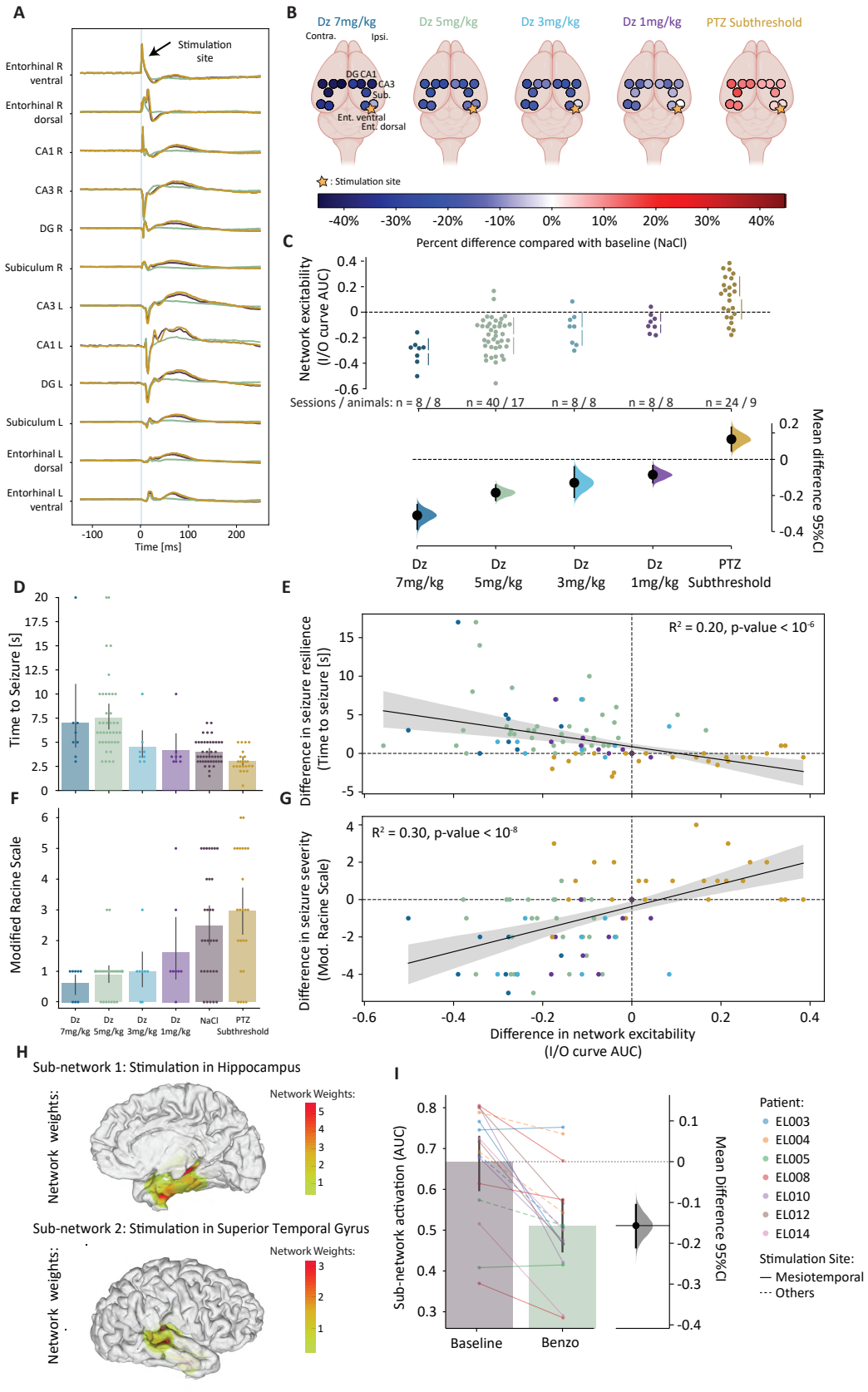

FIGURE 3.4: Network excitability, resilience and seizure severity

A. Average cortical response to optogenetic single-pulse stimulation in the right entorhinal cortex and propagation across the limbic circuit in a single animal in three pharmacological conditions. B. Single channel level analysis of the GABAergic modulation of response to single-pulse stimulation of maximal intensity. Dots correspond to single electrodes colored by the difference of the average cortical response compared to the NaCl condition. Mean differences that were not different from baseline after bootstrapping were left blank. C. Network responses to perturbation, computed across electrodes, intensities and conditions using a dimensionality reduction algorithm (NMF) and normalized by subtracting the value in control condition (NaCl) for each session. Bottom panel reports mean difference after bootstrapping and 95%CI (black vertical bar). D. GABAergic modulation of seizure resilience, measured as the duration of 20 Hz stimulation necessary to induce a seizure (Time to Seizure). E. Resilience to seizure inversely correlates with the network response to single-pulse stimulation. F. GABAergic modulation of seizure severity scored on a modified Racine scale. Three animals (18 sessions) were not filmed and couldn't be included in the analysis. G. Seizure severity directly correlates with network response to single-pulse stimulation. H. In a representative human subject, two examples of subnetworks in the right hippocampus and the right superior temporal gyrus, identified by NMF and projected to the cortical surface I. Sixteen sub-networks identified across seven patients (colors) showing decreased excitability after infusion of a benzodiazepine. Full lines are for stimulation sites in the mesiotemporal cortex, dotted lines for stimulation in the neocortex. A table with clinical characteristics of the patients can be found in supplementary.

passive makers or active probing of cortical excitability were more informative about the momentary state of the system. In CA1 R, both the variance and the skewness of the baseline signal were significantly increased for high excitability (PTZ) but only showed a minimal trend towards decreased values for low excitability (BZD, Fig 3.5 A-E shows one illustrative animal, group level normalized value and statistics in Supp. Fig. 16). The $1/f$ spectral exponent and autocorrelation capture a significant slowing of the EEG when cortical excitability is low, but only the latter show an opposite effect for high excitability (Fig. 3.5C-D and Supp. 16). Finally, spatial correlation between electrodes in the limbic circuit shows significant global decrease and increase proportionally to cortical excitability (Fig. 3.5E and Supp. Fig. 16).

3.13 Decoding excitability from the EEG

Next, we adopted a machine-learning approach to decode momentary states of cortical excitability at the single trial level, using short segments of EEG. To do this, we trained logistic regression algorithms to classify the pharmacological conditions corresponding to states of low, normal, and high excitability (BZD, NaCl and PTZ). The first of these multilabel classifiers was trained on the multichannel EEG response to single pulse over 0.25s without feature extraction (SP classifier). The second was trained on 4s segments of baseline multichannel EEG (without stimulation) and uses the 6 passive features described above (autocorrelation, variance, skewness, line-length, $1/f$ exponent, and spatial correlation) for each channel. The third classifier combines passive markers and active probing, incorporating the 6 passive features with the magnitude of the probed cortical response measured as line-length in each channel. All three classifiers performed well above empirical chance level with F1-score for SP-classifier = 0.89, $p<0.01$; Passive-classifier =0.86, $p<0.01$; Passive + Active classifier = 0.88,$p<0.01$, (Fig. 3.5G). The F1-score was statistically higher when active probing was included as an input to the classifier (Fig 3.5G, Passive+Active > Passive: $p<0.05$, paired Wilcoxon rank test).

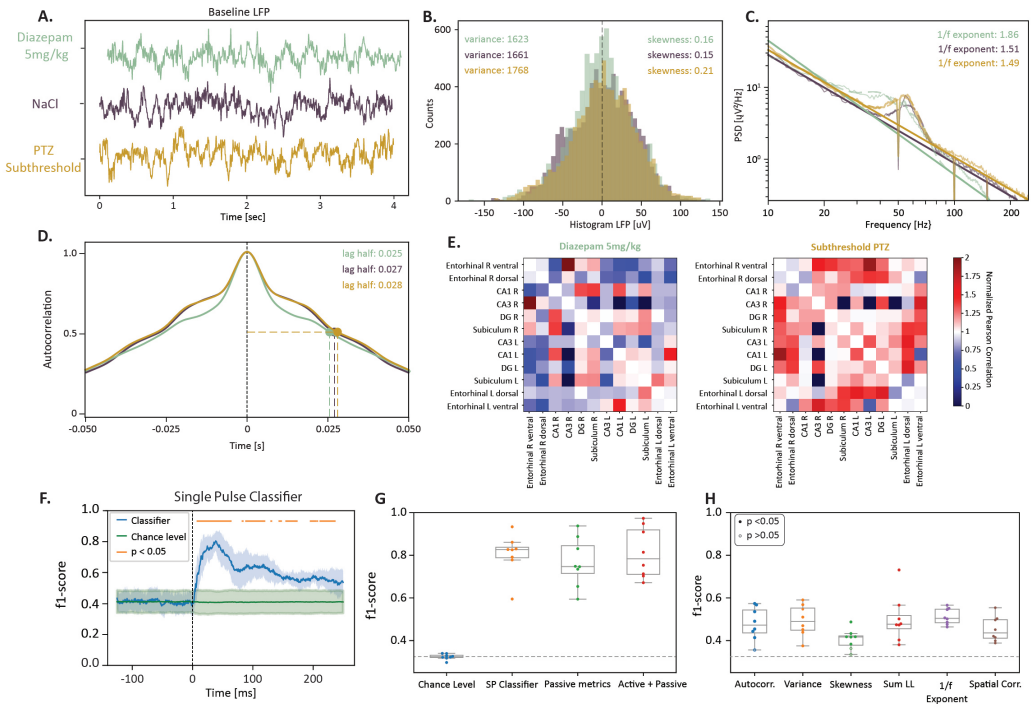

FIGURE 3.5: Decoding excitability from the EEG

For each animal, cortical responses and passive markers of excitability were respectively characterized on the stimulated EEG (0-0.25s post-stimulation) and on the rest EEG (4-8 seconds post-stimulation) for comparison. A: Example of rest EEG traces in absence of stimulation for the three pharmacological conditions, recorded in the CA1 hippocampus over 4s in a representative animal. B: Histogram of the EEG voltage values across the three conditions in the same animal and channel drawn from 50 4s rest EEG blocks. C: Power spectrum density of the LFP signal and estimation of the 1/f power law exponent by linear fitting between 10 and 250Hz on a log-log plot. D: Autocorrelogram of the signal with calculation of the lag value at half-maximum. E: Example of Pearson correlation between all pairs of electrodes normalized to the control condition (NaCl). F: Average accuracy across animals (blue line) of a multilabel classifier of the pharmacological condition based on the network response to single-pulse stimulation (0-0.25s) against the mean empirical chance level (green, 100 label permutations). Orange dots show significant timepoints . G: Comparison across three classifiers using: 1) the raw cortical response to single-pulse stimulations, 2) the 6 passive indicators on rest EEG and 3) the six passive indicators and the magnitude of the response to the single pulse. H: Comparison across classifiers using individual passive indicators. Each dot (N=8) corresponds to one animal that underwent both Dz and PTZ sessions, filled if the classifier is significantly above chance level ($p<0.05$). Dotted line is the mean empirical chance level across animals.

Post-hoc analysis by training SP classifiers on single timepoints confirmed the absence of classification ability from baseline EEG without feature extraction (Fig. 3.5F before stim at 0), and then sustained above chance level in almost all the duration of the response (0-250ms), although the beginning of the cortical response seemed most informative. Post-hoc analysis by training passive classifiers for individual passive markers showed that all scored poorly (Fig 3.5H) pointing toward the necessity to combine these metrics to decode excitability accurately.

3.14 Precursors sign of ictal transition

All the previous experiments characterized cortical stability in a situation of bistability, where the cortex needs large external perturbations to reach seizure threshold (green, brown, and yellow landscape in Fig. 3.1A). However, for even higher cortical excitability, the system passes the ('saddle-node') bifurcation point and the non-ictal attractor (stable fixed point or 'node') coalesces with the seizure threshold (unstable fixed point or 'saddle') forcing the transition into seizures, as the only remaining possible state. This transition is predicted to occur with minimal or even in absence of imposed perturbations (red landscape in Fig. 1). This case can be modeled with Epileptor by imposing higher values on the variable x_0, and correspond to most of its previous utilisations (Fig. 3.6A). Predictively, approaching the bifurcation leads to larger, sometimes massive, cortical responses to small perturbations and a brittle cortical stability (Fig. 3.6B).

These predictions could also be verified experimentally in mice. In the presence of high doses of PTZ (30-40mg/kg, subthreshold doses used before were 10-20mg/kg), the non-epileptic cortex gradually approaches and then passes the bifurcation, resulting in a spontaneous seizure. Before the transition, cortical responses to small perturbations increase when the distance to the bifurcation decreases, both at the single channel and network level, when serially probed with single-pulses every 8-12s (Fig 3.6C-E). Progressive loss of cortical stability could be seen up to 15 minutes before the ictal transition , but a massive increase in cortical response was visible in the last four minutes. As predicted, seizures could then be triggered by mere single-pulses (4 out of 4 sessions with suprathreshold PTZ doses and single-pulse stimulations) or in the absence of stimulation (5 out of 5 sessions with suprathreshold PTZ doses but without single-pulse stimulations).
Passive metrics of critical transition also showed a significant increase before the seizure, but it was only restricted to the very last minutes and were less consistent (Fig. 3.6G-L).

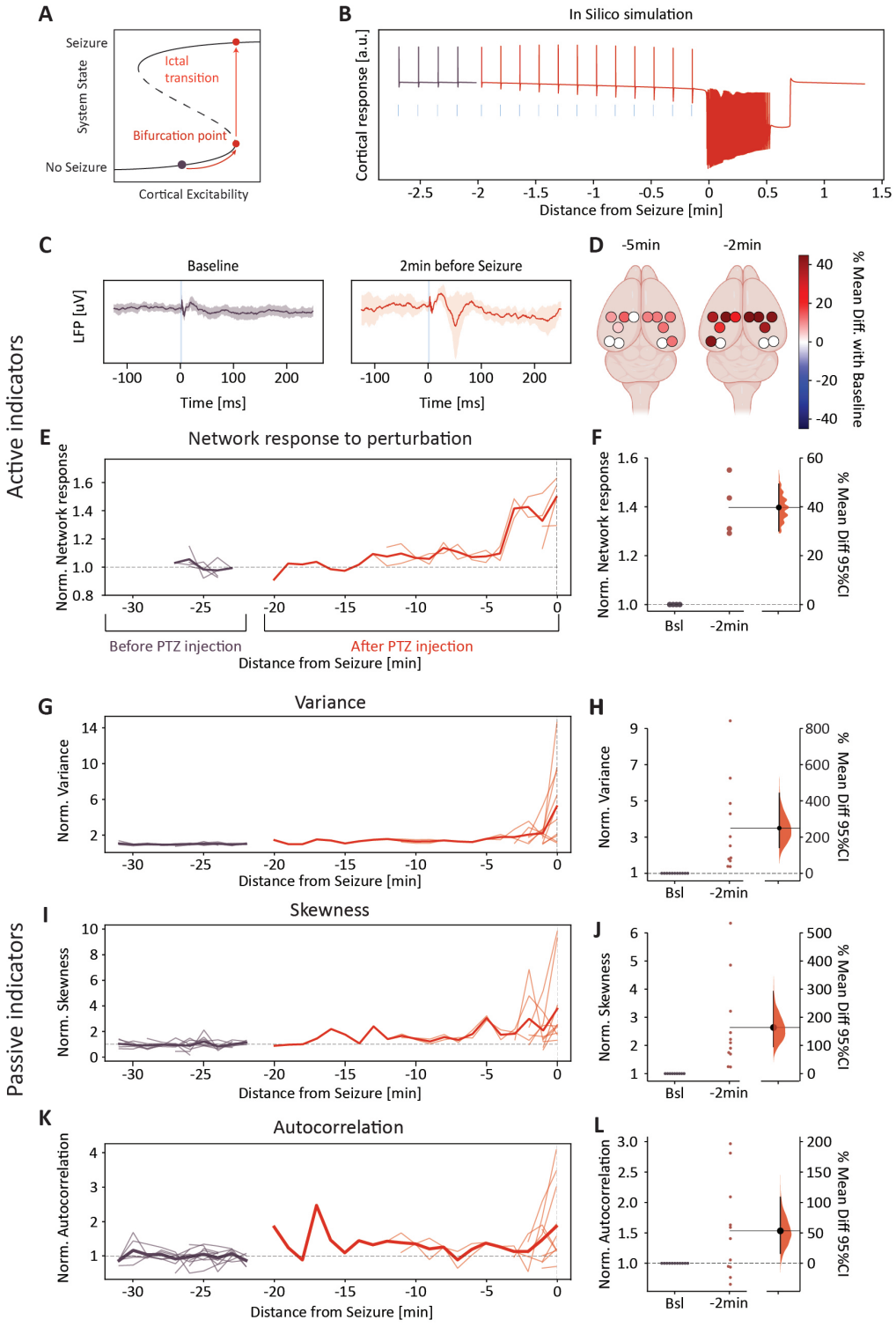

FIGURE 3.6: Precursors sign of critical transition

A: Bifurcation diagram: progressive increase in cortical excitability leads the system to the bifurcation point, resulting in an ictal transition. B: In Silico single pulse stimulations during shifting in cortical excitability until the bifurcation point. First pulses are baseline (brown). Blue bars are single-pulse timestamps. The last pulse starts a seizure. C: In vivo optogenetic stimulations in mice, example of CA1 EEG responses to single pulse stimulation (blue line) during baseline and two minutes before a suprathreshold PTZ-induced seizure (30-40mg/kg). Thick lines are the mean across 12 stimulations in a 2 minutes window, shading the standard deviation. D: Differences in evoked responses (LL) to single pulse for each electrode. Each dot shows the mean difference compared to baseline after bootstrapping, across animals. Empty dots are not significant.

E: Network response to single pulse during the shift in cortical excitability. After the PTZ injection, the response to single pulse increases until the seizure occurs. Thin lines show responses for individual sessions, the thick line is the average. For each session, values are normalized to the mean response during baseline. F: Quantification of the network response during baseline and in the 2 minutes before the seizure. Each point is the mean for a session, normalized by the network response at baseline. Violin plot shows the mean difference after bootstrapping, vertical black line is the 95%CI. For D-F, n = 270 single pulse responses during 4 sessions in 2 animals. G-L: Passive indicators of critical transition (Variance, Skewness and Autocorrelation of the EEG), either in sessions without stimulation (n=5) or in between single pulse stimulations (n=6). A 10-minute period before the PTZ injection was used as baseline (brown line), and all the values were normalized to the mean of this baseline. N = 11 sessions across 8 animals.

Discussion and Outlook

My PhD research project aims at bridging recent theoretical developments in the understanding of epileptic seizure with in vivo biological mechanisms as well as its clinical application. One strong prediction emerging from the application of the dynamical system theory to epilepsy, is that latent changes in seizure resilience should be accompanied by measurable changes in response to small perturbations (Scheffer, Bascompte, et al., 2009; Baud et al., 2020). In this study, we combined theoretical, experimental and clinical approaches to test this hypothesis, and developed methodology to delineate the landscape of physiological and pathological cortical excitability, including quantification of seizure thresholds.

For the first time, we used the seizure mathematical model Epileptor to explore brain stability in a non-epileptogenic state and to study how it reacts to small and large perturbations. We then tested these findings using a circuit and cell type specific stimulation on mice and confirmed their translational aspect to human studies using intracranial electrical stimulations. Crucially, we have shown that in vivo modulation of the GABAergic system corresponds to fixing a control parameter in the model, leading to both measurable changes in markers of cortical stability and seizure resilience. Finally, we confirmed that active and passive EEG markers can decode momentary states of cortical excitability and reflect distance to the seizure threshold.
Our study expands previous work in several ways. First of all, we characterize cortical stability in a large range of different cortical excitabilities, going from non-epileptic brain with increased inhibition to very high level of cortical excitability in the seconds preceding a critical bifurcation to seizure. Secondly, we establish two direct ways of quantifying seizure resilience (distance and time-to-seizure), circumventing the problem of only inferring it from a hypothetical pre-seizure state. Finally, we causally link changes in cortical excitability and seizure resilience in the Epileptor model with a biological mechanism in vivo, the activity of the GABAergic system.

3.15 Bistability and seizure transition

Observations that electrical (S. Kalitzin et al., 2005; Lisanby, 2002; Zangaladze et al., 2008), magnetic (Lisanby, 2007) or optogenetic (Osawa et al., 2013) repetitive stimulation can induce seizures in a healthy brain led to the conclusion that seizure is a natural latent state of the brain ("any brain can seize").
From a dynamical system perspective, it can be described as a bistable system composed of the 'non-ictal' and 'ictal' states, separated by a threshold that prevents spontaneous ictal transitions in healthy brains (Fig. 3.1). In this perspective, epilepsy is simply a condition of decreased resilience to a transition into the ictal state (Baud

et al., 2020), and sustained stimulations can be seen as a perturbation which forces the system to pass the seizure threshold (Lopes Da Silva et al., 2003; Jirsa et al., 2014; W. C. Chang et al., 2018).

A dynamical system which undergoes a catastrophic bifurcation such as an ictal transition can only follow a limited number of mathematically defined bifurcation types (Izhikevich, 2007). Previous studies classified seizures based on their bifurcation type (so-called dynamotypes, Saggio et al., 2020; Jirsa et al., 2014, but relied solely on passive recordings. Taking advantage of the fact that we could actively induce seizures in the mice and human limbic system, we tested several predictions made by Epileptor. In non-epileptic animals, seizures could be induced by different types of excitatory stimuli, at different frequencies and with regular or irregular stimulations, but not, as described before (Lévesque, Biagini, et al., 2021), by solely inhibitory stimuli. These characteristics point toward the fact that induced seizures follow an integrator type of bifurcation (saddle-node or saddle-node on invariant circle bifurcations). Consequently, non-epileptic dynamics in the limbic circuit are intrinsically organized around a saddle-node bifurcation, likely explaining how this circuit can easily generate seizures. These dynamotypes have also been described in several species and are believed to be more common in humans with epilepsy (**Jirsa 2014**; Saggio et al., 2020). Thus, minor disturbances to the fine physiological equilibrium controlling adequate cortical excitability in the limbic circuit (enough, but not too much) can move this cortex closer to the bifurcation point and result in epilepsy.

3.16 Measuring seizure resilience

In-silico simulations predict that increasing levels of cortical excitability decrease the distance to the seizure threshold and therefore the amount of perturbations needed to tip the system into a seizure state (Jirsa et al., 2014; Baud et al., 2020). Validation of these relationships in-vivo requires specific tools to both modulate cortical excitability and measure seizure resilience. Bi-directional pharmacological modulation of the GABA-A receptor is well known to either prevent or promote seizures and was a natural candidate to control cortical excitability (Yonekawa, Kupferberg, and Woodbury, 1980; Yoong et al., 1986). In our study, agonists (BZD) showed tight dose-dependent modulation of cortical stability, and antagonists (PTZ and PTX) could be used either to get closer (subthreshold) and pass the bifurcation point (suprathreshold). Repetitive train stimulations (either by optogenetic or electrically) allow to study 'on-demand' seizure resilience in awake freely moving mice as well as in human patients. Due to stimulation artifacts with electrical stimulation, only optogenetics allow to capture the dynamics of cortical responses during the stimulation pulse.

Time-to-seizure is a simple and translational way of measuring seizure resilience. It can be used in experimental epilepsy both to study the fundamental mechanisms governing the fluctuations of cortical excitability and to develop and validate new anti-seizure drugs. As it doesn't require any signal analysis, it is unaffected by magnetic or electrical artifacts and can also be used in clinical settings to measure changes in seizure threshold in patients. Train of optogenetic stimulation has already been used to measure seizure threshold (Paschen et al., 2020; Klorig et al., 2019), and importantly Paschen and colleagues showed that time-to-seizure was

also able to capture the chronic loss of seizure resilience in epileptic animals. Going beyond the irreversible changes in sclerotic hippocampi, our study completes this work by showing acute pharmacological modulation of seizure resilience both in non-epileptic mice and in a human subject.
We also took advantage of the optogenetic artifact free stimulations to calculate a second measurement of seizure resilience: the distance-to-seizure. This new metric presents the advantage to be directly linked to a mathematical definition of seizure resilience. It is defined as the minimal deviation from a stable state, induced by perturbations, required to initiate a seizure. It can be computed from the EEG signal as the cumulative voltage change (line-length) induced by the stimulations. From a dynamical system perspective, it corresponds to the distance between the non-ictal state and the seizure threshold in a phase space (Scheffer, 2009; Jirsa et al., 2014; Baud et al., 2020), and can also be easily calculated in neural mass models such as the Epileptor. Both metrics showed significant changes in seizure resilience across drugs and dosages but distance-to-seizure might be more precise as it showed a consistently smaller confidence interval.
In the mice experiment, different levels of cortical excitability were also correlated with seizure clinical severity. In a bifurcation diagram, this corresponds to differences in the position of the ictal state along the y-axis once the threshold is passed. No consistent change was observed in seizure duration.

3.17 Small perturbations as indicators of cortical stability

Previous studies observed an increased response to stimulation in pre-ictal state in in vitro seizure model (W. C. Chang et al., 2018; Graham et al., 2022). In these studies, the pro-convulsive artificial milieu creates a deterministic "ictogenic ramp" (**Graham**) toward seizure, which is putatively correlated with an underlying loss in seizure resilience. In Epileptor, this corresponds to increase in the state parameter until the bifurcation point, and larger responses to stimulations are visible in silico.
We replicated these findings in vivo using suprathreshold PTZ injections combined with single pulse stimulations. As for lower doses of PTZ, we first observed an increase in response due to the presence of the GABA-A antagonist. Interestingly, a second sharp increase in response to perturbations happened just before seizure (2 minutes), reminiscent of the "pre-ictal transformation" recently described by Graham and colleagues. In this specific state of extremely high excitability, the system is adjacent to the bifurcation point and even single pulses can induce seizure.

However, both epileptic and non-epileptic brains live most of the time far from these extremely unstable conditions. The possibility to infer seizure resilience from the response to small perturbations in condition of normal or subnormal cortical excitability remains open. Human studies of evoked cortical responses by TMS-EEG showed modulations by diverse anti-epileptic drugs (Šulcová et al., 2022; Premoli, Castellanos, et al., 2014; Premoli, Bergmann, et al., 2017) but direct correlations with changes in seizure resilience are lacking. In our study, we show that the modification in the response to single pulse was accompanied with changes in time-to-seizure. A machine-learning classifier confirmed that current states of cortical excitability could be inferred from individual single pulses, without relying on probabilistic thresholds that require several trials for their determination (Klorig et al., 2019).
In presurgical epileptology, intra-cranial electrical stimulation has been previously used to localize epileptic parenchyma (Valentín et al., 2002) but to our knowledge

never before to investigate drug effects on cortical stability. Although being naturally limited by the clinical choice of electrodes localization, cortico-cortical stimulation allows the study of the human cortex with high temporal and spatial resolution. Our results show that single pulse stimulations in these patients could be used to study the different determinants of cortical excitability.

3.18 Putative biological mechanism

In Epileptor, the responses to perturbations correspond to short or long excursions away from a point of stability. The shape and intensity of these responses can be explained by the study of the stability landscape for a given cortical excitability. However, biological interpretations of these responses are limited, and different mechanisms may play a role in vivo. In mice, differences in response to circuit-specific single pulse stimulations could be observed from the site of stimulation (entorhinal right) up to the contralateral limbic structures. This suggests changes in neuronal response both at a cellular level and network level. In human patients, GABAergic modulations of the response to small perturbations were also observed in putative mono-synaptic connections (hippocampus-entorhinal) as well as in larger networks. Interestingly, Graham and colleagues (Graham et al., 2022) observed a pre-ictal increase response to single pulse even in absence of synaptic transmission and proposed different cellular mechanisms to explain it, including increased concentrations of intracellular chloride and dendritic plateau potentials due to large entry of calcium.
At the level of individual neurons, modification of intracellular chloride could be a suitable explanation for smaller changes observed far from the bifurcation point. The GABA-A receptor is a ligand-gated ion channel permeable to chloride (Cl-), and modulation of tonic inhibition might explain the local differences in response to single pulse. Dendritic plateaux at the population level are believed to happen only in frankly abnormal levels of cortical excitability and could explain the specific preictal sharp increase observed with suprathreshold PTZ.

At the network level, GABAergic interneurons are known to provide inhibitory restraint through feed-back and feed-forward inhibition to prevent runaway excitation and thereby seizure. In presence of increased excitation, GABAergic interneurons prevent seizure onset (Miri et al., 2018; Trevelyan, Sussillo, Watson, et al., 2006; Parrish et al., 2019) or spatial propagation (Schevon et al., 2012; Parrish et al., 2019; Liou et al., 2018). The observation that the maximum GABAergic modulation was observed in electrodes with the higher response latency point toward a cumulative effect across synapses, which may be due to a respectively increase or decrease in feed-forward inhibition (Trevelyan, Sussillo, and Yuste, 2007; Parrish et al., 2019).

During train stimulations, responses to single pulse followed a bell-shaped curve both in the Epiletor and in vivo experiment. In the model, this shape was governed by changes in the gradients encountered in the trajectory toward the seizure threshold. Their visualizations in the mice recording allow to study dynamical trajectories toward seizures in vivo. As predicted by the model, changes in cortical excitability modify the trajectories toward seizure, resulting in shrunk or elongated bell curves. Recently both animal (Wenzel et al., 2017) and human studies (Truccolo, J. A. Donoghue, et al., 2011; Karoly, Kuhlmann, et al., 2018; M. Schroeder et al., 2020; G. M. Schroeder

et al., 2022) showed that seizures generally follow stereotypical dynamical pathways, but the speed at which they progress along these can vary, resulting in 'elastic' trajectories (Wenzel et al., 2017; G. M. Schroeder et al., 2022). WWnzel and colleagues showed that the speed of progressions along these paths are critically dependent on GABAergic inhibition. Although the trajectories which we described are different (path to seizure, during stimulation, instead of pathways followed during seizures), we observed a similar elastic modulation. These observations suggest that modulation of the GABAergic system shapes abstract dynamical trajectories both outside and during seizures and provide a first step toward bridging abstract dynamical models with tangible biological mechanisms.

3.19 Comparing maker of cortical stability

The apparent randomness of seizures is a profound cause of anxiety for patients with epilepsy and seizure prediction has been a holy grail for epileptologists for decades. With the conceptualization of seizures as critical transitions, a list of generic markers called 'precursor signs' or 'early warning signs' has been proposed to anticipate seizure. When a system progressively loses its resilience (getting closer to a bifurcation point), it becomes increasingly sensitive to small perturbations. This should be reflected in a given time series both as an increased impact of stochastic noise (variance, skewness, line-length) and as a general 'slowing down', resulting from a longer recovery rate to these perturbations (autocorrelation, spatial correlation, frequency shift) (Scheffer). These markers have been successfully used in diverse fields (ecology, finance) but their application to seizure prediction has produced conflicting results (Meisel and Kuehn, 2012; Milanowski and Suffczynski, 2016; Wilkat, Rings, and Lehnertz, 2019; Maturana et al., 2020).

An intrinsic limitation of these observational studies is the absence of actual probing and measurements of the system's resilience. In passive recordings, the proposed makers cannot be compared to any ground truth and the analysis relies solely on seizure occurrences which are by nature very sparse events. Moreover, precursor signs could be present in the absence of seizures, when the system approaches the bifurcation point without crossing it, resulting in misinterpreting precursor signs as "false positives". In particular, the time window at which such resilience loss would occur in epilepsy is still unknown, with some studies focusing on seconds or minutes before a seizure (Milanowski and Suffczynski, 2016; W. C. Chang et al., 2018; Wilkat, Rings, and Lehnertz, 2019) and others on multi-days fluctuations (Maturana et al., 2020). Empirical validation of the proposed markers with a direct comparison to seizure threshold and controlled changes in cortical excitability is provided for the first time by this work. In addition, a better understanding of the biological correlates to these observed changes in the EEG would be necessary for future pharmacological intervention.
In this study, the ground truth was the drug and dosage injected. We showed that these markers reflect the current level of GABAergic inhibition and that they are accompanied with measurable change in the seizure threshold. Interestingly, we showed that some markers are better at capturing changes in seizure resilience far from the bifurcation (autocorrelation, $1/f$ exponent) and others only at high levels of cortical excitability (variance, skewness).
In the past, several different makers were used and active probing was proposed to

be superior to passive metrics (S. Kalitzin et al., 2005; Suffczynski et al., 2008; Freestone et al., 2011; Carvalho et al., 2021). To test this, we trained machine-learning based classifiers to detect the changes in cortical excitability from EEG snapshot. Evoked responses to single pulse reached high classification performance on its own. Although all six passive metrics got scores above empirical chance level, they performed quite poorly individually. However, when combined they achieved performance approaching that of active probing. Taken together, these results confirmed the ability of precursor signs based on EEG recording to detect loss of cortical resilience, but highlight the advantage of using active probing and/or combining several different markers.

3.20 Limitations

Although we believe our study provides important new contributions to the field, it has some limitations. First, we focus only on one modulator of cortical resilience: the GABAerigc system. Although it is known to be one of the key contributors, other factors also influence seizure threshold. Several anti-epileptic drugs are not acting on the GABA-A receptor, multiple other substances can cause seizure in a non-epileptic brain and in patient with epilepsy, seizure risk is known to cycle on circadian and multidien timescale (Karoly, Rao, et al., 2021). Although all of these factors presumably converge onto one latent variable - cortical excitabiltiy - each one would have to be tested separately as in the present study to confirm this intuition. Here we developed tools and rigorism that can be used to study cortical stability more broadly and systematically, from animal experiment to clinical settings and in silico modeling.
Second, for the sake of consistency, all our investigations were done in awake animals and patients. Sleep stages are known to influence both seizure risk (Ng and Pavlova, 2013), response to stimulation (Massimini et al., 2005) and passive markers (Wilkat, Rings, and Lehnertz, 2019). However, in patients with epilepsy, this influence seems to be negligible compared to the underlying cycles of cortical excitability (Maturana et al., 2020).
Third, our ability to study seizure threshold in humans was limited. Seizures were always induced for clinical reasons, and only in one case were we able to compare cortical resilience at different states of cortical excitability. Future data collection of such cases would be necessary to confirm it, but in the meantime our data indicate that responses to single pulse are good proxies in clinical settings.
Finally, in order to remain comparable with clinical data and model outputs, our animal study focused on population level activity recorded as intracranial EEG. In order to study in more detail, the biological determinants of seizure resilience, the optogenetic probing methods developed here could be, in the future, combined with modern tools of calcium imaging (Wenzel et al., 2017; Khoshkhoo, Vogt, and Sohal, 2017) as well as extra and intracellular electrophysiology.

3.21 Outlooks

The methods developed in this study allow to characterize precisely changes in cortical excitability and seizure resilience, together in dynamical models, experimental epilepsy and clinical settings. From a fundamental research standpoint, it opens new possibilities for studying biological mechanisms of cortical resilience such as the role

of the different cell type (Khoshkhoo, Vogt, and Sohal, 2017), ion concentrations (Magloire et al., 2019), brain states (Ng and Pavlova, 2013) or genetic mutation (Mattis et al., 2022). In addition, determining seizure thresholds has been the workhorse of pharmacological developments in epilepsy for decades (Yonekawa, Kupferberg, and Woodbury, 1980) but the recent low success rate of clinical studies for anti-epileptic drugs led to questioning the current methods (Simonato et al., 2013). Our experimental paradigm proved its translational value and could be easily applied in the context of drug screening and development.

From a clinical standpoint, our study validates the dynamical system approach and confirms its ability to be used in seizure prediction (Maturana et al., 2020). Implementation of real time estimation of the cortical excitability based on active and/or passive markers of critical transition could improve current seizure prediction models and allow the development of dynamically targeted interventions.

Finally, with the fast development of closed-loop neurostimulation devices for the treatment of neurological or psychiatric conditions, tractable markers of cortical dynamics will be crucial to inform the choice of stimulation timing and parameters in the future (Krauss et al., 2020; Vonck and Boon, 2015; Scangos et al., 2021; M. Zhang, Riddle, and Frohlich, 2022). In epilepsy, even simple single pulse stimulation can have dramatically different effects, capable of either starting or delaying seizure depending on the underlying dynamics (W. C. Chang et al., 2018). Measurements and understandings of these dynamics will therefore be a prerequisite to substantial developments of these therapeutic approaches.

Supplementary figures

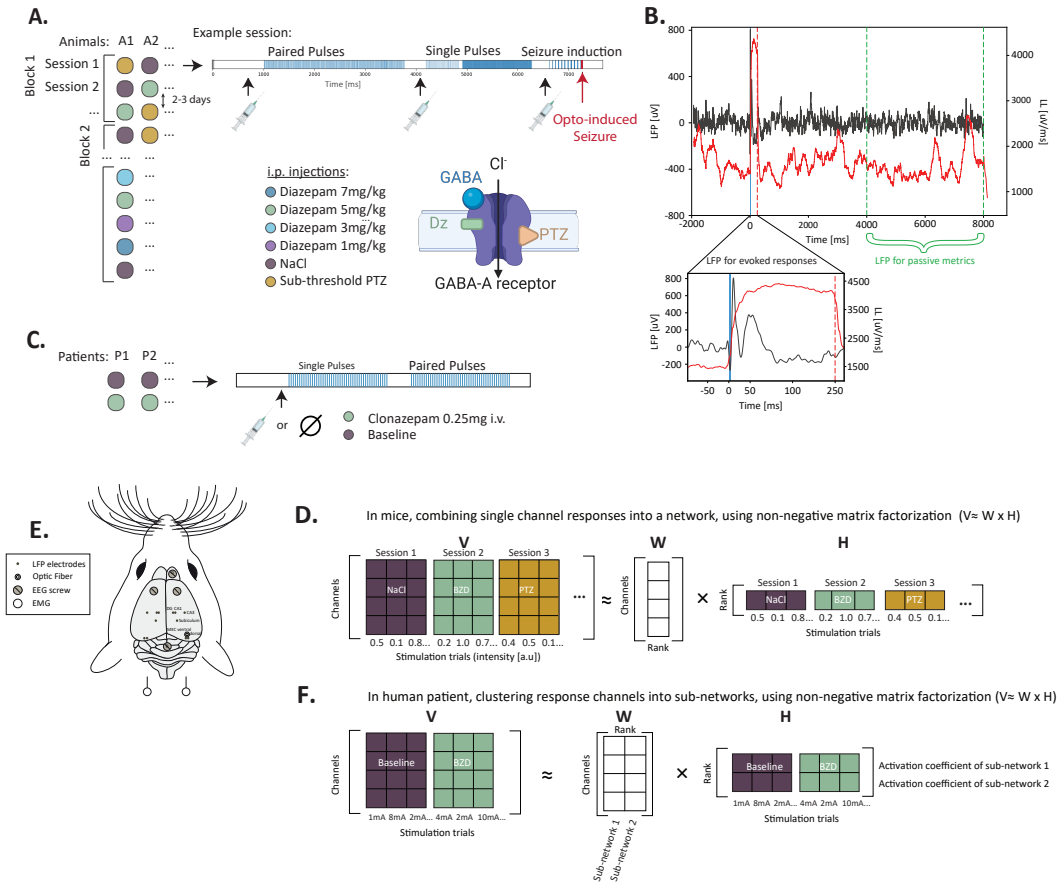

FIGURE 7: Methods

A. Recording session in mice: Each of the recording blocks included usually three 90-min afternoon sessions with three different pharmacological conditions (Diazepam (BZD), Sub-threshold Pentylenetetrazole (PTZ) and NaCl) in a random order at intervals of 48-72h. Each session started with two different protocol of paired and single pulses, and the seizure induction was done only a the end. B. Example of line-length calculation (see methods). Black trace in the EEG (CA1 R), red trace the line-length calculated on a 250ms window. C. Recording session in human patients: a first session with both single and paired pulses protocol was first done at baseline and then after the injection of clonazepam (for clinical reason). E. Montage of the multi-site intracranial electrodes. D-E. Schematic of the Non-negative Matrix Factorization (NMF), respectively for mice and human. See methods for explanations.

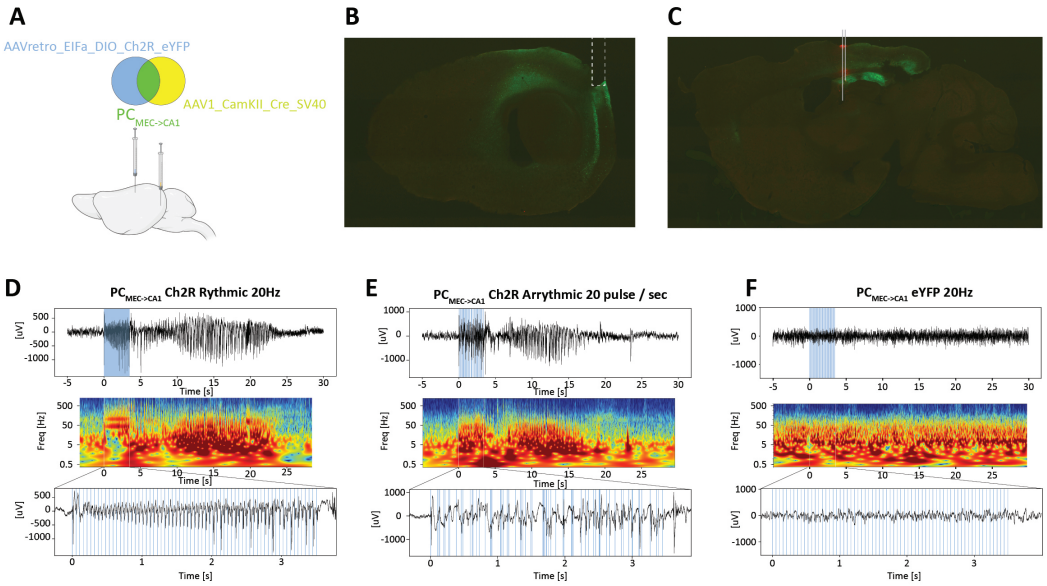

FIGURE 8: Optogenetically induced seizures in non-epileptic mice, Entorhinal cortex.

A. Channelrhodopsin was expressed in a cell-type circuit specific manner using intersectional viral strategy, targeting only excitatory neurons (pyramidal cells) projecting from the medial entorhinal cortex to the CA1 region of the hippocampus ($PC_{MEC->CA1}$). B. Sagittal view of the transfection (eYFP in green) in the entorhinal layer III and the position of the optic fiber. C. Sagittal view of the projections (eYFP in green) to CA1 (stratum lacunosum moleculare). The dye applied to the electrodes is visible in red, two electrodes tracks are visible, corresponding to electrodes in CA1 and DG. D. Example of seizure induced by optogenetic stimulation at 20Hz of the $PC_{MEC->CA1}$. E. Example, in the same mice, of a seizure induced by irregular stimulations (20 pulse per seconds but with randomly inter-pulse intervals). F. Example of stimulation in a control animal, which underwent the same procedure and stimulation protocol as in D, but received a virus without the Channelrhodopsin. Upper panels are the EEG trace recorded in CA1, middle panels are spectrograms after wavelet transform, and lower panels are a zoom-in during the stimulation.

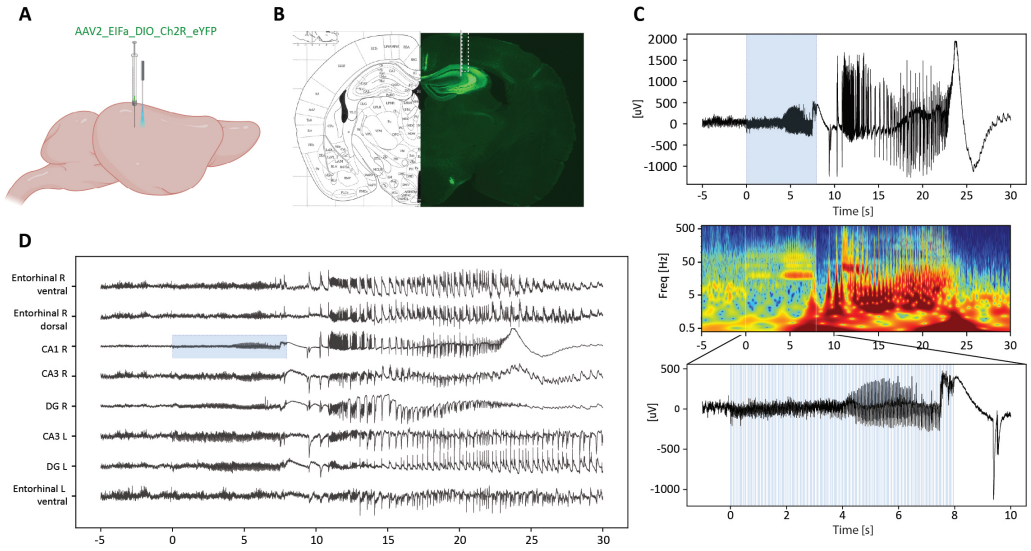

FIGURE 9: Optogenetically induced seizures in non-epileptic mice, CA1 cortex

Channelrhodopsin was expressed in CA1 Pyramidal cells using 450nl of AAV2-CamK2-Ch2R-eYFP. B. Transfection of Pyramidal cells in the right hippocampus. White dashed lines marked the optic fiber location, and the gray line is the CA1 electrodes glue to it. C. Example of seizure induced by optogenetic stimulation at 20Hz and recorded in CA1 R. D. Same seizure across all channels, blue square marks the channel corresponding to the optogenetic stimulation.

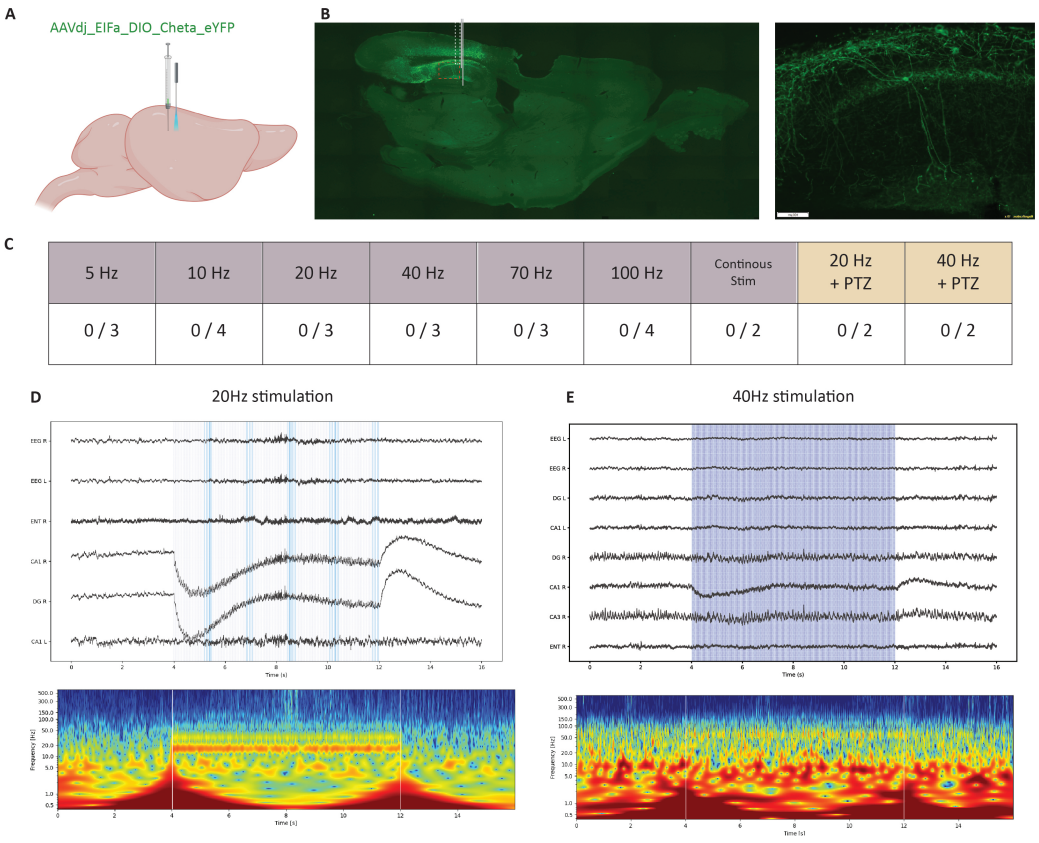

FIGURE 10: Seizure couldn't be induced by stimulation of CA1 PV interneuron

A. Experiment schematic: 450nl of the virus AAVdf-EIFa-DIO-Cheta-eYFP were injected in CA1 right. Four weeks later, multi-site depth electrodes and optic fiber in CA1 R were implanted. B. Left panel: Sagittal slice showing viral transfection in the CA1 region of the hippocampus. Right panel: 40x zoom. C. All the different simulation frequencies tested, none induce seizure. In two animals, 20Hz and 40Hz were also tested in presence of subthreshold doses of PTZ (20mg/kg). D-E. Stimulation of PV interneurons produced a visible EEG entrainment at the stimulation frequency, visible as a band in the spectrogram (wavelet transform), but no seizure.

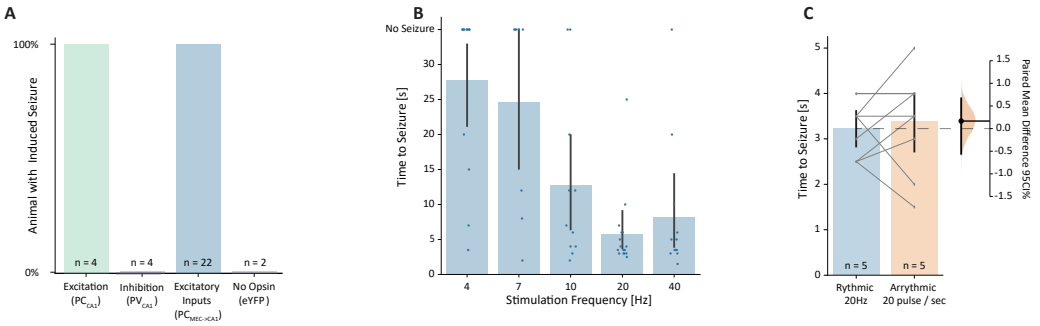

	Integrators:	Resonators:
Characteristics	-> No frequency preference -> No Inhibition -induced transition	-> Frequency preference -> Inhibition-induced transition
Type of Bifurcations	-> Saddle-Node -> Saddle-Node on invariant cycle	-> Supercritical Andronov-Hopf -> Subcritical Andronov-Hopf

FIGURE 11: Ictal transition in mice limbic circuit follows a bifurcation of the type integrator

A. In awake non-epileptic mice, limbic seizure can be induced by both direct excitation of the CA1 pyramidal cells (PC_{CA1}) or by upstream stimulation of entorhinal excitatory inputs ($PC_{MEC->CA1}$) but not by inhibition (PV_{CA1}: local parvalbumin interneurons). In absence of the opsin (eYFP), no EEG activity nor seizure could be triggered. B. Stimulation of $PC_{MEC->CA1}$ could induce seizure at all frequencies tested (4, 7, 10, 20 and 40Hz) but the time of stimulation needed to induce a seizure was decreased for higher frequencies. C. For $PC_{MEC->CA1}$ stimulation, irregular stimulations (20 pulse per seconds but with randomly inter-pulse intervals) were also systematically able to induce seizure, with a time to seizure comparable to a regular 20Hz stimulation. D.: Table of the four possible bifurcations and their respective characteristic, adapted from (Izhikevich, 2007). F-G: Stimulation in the Epileptor reproduce the InVivo findings.

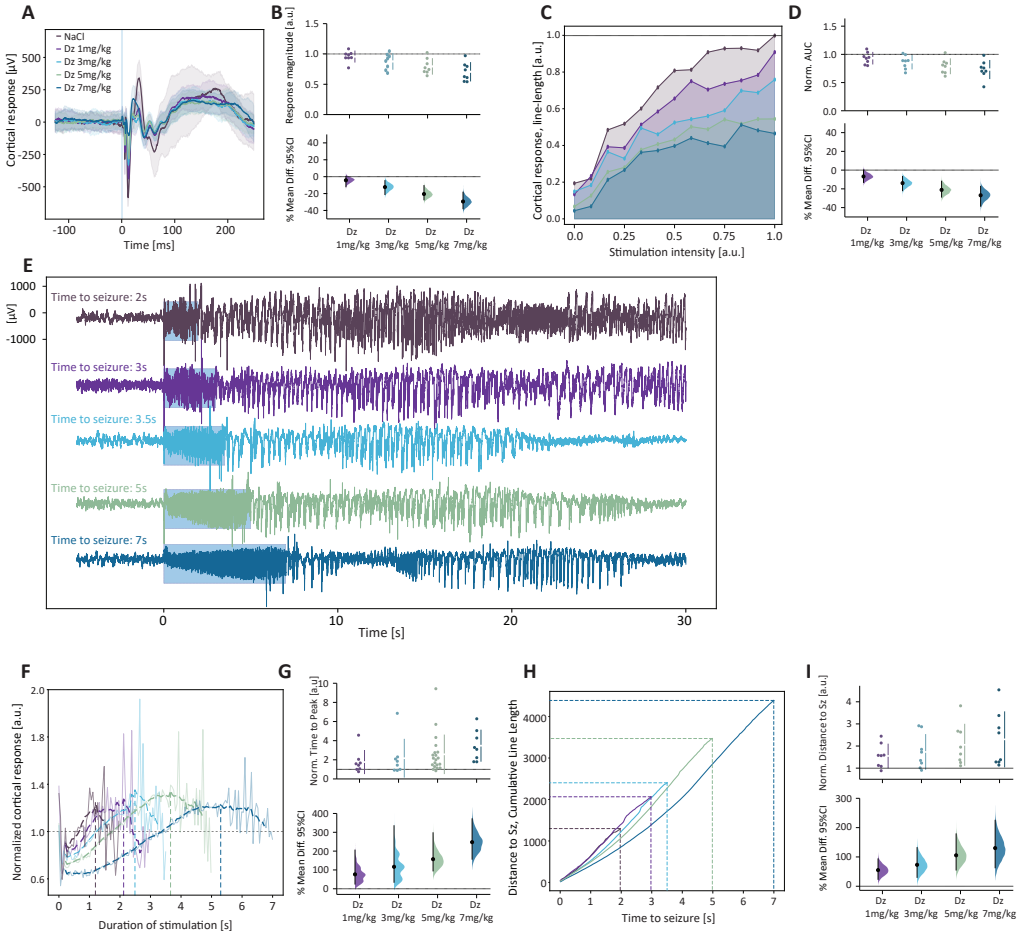

FIGURE 12: Dose-dependent increases in cortical stability under benzodiazepine.

In mice, cortical response to small perturbation (optogenetic single-pulse, max intensity) for different levels of benzodiazepine (diazepam, Dz). B. Quantification of the response across animals, as the line-length of the signal on a 250ms window, normalized to NaCl value. C. Input-output curve of the cortical response for different stimulation intensity. D. Quantification of the area under the input-output curve (AUC) and corresponding bootstrapped estimation statistics. E. Example, in one representative animal, of seizures induced by 20Hz train stimulation. F. Pulse by pulse quantification of cortical response during the stimulation shown in E. Time-to-peak is measured as the time necessary to reach the peak of the bell-shaped curves. G. Time-to-peak across animals, normalized by NaCl value and corresponding estimation statistics. H. Cumulative line-length of the responses to each pulse during stimulation train correspond to the 'Distance-to-seizure', a measure of seizure resilience. I. Quantification of 'Distance-to-seizure' across animals and corresponding estimation statistics (mean difference and 95%CI): Dz 1mg/kg: +55%[24,93], Dz 3mg/kg: +73%[30,132], Dz 5mg/kg: +106%[55,170], Dz 7mg/kg: +130%[63,225)]. N = 8 animals, 1 session in each condition, randomized.

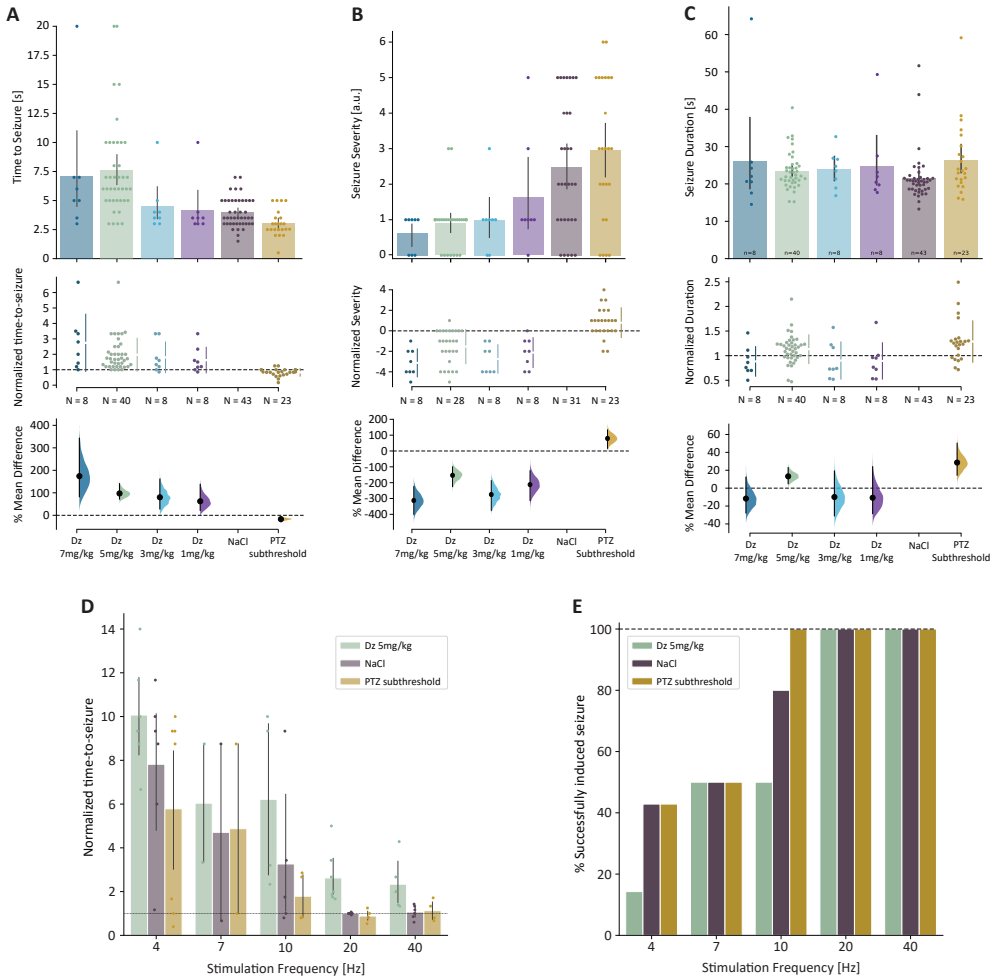

FIGURE 13: Time-to-seizure, seizure severity and seizure duration in mice

A-C: Time-to-seizure, seizure severity and duration in mice for 20Hz stimulation in mice. Upper panel shows absolute values, middle panel normalized values by block, lower panel mean difference with 95%CI (black bar) after bootstrapping. Severity is scored using a modified Racine scale (see methods), duration is calculated from the end of the stimulation until the end of the seizure. D: Time-to-seizure across stimulation frequencies. The BZD and PTZ effect on seizure resilience seems to be independent of the frequency. Only animals which were stimulated at different frequencies were included (n=7) E: Percentage of successfully induced seizures by condition. For 20Hz or higher frequencies, seizures could always be induced by train stimulation (max 30s). Pharmacological modulation of cortical excitability could have an impact on the possibility to induce seizure with lower frequencies.

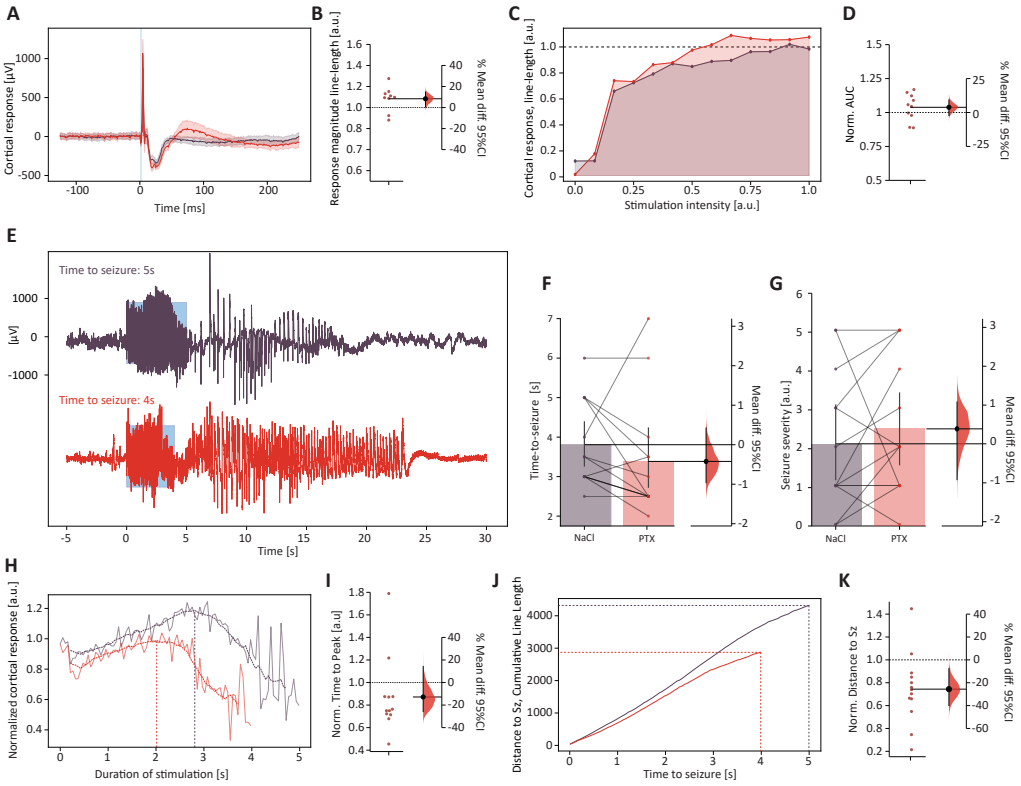

FIGURE 14: PTZ effects were reproduced with Picrotoxin

A-D: After injection of subthreshold picrotoxin (PTX, 0.75 mg/kg i.p.) in mice, response to small perturbation was significantly increased for stimulation at maximum intensity (Panel B, +8% 95%CI [5,15]), and overall response across intensities showed a trend toward increased responses (Panel D, +3% [-3,9]). E. Representative example of induced seizure in one animal in either NaCl or PTX condition. F-J-K: As for PTZ, seizure resilience was reduce in presence of PTX, with a significant effect on 'distance-to-seizure' (Panels J-K, -26% [-40,-8]) and a trend on 'time-to-seizure' (-10% [-22,+13]). G. A small trend toward an increased seizure severity (+0.4 [-0.9,+1.1]) was also found. H-I. The bell-shaped curves observed during stimulation tend to be shrinked in presence of PTX (-12%[-25,14]). N = 5 animals

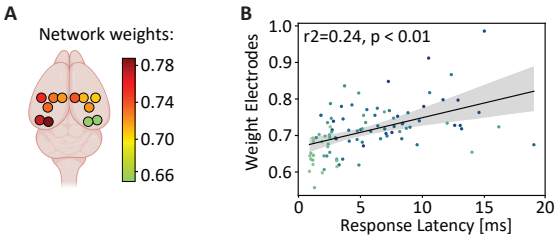

FIGURE 15: NMF weights by electrodes in mice

A. Mean weights attributed by the NMF analysis to each electrode. B. Positive linear correlation between the network weights assigned by the NMF and the latency of the response to single pulse, pointing towards a bigger GABAergic modulation at distance from the stimulation site. Each dot represents one electrode in one animal. In order to balance their respective effects, only animals which had both sessions with GABA agonist (Dz) and antagonist (PTZ) were included (n = 9).

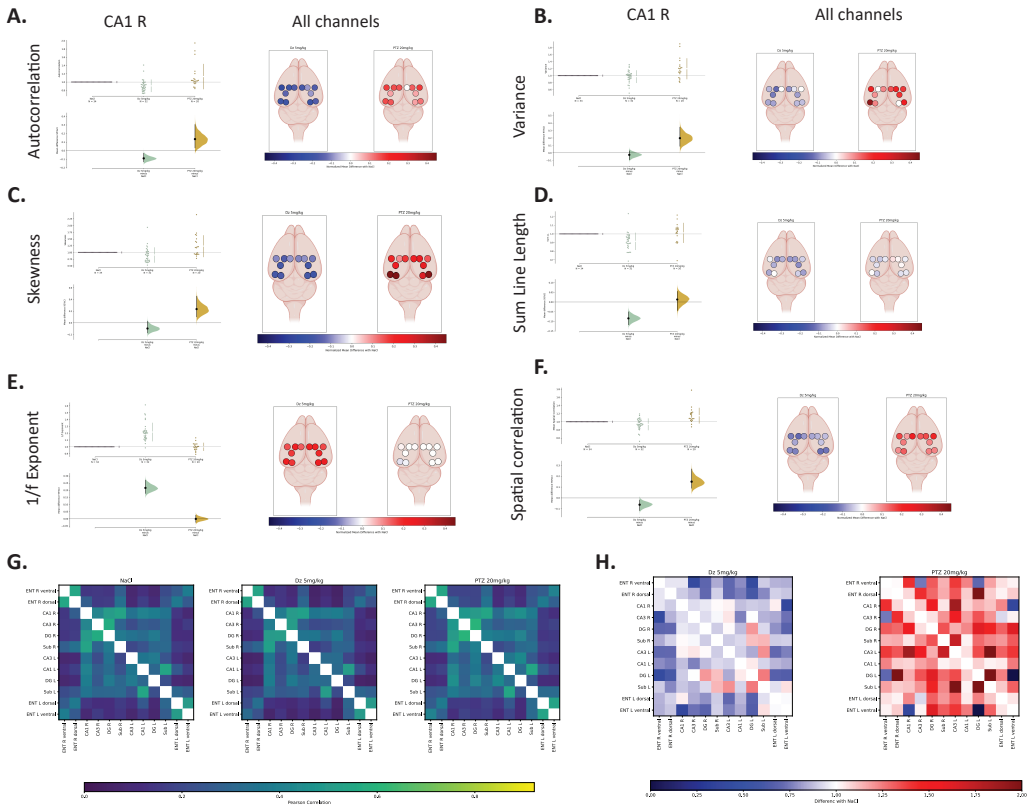

FIGURE 16: Passive markers of cortical stability by channels

A-F. For each of the six passive markers, the right panel shows normalized values by conditions and mean difference after bootstrapping with 95%CI measured in CA1 R. Left panel shows the mean difference with the control condition (NaCl), after bootstrapping, for each channel. G. Mean correlation across electrodes for each condition. H. Mean differences with the control condition (NaCl).

Table 1: Patient characteristics:

N	ID	Age	Gender	SOZ	Etiology	# leads	Single Pulse	Seizure induction	Figures
1	EL003	33	F	Temporal R	Unknown	8	Yes	No	4
2	EL004	38	M	Subcentral gyrus R	Unknown	11	Yes	No	4
3	EL005	26	F	Superior temporal gyrus L	Post-traumatic lesion	9	Yes	No	4
4	EL008	20	F	Temporal R	Encephalitis	4	Yes	*Yes*	4
5	EL010	45	F	Mesiotemporal L	Lesion	6	Yes	*Yes*	4
6	EL012	56	F	Temporal L	Unknown	8	Yes	Yes	4
7	EL014	42	M	Temporal R	Hippocampal sclerosis	5	Yes	Yes	4
8	EL015	49	M	Temporal L	Hippocampal sclerosis	6	No	Yes	2
9	EL017	48	M	Temporal L	cerebral venous sinus thrombosis	9	No	Yes	3

FIGURE 17: Patient characteristics:

Table 2: Animals with then main viral construct ($PC_{MEC->CA1}$):

N	ID	Series	Total sessions	Condition	Frequency tested	Figures
1	Ent_CamK2_03	$PC_{MEC->CA1}$	6	BZD	20Hz	3,4
2	Ent_CamK2_04	$PC_{MEC->CA1}$	6	BZD	20Hz	3,4
3	Ent_CamK2_06	$PC_{MEC->CA1}$	6	BZD	20Hz	3,4
4	Ent_CamK2_09	$PC_{MEC->CA1}$	13	PTZ, BZD, PTX	20Hz	3,4,5
6	Ent_CamK2_10	$PC_{MEC->CA1}$	24	PTZ, multi-dose BZD, PTX	20Hz	3,4,5
7	Ent_CamK2_11	$PC_{MEC->CA1}$	22	PTZ, multi-dose BZD, PTX	20Hz	3,4,5
8	Ent_CamK2_15	$PC_{MEC->CA1}$	7	PTZ, BZD, PTX	20Hz	3,4,5
9	Ent_CamK2_16	$PC_{MEC->CA1}$	24	PTZ, multi-dose BZD, PTX	20Hz	3,4,5
10	Ent_CamK2_22	$PC_{MEC->CA1}$	19	PTZ, BZD	4, 10, 20, 40Hz	Supp
11	Ent_CamK2_24	$PC_{MEC->CA1}$	20	PTZ, BZD	4, 7, 10, 20, 40Hz	Supp
12	Ent_CamK2_34	$PC_{MEC->CA1}$	13	PTZ, BZD	4, 10, 20, 40Hz	3,4,5
13	Ent_CamK2_35	$PC_{MEC->CA1}$	5	/	4, 7, 10, 20, 40Hz	Supp
14	Ent_CamK2_39	$PC_{MEC->CA1}$	19	PTZ, BZD	4, 7, 10, 20, 40Hz	3,4,5
15	Ent_CamK2_40	$PC_{MEC->CA1}$	12	PTZ, BZD	4, 7, 10, 20, 40Hz	3,4,5
16	Ent_CamK2_42	$PC_{MEC->CA1}$	15	PTZ, BZD	4, 7, 10, 20, 40Hz	3,4,5
17	Ent_CamK2_43	$PC_{MEC->CA1}$	5	/	4, 7, 10, 20, 40Hz	Supp
18	Ent_CamK2_54	$PC_{MEC->CA1}$	5	multi-dose BZD	20Hz	4
19	Ent_CamK2_55	$PC_{MEC->CA1}$	5	multi-dose BZD	20Hz	4
20	Ent_CamK2_56	$PC_{MEC->CA1}$	5	multi-dose BZD	20Hz	4
21	Ent_CamK2_57	$PC_{MEC->CA1}$	5	multi-dose BZD	20Hz	4
22	Ent_CamK2_58	$PC_{MEC->CA1}$	5	multi-dose BZD	20Hz	4

FIGURE 18: Animals with then main viral construct ($PC_{MEC->CA1}$):

Table 3: Additional animals (other viral constructs):

N	ID	Series	Total sessions	Condition	Frequency tested	Figures
1	CA1_CamK2_01	PC_{CA1}	6	/	4, 7, 10, 20, 30, 40Hz	Supp
2	CA1_CamK2_02	PC_{CA1}	6	/	4, 7, 10, 20, 30, 40Hz	Supp
3	CA1_CamK2_03	PC_{CA1}	18	BZD	20Hz	Supp
4	CA1_CamK2_04	PC_{CA1}	14	BZD	20Hz	Supp
5	CA1_PV_Cheta_01	PV_{CA1}	9	PTZ	5, 10, 20, 40, 70, 100Hz	Supp
6	CA1_PV_Cheta_01	PV_{CA1}	9	/	5, 10, 20, 40, 70, 100Hz	Supp
7	CA1_PV_Cheta_03	PV_{CA1}	2	/	10, 100Hz	Supp
8	CA1_PV_Cheta_04	PV_{CA1}	9	PTZ	5, 10, 20, 40, 70, 100Hz	Supp
9	Ent_CamK2_17	eYFP $PC_{MEC->CA1}$	24	PTZ, multi-dose BZD, PTX	20Hz	Supp
10	Ent_CamK2_18	eYFP $PC_{MEC->CA1}$	24	PTZ, multi-dose BZD, PTX	20Hz	Supp

FIGURE 19: Additional animals (other viral constructs)

Bibliography

Ang, Chyze Whee, Gregory C. Carlson, and Douglas A. Coulter (Nov. 2006). "Massive and specific dysregulation of direct cortical input to the hippocampus in temporal lobe epilepsy." In: *The Journal of neuroscience : the official journal of the Society for Neuroscience* 26.46, pp. 11850–11856. ISSN: 02706474. DOI: 10.1523/JNEUROSCI.2354-06.2006. URL: http://www.jneurosci.org/content/26/46/11850.abstract%20papers3://publication/doi/10.1523/JNEUROSCI.2354-06.2006.

Assaf, Fadi and Yitzhak Schiller (2016). "The antiepileptic and ictogenic effects of optogenetic neurostimulation of PV-expressing interneurons". In: *Journal of Neurophysiology* 116.4, pp. 1694–1704. ISSN: 15221598. DOI: 10.1152/jn.00744.2015. URL: www.jn.org.

Avoli, Massimo et al. (2016). "Specific imbalance of excitatory/inhibitory signaling establishes seizure onset pattern in temporal lobe epilepsy". In: *Journal of Neurophysiology* 115.6, pp. 3229–3237. ISSN: 15221598. DOI: 10.1152/jn.01128.2015.

Baud, Maxime O. et al. (2020). "Chance and risk in epilepsy". In: *Current opinion in neurology* 33.2, pp. 163–172. ISSN: 14736551. DOI: 10.1097/WCO.0000000000000798.

Baulac, Stéphanie et al. (2001). "First genetic evidence of GABAA receptor dysfunction in epilepsy: A mutation in the γ2-subunit gene". In: *Nature Genetics* 28.1, pp. 46–48. ISSN: 10614036. DOI: 10.1038/ng0501-46.

Buckmaster, Paul S. and Felicia H. Lew (2011). "Rapamycin suppresses mossy fiber sprouting but not seizure frequency in a mouse model of temporal lobe epilepsy". In: *Journal of Neuroscience* 31.6, pp. 2337–2347. ISSN: 02706474. DOI: 10.1523/JNEUROSCI.4852-10.2011.

Buzsáki, György, Costas A. Anastassiou, and Christof Koch (2012). "The origin of extracellular fields and currents-EEG, ECoG, LFP and spikes". In: *Nature Reviews Neuroscience* 13.6, pp. 407–420. ISSN: 1471003X. DOI: 10.1038/nrn3241. URL: http://www.ncbi.nlm.nih.gov/pubmed/22595786%0Ahttp://www.pubmedcentral.nih.gov/articlerender.fcgi?artid=PMC4907333.

Călin, Alexandru et al. (Sept. 2018). "Chemogenetic Recruitment of Specific Interneurons Suppresses Seizure Activity". In: *Frontiers in Cellular Neuroscience* 12. DOI: 10.3389/fncel.2018.00293.

Carvalho, Vinícius Rezende et al. (2021). "Active probing to highlight approaching transitions to ictal states in coupled neural mass models". In: *PLoS Computational Biology* 17.1, pp. 1–24. ISSN: 15537358. DOI: 10.1371/journal.pcbi.1008377.

Cela, Elvis et al. (Dec. 2019). "An Optogenetic Kindling Model of Neocortical Epilepsy". In: *Scientific Reports* 9.1, p. 5236. ISSN: 20452322. DOI: 10.1038/s41598-019-41533-2. URL: http://www.nature.com/articles/s41598-019-41533-2.

Chang, Michael et al. (Jan. 2018). "Brief activation of GABAergic interneurons initiates the transition to ictal events through post-inhibitory rebound excitation". In: *Neurobiology of Disease* 109, pp. 102–116. ISSN: 1095953X. DOI: 10.1016/j.nbd.2017.10.007.

Chang, Wei Chih et al. (Dec. 2018). "Loss of neuronal network resilience precedes seizures and determines the ictogenic nature of interictal synaptic perturbations". In: *Nature Neuroscience* 21.12, pp. 1742–1752. ISSN: 15461726. DOI: 10.1038/s41593-018-0278-y.

Chuang, Shu-Hui and Doodipala Samba Reddy (Jan. 2018). "Genetic and Molecular Regulation of Extrasynaptic GABA-A Receptors in the Brain: Therapeutic Insights for Epilepsy". In: *Journal of Pharmacology and Experimental Therapeutics* 364.2, pp. 180–197. ISSN: 0022-3565. DOI: 10.1124/jpet.117.244673. URL: http://dx.doi.org/10.1124/jpet.117.244673%20papers3://publication/doi/10.1124/jpet.117.244673.

Chvojka, Jan et al. (2021). "The role of interictal discharges in ictogenesis — A dynamical perspective". In: *Epilepsy and Behavior* 121, p. 106591. ISSN: 15255069. DOI: 10.1016/j.yebeh.2019.106591. URL: https://doi.org/10.1016/j.yebeh.2019.106591.

Cossart, R. et al. (2001). "Dendritic but not somatic GABAergic inhibition is decreased in experimental epilepsy". In: *Nature Neuroscience* 4.1, pp. 52–62. ISSN: 10976256. DOI: 10.1038/82900. URL: https://www.nature.com/articles/nn0101_52?draft=collection.

Dakos, Vasilis et al. (2012). "Methods for detecting early warnings of critical transitions in time series illustrated using simulated ecological data". In: *PLoS ONE* 7.7. ISSN: 19326203. DOI: 10.1371/journal.pone.0041010.

De Lanerolle, Nihal C. et al. (2003). "A retrospective analysis of hippocampal pathology in human temporal lobe epilepsy: Evidence for distinctive patient subcategories". In: *Epilepsia* 44.8, p. 1131. ISSN: 00139580. DOI: 10.1046/j.1528-1157.2003.00448.x.

Dehghani, Nima et al. (2016). "Dynamic balance of excitation and inhibition in human and monkey neocortex". In: *Scientific Reports* 6, pp. 1–12. ISSN: 20452322. DOI: 10.1038/srep23176.

Devarajan, Karthik (2008). "Nonnegative matrix factorization: An analytical and interpretive tool in computational biology". In: *PLoS Computational Biology* 4.7. ISSN: 15537358. DOI: 10.1371/journal.pcbi.1000029.

Donoghue, Thomas et al. (2020). "Parameterizing neural power spectra into periodic and aperiodic components". In: *Nature Neuroscience* 23.12, pp. 1655–1665. ISSN: 15461726. DOI: 10.1038/s41593-020-00744-x. URL: http://dx.doi.org/10.1038/s41593-020-00744-x.

Drexel, Meinrad et al. (Aug. 2017). "Selective Silencing of Hippocampal Parvalbumin Interneurons Induces Development of Recurrent Spontaneous Limbic Seizures in Mice". In: *Journal of Neuroscience* 37.34, pp. 8166–8179. URL: http://www.jneurosci.org/lookup/doi/10.1523/JNEUROSCI.3456-16.2017.

Dubanet, Olivier et al. (2021). "Probing the polarity of spontaneous perisomatic GABAergic synaptic transmission in the mouse CA3 circuit in vivo". In: *Cell Reports* 36.2, p. 109381. ISSN: 22111247. DOI: 10.1016/j.celrep.2021.109381. URL: https://doi.org/10.1016/j.celrep.2021.109381.

During, M. J. and D. D. Spencer (1993). "Extracellular hippocampal glutamate and spontaneous seizure in the conscious human brain". In: *The Lancet* 341.8861, pp. 1607–1610. ISSN: 01406736. DOI: 10.1016/0140-6736(93)90754-5.

El Houssaini, Kenza et al. (2015). "Seizures, refractory status epilepticus, and depolarization block as endogenous brain activities". In: *Physical Review E - Statistical, Nonlinear, and Soft Matter Physics* 91.1, pp. 2–6. ISSN: 15502376. DOI: 10.1103/PhysRevE.91.010701.

Elahian, Bahareh et al. (2018). "Low-voltage fast seizures in humans begin with increased interneuron firing". In: *Annals of Neurology* 84.4, pp. 588–600. ISSN: 15318249. DOI: 10.1002/ana.25325.

Freestone, Dean R. et al. (2011). "Electrical probing of cortical excitability in patients with epilepsy". In: *Epilepsy and Behavior* 22.SUPPL. 1, S110–S118. ISSN: 15255050. DOI: 10.1016/j.yebeh.2011.09.005. URL: http://dx.doi.org/10.1016/j.yebeh.2011.09.005.

Fröhlich, Flavio, Terrence J. Sejnowski, and Maxim Bazhenov (2010). "Network bistability mediates spontaneous transitions between normal and pathological brain states". In: *Journal of Neuroscience* 30.32, pp. 10734–10743. ISSN: 02706474. DOI: 10.1523/JNEUROSCI.1239-10.2010.

Goldberg, Ethan M. and Douglas A. Coulter (2013). "Mechanisms of epileptogenesis: A convergence on neural circuit dysfunction". In: *Nature Reviews Neuroscience* 14.5, pp. 337–349. ISSN: 1471003X. DOI: 10.1038/nrn3482.

Graham, Robert T et al. (2022). "Optogenetic stimulation reveals a latent tipping point in cortical networks during ictogenesis". In: *Brain*.

Griffiths, GwenvronM. and J.Tylor Fox (Aug. 1938). "Rhythm in Epilepsy". In: *The Lancet* 232.5999, pp. 409–416. ISSN: 01406736. DOI: 10.1016/S0140-6736(00)41614-4. URL: https://linkinghub.elsevier.com/retrieve/pii/S0140673600416144.

Groen, Thomas van, Pasi Miettinen, and Inga Kadish (2003). "The entorhinal cortex of the mouse: Organization of the projection to the hippocampal formation". In: *Hippocampus* 13.1, pp. 133–149. ISSN: 10509631. DOI: 10.1002/hipo.10037.

Heinemann, U. et al. (1992). "The dentate gyrus as a regulated gate for the propagation of epileptiform activity." In: *Epilepsy research. Supplement* 7, pp. 273–280. ISSN: 09229833.

Ho, Joses et al. (2019). "Moving beyond P values: data analysis with estimation graphics". In: *Nature Methods* 16.7, pp. 565–566. ISSN: 15487105. DOI: 10.1038/s41592-019-0470-3. URL: http://dx.doi.org/10.1038/s41592-019-0470-3.

Hofmann, Gabrielle et al. (2016). "Hilar somatostatin interneuron loss reduces dentate gyrus inhibition in a mouse model of temporal lobe epilepsy". In: *Epilepsia* 1.028579, pp. 977–983. DOI: 10.1111/epi.13376.

Holling, C S (1973). "Resilience and stability of ecological systems". In: *Annu.Rev.Ecol.Syst.* 4, pp. 1–23.

Huberfeld, Gilles et al. (2011). "Glutamatergic pre-ictal discharges emerge at the transition to seizure in human epilepsy". In: *Nature Neuroscience* 14.5, pp. 627–635. ISSN: 10976256. DOI: 10.1038/nn.2790.

Igarashi, Kei M. et al. (2014). *Functional diversity along the transverse axis of hippocampal area CA1*. DOI: 10.1016/j.febslet.2014.06.004.

Izhikevich, Eugene M. (2007). *Dynamical Systems in Neuroscience*. Vol. 25, pp. 227–256. ISBN: 978-0262514200.

Jirsa, Viktor K. et al. (2014). "On the nature of seizure dynamics". In: *Brain* 137.8, pp. 2210–2230. ISSN: 14602156. DOI: 10.1093/brain/awu133.

Kalitzin, S. et al. (2005). "Electrical brain-stimulation paradigm for estimating the seizure onset site and the time to ictal transition in temporal lobe epilepsy". In: *Clinical Neurophysiology* 116.3, pp. 718–728. ISSN: 13882457. DOI: 10.1016/j.clinph.2004.08.021.

Kalitzin, Stiliyan N., Demetrios N. Velis, and Fernando H. Lopes da Silva (2010). "Stimulation-based anticipation and control of state transitions in the epileptic brain". In: *Epilepsy and Behavior* 17.3, pp. 310–323. ISSN: 15255050. DOI: 10.1016/j.yebeh.2009.12.023. URL: http://dx.doi.org/10.1016/j.yebeh.2009.12.023.

Karoly, Philippa J., Levin Kuhlmann, et al. (2018). "Seizure pathways: A model-based investigation". In: *PLoS Computational Biology* 14.10. ISSN: 15537358. DOI: 10.1371/journal.pcbi.1006403.

Karoly, Philippa J., Vikram R. Rao, et al. (2021). "Cycles in Epilepsy". In: *Nature Reviews Neurology* in press. ISSN: 1759-4766. DOI: 10.1038/s41582-021-00464-1. URL: http://dx.doi.org/10.1038/s41582-021-00464-1.

Keller, Corey J. et al. (2018). "Induction and quantification of excitability changes in human cortical networks". In: *Journal of Neuroscience* 38.23, pp. 5384–5398. ISSN: 15292401. DOI: 10.1523/JNEUROSCI.1088-17.2018.

Khoshkhoo, Sattar, Daniel Vogt, and Vikaas S Sohal (Jan. 2017). "Dynamic, Cell-Type-Specific Roles for GABAergic Interneurons in a Mouse Model of Optogenetically Inducible Seizures." In: *Neuron* 93.2, pp. 291–298.

Kiss, Jozsef et al. (1996). "Entorhinal cortical innervation of parvalbumin-containing neurons (basket and chandelier cells) in the rat ammon's horn". In: *Hippocampus* 6.3, pp. 239–246. ISSN: 10509631. DOI: 10.1002/(SICI)1098-1063(1996)6:3<239::AID-HIPO3>3.0.CO;2-I.

Kitamura, Takashi et al. (2014). "Island Cells Control Temporal Association Memory". In: *Science* 231.February, pp. 896–902.

Klorig, D. C. et al. (Oct. 2019). "Optogenetically-induced population discharge threshold as a sensitive measure of network excitability". In: *eNeuro* 6.6, pp. 0229–18. ISSN: 23732822. DOI: 10.1523/ENEURO.0229-18.2019. URL: http://eneuro.org/lookup/doi/10.1523/ENEURO.0229-18.2019.

Krauss, Joachim K. et al. (2020). "Technology of deep brain stimulation: current status and future directions". In: *Nature Reviews Neurology*. ISSN: 17594766. DOI: 10.1038/s41582-020-00426-z. URL: http://dx.doi.org/10.1038/s41582-020-00426-z.

Krook-Magnuson, Esther, Caren Armstrong, Anh D Bui, et al. (May 2015). "In vivo evaluation of the dentate gate theory in epilepsy". In: *The Journal of Physiology* 593.10, pp. 2379–2388. URL: https://physoc.onlinelibrary.wiley.com/doi/full/10.1113/JP270056%20papers3://publication/doi/10.1113/JP270056.

Krook-Magnuson, Esther, Caren Armstrong, Mikko Oijala, et al. (Jan. 2013). "On-demand optogenetic control of spontaneous seizures in temporal lobe epilepsy". In: *Nature Communications* 4, p. 1376. URL: https://www.nature.com/articles/ncomms2376%20papers3://publication/doi/10.1038/ncomms2376.

Kudlacek, Jan et al. (2021). "Long-term seizure dynamics are determined by the nature of seizures and the mutual interactions between them". In: *Neurobiology of Disease* 154, p. 105347. ISSN: 1095953X. DOI: 10.1016/j.nbd.2021.105347. URL: https://doi.org/10.1016/j.nbd.2021.105347.

Kuehn, Christian (2011). "A mathematical framework for critical transitions: Bifurcations, fastslow systems and stochastic dynamics". In: *Physica D: Nonlinear Phenomena* 240.12, pp. 1020–1035. ISSN: 01672789. DOI: 10.1016/j.physd.2011.02.012. URL: http://dx.doi.org/10.1016/j.physd.2011.02.012.

Ladino, Lady D, Farzad Moien-afshari, and J.F Téllez-Zenteno (2014). "A Comprehensive Review of Temporal lobe epilepsy". In: *Epilepsy Research and Treatment*.

Lagarde, Stanislas et al. (2019). "The repertoire of seizure onset patterns in human focal epilepsies: Determinants and prognostic values". In: *Epilepsia* 60.1, pp. 85–95. ISSN: 15281167. DOI: 10.1111/epi.14604.

Lai, Nanxi et al. (2022). "Interictal-period-activated neuronal ensemble in piriform cortex retards further seizure development ll Interictal-period-activated neuronal ensemble in piriform cortex retards further seizure development". In: *CellReports*

41.11, p. 111798. DOI: 10.1016/j.celrep.2022.111798. URL: https://doi.org/10.1016/j.celrep.2022.111798.

Lambrecq, Virginie et al. (2017). "Single-unit activities during the transition to seizures in deep mesial structures". In: *Annals of Neurology* 82.6, pp. 1022–1028. ISSN: 15318249. DOI: 10.1002/ana.25111.

Lanerolle, N. C. de et al. (Aug. 1989). "Hippocampal interneuron loss and plasticity in human temporal lobe epilepsy". In: *Brain Research* 495.2, pp. 387–395. ISSN: 00068993. DOI: 10.1016/0006-8993(89)90234-5.

Langdon-Down, Mary and W. Russell Brain (1929). "Time of Day in Relation to Convulsions in Epilepsy". In: *Lancet*, pp. 1029–1032.

Leguia, Marc G et al. (2021). "Seizure Cycles in Focal Epilepsy". In: *JAMA Neurology* In press.

Lévesque, Maxime, Giuseppe Biagini, et al. (2021). "The pilocarpine model of mesial temporal lobe epilepsy: Over one decade later, with more rodent species and new investigative approaches". In: *Neuroscience and Biobehavioral Reviews* 130.June, pp. 274–291. ISSN: 18737528. DOI: 10.1016/j.neubiorev.2021.08.020.

Lévesque, Maxime, Li Yuan Chen, et al. (Nov. 2019). "Paradoxical effects of optogenetic stimulation in mesial temporal lobe epilepsy". In: *Annals of Neurology* 86.5, pp. 714–728. ISSN: 15318249. DOI: 10.1002/ana.25572.

Lévesque, Maxime, Siyan Wang, et al. (2022). "Bilateral optogenetic activation of inhibitory cells favors ictogenesis". In: *Neurobiology of Disease* 171.June, p. 105794. ISSN: 09699961. DOI: 10.1016/j.nbd.2022.105794.

Liou, Jyun-You et al. (July 2018). "Role of inhibitory control in modulating focal seizure spread." In: *Brain* 141.7, pp. 2083–2097. URL: https://academic.oup.com/brain/article/141/7/2083/4994808%20papers3://publication/doi/10.1093/brain/awy116.

Lisanby, Sarah H. (2002). "Update on magnetic seizure therapy: A novel form of convulsive therapy". In: *Journal of ECT* 18.4, pp. 182–188. ISSN: 10950680. DOI: 10.1097/00124509-200212000-00003.

— (2007). "Electroconvulsive Therapy for Depression". In: *New England Journal of Medicine* 357.19, pp. 1939–1945. ISSN: 0028-4793. DOI: 10.1056/nejmct075234.

Liu, Anli A. et al. (2022). "A consensus statement on detection of hippocampal sharp wave ripples and differentiation from other fast oscillations". In: *Nature Communications* 13.1. ISSN: 20411723. DOI: 10.1038/s41467-022-33536-x.

Lopes Da Silva, Fernando H. et al. (2003). "Epilepsies as Dynamical Diseases of Brain Systems: Basic Models of the Transition between Normal and Epileptic Activity". In: *Epilepsia* 44.12 SUPPL. Pp. 72–83. ISSN: 00139580. DOI: 10.1111/j.0013-9580.2003.12005.x.

Lothman, E. W., J. L. Stringer, and E. H. Bertram (1992). "The dentate gyrus as a control point for seizures in the hippocampus and beyond." In: *Epilepsy research. Supplement* 7, pp. 301–313. ISSN: 09229833.

Magloire, Vincent et al. (Mar. 2019). "KCC2 overexpression prevents the paradoxical seizure-promoting action of somatic inhibition." In: *Nature Communications* 10.1, p. 1225. URL: http://eutils.ncbi.nlm.nih.gov/entrez/eutils/elink.fcgi?dbfrom=pubmed&id=30874549&retmode=ref&cmd=prlinks%20papers3://publication/doi/10.1038/s41467-019-08933-4.

Maguire, Jamie et al. (May 2005). "Ovarian cycle–linked changes in GABAA receptors mediating tonic inhibition alter seizure susceptibility and anxiety". In: *Nature Neuroscience* 8.6, pp. 797–804. URL: http://www.nature.com/articles/nn1469%20papers3://publication/doi/10.1038/nn1469.

Massimini, Marcello et al. (2005). "Breakdown of cortical effective connectivity during sleep". In: *Science* 309.5744, pp. 2228–2232. ISSN: 00368075. DOI: 10.1126/science.1117256.

Mathern, Gary W et al. (1995). "Reactive synaptogenesis and neuron densities for neuropeptide Y, somatostatin, and glutamate decarboxylase immunoreactivity in the epileptogenic human fascia dentata". In: *Journal of Neuroscience* 15.5 II, pp. 3990–4004. ISSN: 02706474. DOI: 10.1523/jneurosci.15-05-03990.1995.

Mattis, Joanna et al. (2022). "Corticohippocampal circuit dysfunction in a mouse model of Dravet syndrome". In: *eLife* 11, pp. 1–30. ISSN: 2050084X. DOI: 10.7554/ELIFE.69293.

Maturana, Matias I et al. (Dec. 2020). "Critical slowing down as a biomarker for seizure susceptibility". In: *Nature Communications* 11.1, p. 2172. ISSN: 2041-1723. DOI: 10.1038/s41467-020-15908-3. URL: http://dx.doi.org/10.1038/s41467-020-15908-3%20http://www.nature.com/articles/s41467-020-15908-3.

McCormick, D. A. and D. Contreras (2001). "On the cellular and network bases of epileptic seizures". In: *Annual Review of Physiology* 63, pp. 815–846. ISSN: 00664278. DOI: 10.1146/annurev.physiol.63.1.815.

Meisel, Christian and Christian Kuehn (2012). "Scaling effects and spatio-temporal multilevel dynamics in epileptic seizures". In: *PLoS ONE* 7.2. ISSN: 19326203. DOI: 10.1371/journal.pone.0030371.

Melzer, Sarah et al. (2012). "Long-Range–Projecting GABAergic Neurons Modulate Inhibition in Hippocampus and Entorhinal Cortex". In: *Science* March, pp. 1506–1510.

Milanowski, Piotr and Piotr Suffczynski (2016). "Seizures Start without Common Signatures of Critical Transition". In: *International Journal of Neural Systems* 26.8, pp. 1–15. ISSN: 17936462. DOI: 10.1142/S0129065716500532.

Miri, Mitra L et al. (Nov. 2018). "Altered hippocampal interneuron activity precedes ictal onset". In: *eLife* 7, pp. 1–20. URL: https://elifesciences.org/articles/40750%20papers3://publication/doi/10.7554/eLife.40750.

Morin, F., C. Beaulieu, and J. C. Lacaille (1998). "Cell-specific alterations in synaptic properties of hippocampal CA1 interneurons after kainate treatment". In: *Journal of Neurophysiology* 80.6, pp. 2836–2847. ISSN: 00223077. DOI: 10.1152/jn.1998.80.6.2836.

Mormann, Florian et al. (2007). "Seizure prediction: The long and winding road". In: *Brain* 130.2, pp. 314–333. ISSN: 14602156. DOI: 10.1093/brain/awl241.

Ng, Marcus and Milena Pavlova (2013). "Why Are Seizures Rare in Rapid Eye Movement Sleep? Review of the Frequency of Seizures in Different Sleep Stages". In: *Epilepsy Research and Treatment* 2013, pp. 1–10. ISSN: 2090-1348. DOI: 10.1155/2013/932790. URL: https://www.hindawi.com/archive/2013/932790/.

Noebels, Jeffrey L. et al. (2012). *Jasper 's Basic Mechanisms of the Epilepsies, 4th edition*. Ed. by Jeffrey L. Noebels et al. 4th editio. Bethesda (MD): National Center for Biotechnology Information (US); ISBN: 0199746540.

Osawa, Shin Ichiro et al. (Apr. 2013). "Optogenetically Induced Seizure and the Longitudinal Hippocampal Network Dynamics". In: *PLoS ONE* 8.4. Ed. by Liset Menendez de la Prida, e60928. ISSN: 19326203. DOI: 10.1371/journal.pone.0060928. URL: https://dx.plos.org/10.1371/journal.pone.0060928.

Parrish, R Ryley et al. (2019). "Feedforward inhibition ahead of ictal wavefronts is provided by both parvalbumin- and somatostatin-expressing interneurons". In: *Journal of Physiology* 597.8, pp. 2297–2314. ISSN: 14697793. DOI: 10.1113/JP277749.

Paschen, E. et al. (2020). "Hippocampal low-frequency stimulation prevents seizure generation in a mouse model of mesial temporal lobe epilepsy". In: *eLife* 9, pp. 1–57. ISSN: 2050084X. DOI: 10.7554/ELIFE.54518.

Pillai, Jyoti and Michael R. Sperling (2006). "Interictal EEG and the diagnosis of epilepsy". In: *Epilepsia* 47.SUPPL. 1, pp. 14–22. ISSN: 00139580. DOI: 10.1111/j.1528-1167.2006.00654.x.

Premoli, Isabella, Til O Bergmann, et al. (2017). "The impact of GABAergic drugs on TMS-induced brain oscillations in human motor cortex". In: *NeuroImage* 163.September, pp. 1–12. ISSN: 1053-8119. DOI: 10.1016/j.neuroimage.2017.09.023. URL: https://doi.org/10.1016/j.neuroimage.2017.09.023.

Premoli, Isabella, Nazareth Castellanos, et al. (2014). "TMS-EEG signatures of GABAergic neurotransmission in the human cortex". In: *Journal of Neuroscience* 34.16, pp. 5603–5612. ISSN: 15292401. DOI: 10.1523/JNEUROSCI.5089-13.2014.

Proix, Timothée, Fabrice Bartolomei, et al. (2017). "Individual brain structure and modelling predict seizure propagation". In: *Brain* 140.3, pp. 641–654. ISSN: 14602156. DOI: 10.1093/brain/awx004.

Proix, Timothée, Viktor K. Jirsa, et al. (Dec. 2018). "Predicting the spatiotemporal diversity of seizure propagation and termination in human focal epilepsy". In: *Nature Communications* 9.1, p. 1088. ISSN: 20411723. DOI: 10.1038/s41467-018-02973-y. URL: http://www.nature.com/articles/s41467-018-02973-y.

Quigg, Mark et al. (2000). "Effects of circadian regulation and rest-activity state on spontaneous seizures in a rat model of limbic epilepsy". In: *Epilepsia* 41.5, pp. 502–509. ISSN: 00139580. DOI: 10.1111/j.1528-1157.2000.tb00202.x.

Robbins, Richard J et al. (1991). "A selective loss of somatostatin in the hippocampus of patients with temporal lobe epilepsy". In: *Annals of Neurology* 29.3, pp. 325–332. ISSN: 15318249. DOI: 10.1002/ana.410290316.

Rosenblueth, Arturo and Norbert Wiener (1945). "The Role of Models in Science". In: *Philosophy of Science* 12.4, pp. 316–321. ISSN: 0031-8248. DOI: 10.1086/286874. URL: http://www.jstor.org/stable/184253.

Ross, Lauren N. (2014). "Dynamical models and explanation in neuroscience". In: *Philosophy of Science* 82.1, pp. 32–54. ISSN: 1539767X. DOI: 10.1086/679038.

Rusina, Evgeniia, Christophe Bernard, and Adam Williamson (2021). "The Kainic acid models of Temporal Lobe Epilepsy". In: *Eneuro*, pp. 0337–20. ISSN: 2373-2822. DOI: 10.1523/eneuro.0337-20.2021.

Saggio, Maria Luisa et al. (2020). "A taxonomy of seizure dynamotypes". In: *Elife*, pp. 1–56. DOI: https://doi.org/10.7554/eLife.55632. URL: https://doi.org/10.7554/eLife.55632.

Saras, Arunesh et al. (2017). "Investigation of seizure-susceptibility in a drosophila melanogaster model of human epilepsy with optogenetic stimulation". In: *Genetics* 206.4, pp. 1739–1746. ISSN: 19432631. DOI: 10.1534/genetics.116.194779.

Scangos, Katherine W. et al. (2021). "Closed-loop neuromodulation in an individual with treatment-resistant depression". In: *Nature Medicine* 27.10, pp. 1696–1700. ISSN: 1546170X. DOI: 10.1038/s41591-021-01480-w. URL: http://dx.doi.org/10.1038/s41591-021-01480-w.

Scheffer, Marten (2009). *Critical Transitions in Nature and Society*. Princeton University Press, pp. 0–379. ISBN: 978-0-691-12204-5. DOI: 10.2307/j.ctv173f1g1.

Scheffer, Marten, Jordi Bascompte, et al. (2009). *Early-warning signals for critical transitions*. DOI: 10.1038/nature08227.

Scheffer, Marten, Stephen R Carpenter, et al. (2012). *Anticipating critical transitions*. DOI: 10.1126/science.1225244.

Schevon, Catherine A. et al. (2012). "Evidence of an inhibitory restraint of seizure activity in humans". In: *Nature Communications* 3. ISSN: 20411723. DOI: 10.1038/ncomms2056.

Schroeder, Gabrielle M. et al. (2022). "Multiple mechanisms shape the relationship between pathway and duration of focal seizures". In: *Brain Communications* 4.4, pp. 1–16. ISSN: 26321297. DOI: 10.1093/braincomms/fcac173.

Schroeder, M et al. (2020). "Seizure pathways change on circadian and slower timescales in individual patients with focal epilepsy". In: *Proceedings of the National Academy of Sciences* 2014958117. DOI: 10.1073/pnas.2014958117.

Sheybani, Laurent et al. (Apr. 2018). "Electrophysiological Evidence for the Development of a Self-Sustained Large-Scale Epileptic Network in the Kainate Mouse Model of Temporal Lobe Epilepsy." In: *The Journal of neuroscience : the official journal of the Society for Neuroscience* 38.15, pp. 3776–3791. URL: http://www.jneurosci.org/lookup/doi/10.1523/JNEUROSCI.2193-17.2018%20papers3://publication/doi/10.1523/JNEUROSCI.2193-17.2018.

Simonato, Michele et al. (2013). "Issues for new antiepilepsy drug development". In: *Current Opinion in Neurology* 26.2, pp. 195–200. ISSN: 13507540. DOI: 10.1097/WCO.0b013e32835efe29.

Skotte, Line et al. (2022). "Genome-wide association study of febrile seizures implicates fever response and neuronal excitability genes". In: *Brain* 2021. ISSN: 0006-8950. DOI: 10.1093/brain/awab260.

Sloviter, Robert S. (1987). "Decreased hippocampal inhibition and a selective loss of interneurons in experimental epilepsy". In: *Science* 235.4784, pp. 73–76. ISSN: 00368075. DOI: 10.1126/science.2879352.

Strien, N M van, Natalie L.M. Cappaert, and M P Witter (Apr. 2009). "The anatomy of memory: an interactive overview of the parahippocampal-hippocampal network." In: *Nature Reviews Neuroscience* 10.4, pp. 272–282. URL: https://www.nature.com/articles/nrn2614.

Suffczynski, Piotr et al. (2008). "Active paradigms of seizure anticipation: Computer model evidence for necessity of stimulation". In: *Physical Review E - Statistical, Nonlinear, and Soft Matter Physics* 78.5, pp. 1–9. ISSN: 15393755. DOI: 10.1103/PhysRevE.78.051917.

Šulcová, Dominika et al. (2022). "Evaluation of GABA A R-mediated inhibition in the human brain using TMS- evoked potentials". In: *bioRvix*, pp. 1–27.

Trevelyan, Andrew J., David Sussillo, Brendon O. Watson, et al. (2006). "Modular propagation of epileptiform activity: Evidence for an inhibitory veto in neocortex". In: *Journal of Neuroscience* 26.48, pp. 12447–12455. ISSN: 02706474. DOI: 10.1523/JNEUROSCI.2787-06.2006.

Trevelyan, Andrew J., David Sussillo, and Rafael Yuste (2007). "Feedforward inhibition contributes to the control of epileptiform propagation speed". In: *Journal of Neuroscience* 27.13, pp. 3383–3387. ISSN: 02706474. DOI: 10.1523/JNEUROSCI.0145-07.2007.

Truccolo, Wilson, Omar J. Ahmed, et al. (July 2014). "Neuronal Ensemble Synchrony during Human Focal Seizures". In: *Journal of Neuroscience* 34.30, pp. 9927–9944. URL: http://www.jneurosci.org/cgi/doi/10.1523/JNEUROSCI.4567-13.2014%20papers3://publication/doi/10.1523/JNEUROSCI.4567-13.2014.

Truccolo, Wilson, Jacob A Donoghue, et al. (May 2011). "Single-neuron dynamics in human focal epilepsy". In: *Nature Neuroscience* 14.5, pp. 635–641. URL: https://www.nature.com/articles/nn.2782%20papers3://publication/doi/10.1038/nn.2782.

Tye, Kay M. and Karl Deisseroth (2012). "Optogenetic investigation of neural circuits underlying brain disease in animal models". In: *Nature Reviews Neuroscience* 13.4, pp. 251–266. ISSN: 1471003X. DOI: 10.1038/nrn3171.

Valentín, A. et al. (2002). "Responses to single pulse electrical stimulation identify epileptogenesis in the human brain in vivo". In: *Brain* 125.8, pp. 1709–1718. ISSN: 00068950. DOI: 10.1093/brain/awf187.

Van De Leemput, Ingrid A. et al. (2014). "Critical slowing down as early warning for the onset and termination of depression". In: *Proceedings of the National Academy of Sciences of the United States of America* 111.1, pp. 87–92. ISSN: 00278424. DOI: 10.1073/pnas.1312114110.

Velíšková, Jana, Michael P. Shakarjian, and Libor Velíšek (2017). "Systemic Chemoconvulsants Producing Acute Seizures in Adult Rodents". In: *Models of Seizures and Epilepsy: Second Edition*. Second Edi. Elsevier Inc., pp. 491–512. ISBN: 9780128040669. DOI: 10.1016/B978-0-12-804066-9.00035-3. URL: http://dx.doi.org/10.1016/B978-0-12-804066-9/00035-3.

Vonck, Kristl and Paul Boon (2015). "Epilepsy: Closing the loop for patients with epilepsy". In: *Nature Reviews Neurology* 11.5, pp. 252–254. ISSN: 17594766. DOI: 10.1038/nrneurol.2015.56.

Wang, Ying, Jiao Liang, et al. (Sept. 2018). "Pharmaco-genetic therapeutics targeting parvalbumin neurons attenuate temporal lobe epilepsy". In: *Neurobiology of Disease* 117.June, pp. 149–160. ISSN: 1095953X. DOI: 10.1016/j.nbd.2018.06.006. URL: https://doi.org/10.1016/j.nbd.2018.06.006.

Wang, Ying, Cenglin Xu, et al. (July 2017). "Depolarized GABAergic Signaling in Subicular Microcircuits Mediates Generalized Seizure in Temporal Lobe Epilepsy". In: *Neuron* 95.1, pp. 92–105. ISSN: 10974199. DOI: 10.1016/j.neuron.2017.06.004. URL: https://linkinghub.elsevier.com/retrieve/pii/S0896627317305020%20papers3://publication/doi/10.1016/j.neuron.2017.06.004%20http://dx.doi.org/10.1016/j.neuron.2017.06.004.

Weiss, Shennan Aibel et al. (2016). "Ictal onset patterns of local field potentials, high frequency oscillations, and unit activity in human mesial temporal lobe epilepsy". In: *Epilepsia* 57.1, pp. 111–121. ISSN: 15281167. DOI: 10.1111/epi.13251.

Wenzel, Michael et al. (June 2017). "Reliable and Elastic Propagation of Cortical Seizures In Vivo". In: *Cell Reports* 19.13, pp. 2681–2693. ISSN: 22111247. DOI: 10.1016/j.celrep.2017.05.090. URL: http://dx.doi.org/10.1016/j.celrep.2017.05.090%20papers3://publication/doi/10.1016/j.celrep.2017.05.090.

Wilkat, Theresa, Thorsten Rings, and Klaus Lehnertz (2019). "No evidence for critical slowing down prior to human epileptic seizures". In: *Chaos* 29.9. ISSN: 10541500. DOI: 10.1063/1.5122759.

Williams, P. A. et al. (2009). "Development of Spontaneous Recurrent Seizures after Kainate-Induced Status Epilepticus". In: *Journal of Neuroscience* 29.7, pp. 2103–2112. ISSN: 0270-6474. DOI: 10.1523/jneurosci.0980-08.2009.

Witter, Menno (2012). "Hippocampus". In: *The Mouse Nervous System*. Elsevier Inc., pp. 112–139. ISBN: 9780123694973. DOI: 10.1016/B978-0-12-369497-3.10005-6. URL: http://dx.doi.org/10.1016/B978-0-12-369497-3.10005-6.

Wittner, L et al. (Jan. 2005). "Surviving CA1 pyramidal cells receive intact perisomatic inhibitory input in the human epileptic hippocampus." In: *Brain* 128.Pt 1, pp. 138–152. URL: https://academic.oup.com/brain/article-lookup/doi/10.1093/brain/awh339.

Wittner, L. et al. (2001). "Preservation of perisomatic inhibitory input of granule cells in the epileptic human dentate gyrus". In: *Neuroscience* 108.4, pp. 587–600. ISSN: 03064522. DOI: 10.1016/S0306-4522(01)00446-8.

Wozny, C. et al. (2005). "Entorhinal cortex entrains epileptiform activity in CA1 in pilocarpine-treated rats". In: *Neurobiology of Disease* 19.3, pp. 451–460. ISSN: 09699961. DOI: 10.1016/j.nbd.2005.01.016.

Wu, K. and L. S. Leung (2001). "Enhanced but fragile inhibition in the dentate gyrus in vivo in the kainic acid model of temporal lobe epilepsy: A study using current source density analysis". In: *Neuroscience*. ISSN: 03064522. DOI: 10.1016/S0306-4522(01)00043-4.

Wu, Siqi et al. (2016). "Stability-driven nonnegative matrix factorization to interpret Spatial gene expression and build local gene networks". In: *Proceedings of the National Academy of Sciences of the United States of America* 113.16, pp. 4290–4295. ISSN: 10916490. DOI: 10.1073/pnas.1521171113.

Yonekawa, Wayne D., H. J. Kupferberg, and Dixon M. Woodbury (1980). "Relationship between pentylenetetrazol-induced seizures and brain pentylenetetrazol levels in mice". In: *Journal of Pharmacology and Experimental Therapeutics* 214.3, pp. 589–593. ISSN: 00223565.

Yoong, Y. L. et al. (1986). *Acute Tolerance To Diazepam in Mice: Pharmacokinetic Considerations*. Tech. rep. 2, pp. 153–158. DOI: 10.1111/j.1440-1681.1986.tb00329.x.

Zangaladze, Andro et al. (2008). "The effectiveness of low-frequency stimulation for mapping cortical function". In: *Epilepsia* 49.3, pp. 481–487. ISSN: 00139580. DOI: 10.1111/j.1528-1167.2007.01307.x.

Zhang, Mengsen, Justin Riddle, and Flavio Frohlich (2022). "Closed-loop control of bistable symptom states". In: *Brain Stimulation* 15.2, pp. 454–456. ISSN: 18764754. DOI: 10.1016/j.brs.2022.02.010.

Zhang, Wei, John R. Huguenard, and Paul S. Buckmaster (2012). "Increased excitatory synaptic input to granule cells from hilar and CA3 regions in a rat model of temporal lobe epilepsy". In: *Journal of Neuroscience* 32.4, pp. 1183–1196. ISSN: 02706474. DOI: 10.1523/JNEUROSCI.5342-11.2012.

Zijlmans, M. et al. (2009). "High-frequency oscillations mirror disease activity in patients with epilepsy". In: *Neurology* 72.11, pp. 979–986. ISSN: 1526632X. DOI: 10.1212/01.wnl.0000344402.20334.81.

Acknowledgements

First and foremost, I would like to express my gratitude to my supervisor, Maxime Baud, for trusting me with this PhD project and then for his support, guidance, and encouragement throughout these four years. Even though being the first PhD in the lab was not without challenges, our almost daily meetings in the first year were crucial to learn all the multiple steps necessary to perform ambitious In Vivo experiment and signal analysis. They say that mentors are important in science, and I consider myself lucky to have found a great one. Your optimism and open-mindedness were crucial in a project which was definitely not straightforward and required changing direction multiple times (from neurosteroids to interneurons to dynamical systems!). Our sometimes long and deep scientific discussions at end of our one-to-one meetings were some of my favorite times in the past four years.

I am also particularly grateful to Antoine Adamantidis for his warm welcome at the ZEN and for the scientific and technical expertise he provided throughout this project.

I would also like to thank all the members of my thesis committee, the Professors Stephan Reichenbach, Stéphane Ciocchi and Přemysl Jiruška, for their constructive feedback and insightful comments.

Many thanks to all the people from the e-Lab, it has been a chance to work alongside you. A special thanks to the 'e-Lab 1.0': Marc, Ellen and of course Kristina which whom I spent a great deal of time creating and debugging experimental set-up and pipeline analysis. And thanks to Richard who gave precious advice on the figures and thesis writing.

A big thank you to all the collaborators on this work and in particular Ellen, who kindly shared her human data, and to Tim who, in addition to his contribution with the modeling, was always keen to provid answers to my dynamic interrogations, even during his holidays.

I am of course grateful for all the ZEN family who provided such a nice work environment, both inside and outside the lab, and this even in time of global pandemic. I cannot cite everyone but the 'Spritz gang' will recognize themselves. These years in Bern would have been much less enjoyable without you.

Thank you also to the people who pushed me to follow my penchant for in-depth thinking and basic science and to take the step to undertake a PhD: my NeuroClub buddy Martin and Prof. Jozsef Kiss for the neuroscience nights organized in Geneva, Mitsouko van Assche and Prof. Assal for the master thesis supervision and all the people who listened to me talking about my PhD aspirations for hours. Here I have a special thought for my brother Jan and Marion.

I would also like to acknowledge the love and support of my family, Jérôme, Sophie, Jan, my grand-parents Brigitte, André and 'bon-papa', who has always been there for me. Again, thank you Sophie for all the last minute -as always- proofreading. And of course, a big thought goes to my mother, Caroline. Her wisdom and kindness continue to be a constant source of inspiration and influence in my life, even after all these years. This work is dedicated to her.

And I don't forget all my friends, thank you for making life just better: Sacha, Mathias, Olivier and all the others ('Bunch of . . . ').

Lastly, I would like to express all my gratitude to Bianca, who has been a tremendous source of support, fun and encouragement during these last months.

Sincerely,

Gregory

License

Declaration of Originality

Last name, first name: Lepeu, Gregory

Matriculation number: 12-331-831

I hereby declare that this thesis represents my original work and that I have used no other sources except as noted by citations.
All data, tables, figures and text citations which have been reproduced from any other source, including the internet, have been explicitly acknowledged as such.
I am aware that in case of non-compliance, the Senate is entitled to withdraw the doctorate degree awarded to me on the basis of the present thesis, in accordance with the "Statut der Universität Bern (Universitätsstatut; UniSt)", Art. 69, of 7 June 2011.

Bern, December 17, 2024

Gregory Lepeu